THE UNIVERSITY OF CALGARY

Theoretical and Experimental Study of Coupled Torsional – Lateral Vibrations in Rotor Dynamics

by

Ittapana Perera

A THESIS

SUBMITTED TO THE FACULTY OF GRADUATE STUDIES

IN PARTIAL FULFILLMENT OF THE REQUIREMENTS FOR THE

DEGREE OF MASTER OF ENGINEERING

DEPARTMENT OF MECHANICAL ENGINEERING

CALGARY, ALBERTA

DECEMBER, 1998

© Ittapana Perera 1998

National Library of Canada
Acquisitions and Bibliographic Services
395 Wellington Street
Ottawa ON K1A 0N4
Canada

Bibliothèque nationale du Canada
Acquisitions et services bibliographiques
395, rue Wellington
Ottawa ON K1A 0N4
Canada

Your file Votre référence

Our file Notre référence

The author has granted a non-exclusive licence allowing the National Library of Canada to reproduce, loan, distribute or sell copies of this thesis in microform, paper or electronic formats.

L'auteur a accordé une licence non exclusive permettant à la Bibliothèque nationale du Canada de reproduire, prêter, distribuer ou vendre des copies de cette thèse sous la forme de microfiche/film, de reproduction sur papier ou sur format électronique.

The author retains ownership of the copyright in this thesis. Neither the thesis nor substantial extracts from it may be printed or otherwise reproduced without the author's permission.

L'auteur conserve la propriété du droit d'auteur qui protège cette thèse. Ni la thèse ni des extraits substantiels de celle-ci ne doivent être imprimés ou autrement reproduits sans son autorisation.

0-612-38558-2

Canada

Abstract

The coupled torsional-lateral vibrations in single and two-disk rotor systems are studied analytically and experimentally over the operational frequency range. A comparison of analytical and experimental results is done for a motor pump assembly. The results presented shows the existence and significance of the coupling phenomenon in rotating machinery.

Acknowledgements

My sincere thanks to Dr. O. Vinogradov not only for his guidance, patience and trust put on this work, but also for the friendly help given through out my study at the University of Calgary.

A special thanks to my loving wife Dharshi for her understanding, help and constant support.

I would like to thank my employer Kadon Electro Mechanical Services of Calgary, and my colleagues Mike Greer, Ray Gibbs, Dr. Don Bayly and Dr. Tony Taylor for their support and encouragement to complete this project.

My special thanks to Victor Obeid and Chuck Yeiser at Rotor Bearing Technology and Software Inc. in Pennsylvania, USA for providing me the algorithm from "Numerical Recipies" to solve the nonlinear differential equations and compute the results.

To Maithri and Shehan

Table of Contents

Approval....ii

Abstract....iii

Acknowledgements....iv

Dedication....v

Table of contents....vi

List of Tables....ix

List of Figures....x

List of Plots....xi

Chapter 1

Introduction....1

1.1 Need for the study....6

1.2 Objectives....7

Chapter 2

State of the art and review of background material....12

Chapter 3

Analysis Model I – Single Disk Rotor System....24

3.1 Lagrange's Equation....25

3.2 Model I – Single Disk Rotor System.....26

3.3 Lateral response.....32

3.4 Conclusion.....35

Chapter 4

Analysis Model II – Two Disk Rotor System.....36

4.1 Two Disk Rotor Model.....37

4.2 Method of Solution.....47

4.3 Two disk Rotor Model Dimensional Data.....48

4.4 Part 1 – Analysis of Response Frequencies of Coupled Torsional-Lateral Vibrations.....49

4.5 Input Test Data and Results.....50

4.6 Part II – Response Analysis of the Coupled Torsional-Lateral Vibrations at Natural Frequencies of the Rotor.....54

4.7 Conclusions.....57

Chapter 5

Analysis of Experimental Data.....60

Chapter 6

Conclusions and Recommendations.....73

Bibliography.....77

Appendix – A.....80

Appendix – B1.....92

Appendix – B2.....108

Appendix – C1.....120

Appendix – C2.....123

Appendix – D2.....125

List of Tables

Table 4.1.....53

Table 4.2.....55

Table 4.3.....57

List of Figures

Figure 1.1 : Imbalance rotating disk.....2

Figure 1.2 : Forces on an imbalance disk.....3

Figure 3.1 : Eccentric disk mounted on a mass-less shaft.....26

Figure 3.2 : Single disk rotor supported on a rigid bearing.....27

Figure 3.3 : Single disk rotor coordinate system.....27

Figure 3.4 : Disk center motion.....33

Figure 3.5 : Polar and Cartesian coordinates.....34

Figure 4.1 : Two eccentric disks mounted on a mass-less shaft.....37

Figure 4.2 : Axis of rotation of two disk rotor system.....38

Figure 4.3 : Cartesian coordinates of two-disk rotor system.....38

Figure 4.4 : Generalized coordinates and dimensions of two disk rotor system.39

List of Plots

Plot 4.1 : Frequency response function.....56

Plot 4.2 : Frequency response function.....59

Plot 5.1 : Detail waveform plot of torsional oscillations.....65

Plot 5.2 : Cascade plot of torsional oscillations.....66

Plot 5.3 : Cascade plot of lateral vibrations.....67

Plot 5.4 : Detail waveform plot of lateral vibration.....68

Plot 5.5 : Dimensional details of pump rotor.....69

Plot 5.6 : First bending mode of pump rotor.....70

Plot 5.7 : Second bending mode of pump rotor.....71

Plot 5.8 : Third flexing mode of pump rotor.....72

Plots A1-A10 : Time Waveforms and Spectra.. .....83 - 91

Plots B1.1-B1.13 : Time Waveforms and Spectra.. ..... .95- 108

Plots B2.1-B2.9 : Time Waveforms and Spectra.....111- 119

CHAPTER 1

INTRODUCTION

The phenomenon of coupling between torsional and lateral vibrations in rotor disk assemblies is described in this chapter. The factors that cause the coupling between the two vibration modes, and the reason for their presence for all configurations of the systems are explained. The differences between the couplings in linear and nonlinear systems are also discussed in the chapter.

Figure 1.1 shows a configuration of a single disk rotor system. A mass-less shaft with a disk at the center is supported on two rigid bearings. The center of the mass of the disk 'm' is offset by eccentricity 'e'.

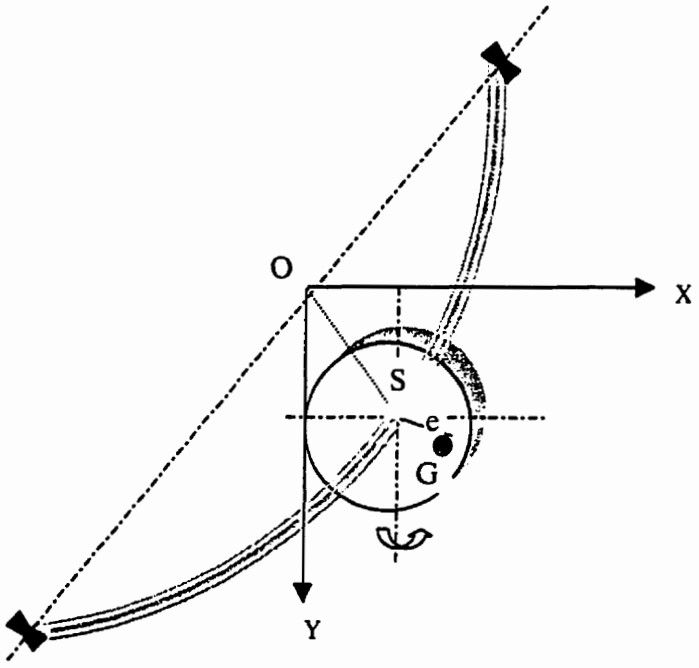

Figure 1.1: Imbalance rotating disk

When the rotor is rotated at a speed of ω_r the mass at eccentricity '*e*' will produce a centrifugal imbalance force on the shaft of magnitude $me\omega_r^2$. This rotating imbalance force will cause the shaft to bend and whirl around the axis of bearing centers. If the vibrations of the shaft are measured in terms of the lateral displacement coordinates X and Y, we will see that the shaft is responding harmonically in the X and Y directions, and the oscillations occur at the frequency of the rotational speed ω_r of the shaft.

If an external oscillatory torque is applied to the rotor, while the shaft is rotating, a torsional oscillation will be superimposed on the rotation of the system. These torsional oscillations will be in addition to the lateral vibration of the system, due to imbalance of the rotor. The torsional oscillations will occur at the same frequency as the oscillatory

torque ω_t, while the lateral vibration occurs at the rotating speed of the shaft assembly at ω_r.

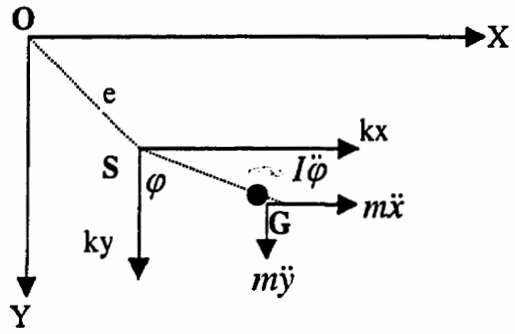

Figure 1.2: Forces on an imbalance disk

Figure 1.2 shows a diagram of forces acting on the shaft and on the center of gravity of the disk. The center of the shaft is at point 'S' and 'O' is the equilibrium point where the center of the shaft lies when the rotor is not rotating. The center of gravity of the disk is at point 'G'. The spring forces *kx* and *ky* are generated due to the bending of the shaft, and $m\ddot{x}$ and $m\ddot{y}$ are the inertia forces due to the lateral motion of the eccentric mass. The angular moment of inertia of the center of gravity of the disk is $I\ddot{\varphi}$.

The torsional oscillations of the disk will cause the eccentric mass to oscillate with angular motion, around the center axis of the shaft. This results in torsional inertia forces on the disk, which will couple with the lateral dynamic forces acting on the shaft. This produces the coupled torsional/lateral vibration of the system. When the forces are coupled the motions associated with the forces, namely torsional and lateral motions, also become coupled, i.e. they interact with each other.

The overall set of equations describing the system becomes coupled and nonlinear.

Because of the coupling, the torsional vibration interacts with the lateral vibration of the system. In the above example, when an oscillatory torque is applied to the rotor, a torsional vibration occurs, and induces a lateral vibration on the rotor assembly. This vibration is in addition to the lateral vibration due to imbalance of the eccentric mass. The frequency of the torsionally induced vibrations will be different from that caused by the imbalance excited vibrations of the system. In a simple way we could state that the lateral vibrations are affected by the torsional oscillations occurring in the system.

As it is known in linear vibrations a set of coupled equations of motion can be uncoupled by a set of principal coordinates, and there is at least one set of principal coordinates for every linear system. The principal coordinates are found by using the orthogonality properties of linear systems. The system characteristics and properties are not affected by using the principal coordinates to define the system. Thus in a linear system the existence of a coupling merely depends on the selection of coordinates to define the system and the coupling is not an inherent property of the system.

In contrast to linear systems, the orthogonality properties do not apply to nonlinear systems. In a nonlinear system, a set of principal coordinates cannot be found to decouple the equations of motion. Thus in a coupled nonlinear system, for all sets of generalized coordinates, the equations of motion will always remain coupled.

Summarizing the above facts we could state the following.

In rotor assemblies where mass imbalances are present, the torsional and lateral vibrations are coupled and the systems are nonlinear. The torsional vibrations interact with the lateral vibrations in the system. When torsional vibrations are present they induce lateral vibrations in the system. Similarly the lateral vibrations induce torsional vibrations in the system. In other words, we could state that lateral vibration will occur in response to a torsional vibration in the system, and a torsional vibration will occur in response to a lateral vibration in the system. No matter how the coordinates are selected to define the configuration of a system the coupling between lateral and torsional vibrations will remain in the system.

As it is seen from the above example both the coupling and the nonlinear properties of the system are induced by the eccentricity 'e' of the unbalanced mass, which is a physical property of the system. In an ideal case, if there is no imbalance, where eccentricity 'e=0', the factors that cause the coupling and the non-linearity in the system are eliminated. In this case the equations of motion for torsional and lateral vibrations can be solved independently.

1.1 NEED FOR THE STUDY AND ITS RELEVENCE TO THE INDUSTRY

Concerns over coupled torsional/lateral vibrations are not new. Their existence, and their frequency response characteristics have often been a concern of vibration analysts and engineers. Typical questions that required answering were:

i. At what frequencies do the coupled torsional-lateral vibrations occur?

ii. How significant is their response?

iii. What are the properties that influence this coupling?

The needs for this project and its application to industry problems are presented in this section. The objectives of the study are outlined in section 1.2.

1.2.1 Because of the fact that some degree of imbalance exists in every rotor, we could state that torsional and lateral vibrations in all rotors are coupled. Thus in rotor dynamics it is important to consider that the lateral and torsional vibrations are interacting with each other.

During engineering design studies, when carrying out response analysis of rotors, or when performing vibration analysis in machines, it was and is often considered that the coupling between torsional and lateral vibrations are weakly non-linear, and thus they have no significant effect on the response characteristics of the system. Because of these assumptions their existence was ignored, and the response analyses of torsional and lateral vibrations were performed independently. It was considered that the torsional vibrations are due to torsional

oscillatory forces only and the lateral vibrations are due to lateral oscillatory forces only. Interaction between the two vibration modes, or one vibration inducing an oscillation in the other coupled mode was never considered a possibility. Nevertheless, when unexplainable peaks occurred, in torsional or lateral vibration spectra, the possibility of torsional vibrations translating into lateral modes or lateral vibrations translating into torsional modes are often suspected.

In the past, vibration analysts and application engineers did not have sufficient knowledge and information with regard to the response frequencies and the characteristics of coupled torsional-lateral vibrations in rotor systems. Hence, when unknown peaks appeared in the frequency spectra, they considered the idea of coupled torsional-lateral vibrations causing the peaks. However, lack of in-depth knowledge and understanding of coupled torsional-lateral vibration left many questions unanswered.

Questions which have been raised in the past with regard to their existence are:

i. Can torsional vibrations transform into lateral modes and what will be their frequency response characteristics?

ii. Similarly, can the lateral vibrations transform into torsional modes and what will be their frequency response characteristics?

ii. Can the coupled torsional-lateral vibrations excite the systems at their natural frequencies?

iv. Can torsional vibration be detected from measurements that are made in lateral directions?

It is envisaged that a study of coupled torsional vibrations will answer these questions and assist the vibration analysts and application engineers in gaining an in-depth knowledge of the subject. It will also aid in developing design considerations to avoid occurrence of the coupled torsional - lateral vibrations in rotor assemblies.

1.2.2 As explained in the Introduction of this Chapter and also proved in Chapter 7, the coupling between the torsional and lateral vibrations in rotor assemblies are due to the eccentricity 'e' of the imbalance mass, which is a physical property of the system. Thus when designing rotors it is always possible to specify tolerances to minimize the imbalance and avoid occurrence of this coupling. This project will stress on the importance of specifying these tolerances, particular in rotors where both torsional and lateral vibrations are expected.

1.2.3 One of the main objectives of this study is to find the magnitudes of the coupled torsional - lateral vibrations in rotor systems and to investigate their frequency dependence. The purpose is also to investigate their significance.

There are many commercially available programs that perform rotor dynamic analyses. In all of these programs the response analyses of lateral and torsional

vibrations are performed independently. The coupled equations of motions are not included in their analyses. The main reason for this is that non-linearity induced due to the coupling makes the solving of equations difficult, in particular with large rotors consisting of many elements. Often equation solvers using numerical analysis methods have to be used to solve these equations.

This project will demonstrate the fact that although the coupling between torsional and lateral vibrations in rotor assemblies is weak, the coupled torsional - lateral vibrations can excite the rotors at their natural frequencies, and increase the vibrations to excessive levels. It will be demonstrated that especially when performing response analyses on rotors, particularly those subjected to both torsional and lateral vibrations, the effects of coupled torsional - lateral vibrations should also be investigated.

1.3.4 Since overall process control, full capacity utilization, high efficiency and energy savings have become major concerns in industry, machinery manufacturers have been compelled to develop advanced complex machinery to cater to their customer's needs. A large number of complex machines, capable of performing many different tasks while operating in a wide range of speeds and operating conditions have been developed. In their operating processes they generate a wide range of forces, including torsional and lateral. They undergo a wide change of forces and operate through a broad range of speeds. These forces often excite the rotors at their natural frequencies.

In the past the torsional and lateral vibrations were analyzed independently. The information and knowledge we had in regard to vibration forces and responses in systems were limited. However, now it has become important to know all the forces and responses occurring in the systems and relate these responses to the corresponding forces in the system.

1.2 Objectives

The principal objective of this study is to analyze the coupling between torsional and lateral vibrations in rotor shaft assemblies. Several studies on this subject have shown that a weak nonlinear coupling could exist between these vibration modes. In this analysis we investigate the parameters that influence the coupling between torsional and lateral vibrations, find the frequency response behavior of the coupled torsional and lateral vibrations, how they could be identified and how their effects could be minimized.

This project will investigate the following

1. When do torsional oscillations affect the lateral vibrations?
2. What parameters affect the coupling between torsional and lateral vibrations?
3. What are the response frequencies of coupled torsional-lateral vibrations in lateral modes?
4. What is the response frequency of torsional vibration induced due to imbalance forces on rotors?
5. Will the coupled torsional-lateral vibrations excite rotors at their natural frequencies?

The second objective of the study is to be able to recommend measures to minimize the effect of coupled torsional and lateral vibrations when designing rotors, and also to show how to identify their occurrence when analyzing the vibrations.

CHAPTER 2

STATE OF THE ART AND REVIEW OF BACKGROUND MATERIAL

This chapter presents a brief review of the literature related and relevant to the subject of this project. The phenomenon of coupling in vibrations, coupled torsional-lateral vibrations in particular, and its applications to various engineering problems are discussed in the chapter.

The use of the word coupling in mechanical vibrations is widely varied. The term static couplings, velocity couplings, dynamic couplings, coupled coordinates, coupled modes and coupled masses are widely used in vibration practice. In many texts the word coupling has been used to describe connection between equations of motion, and in general the term is used to describe interconnection between events, referred to as coupled events. The coupling has been introduced as a phenomenon as a result of some

physical properties of the system or due to selection of coordinates to describe the system.

Until Mahalingam and Bishop (1974) showed that any linear system can be decoupled by using orthogonal properties, the coupling was regarded as a phenomenon due to physical properties of a system. However, once it came to light that a set of principal coordinates exist for every linear system and any linear system can be decoupled by these coordinates, the coupling in a linear system came to known as a existence of connection between motion due to the selection of the system of coordinates, but not an inherent property of the system.

Nevertheless, as already mentioned in the previous chapter the orthogonal properties do not apply to nonlinear systems and thus principal coordinates are not found to decouple these systems. In a nonlinear system the coupling is a phenomenon associated with the physical properties of the system, and no matter how the coordinates are selected the coupled modes remain in the system.

Coupling can exist between lateral vibration modes, torsional vibration modes or between torsional and lateral vibration modes. This study is focussed on the coupling between torsional and lateral vibration modes, particular in application to rotor dynamic systems. Thus the coupling in other modes are not discussed in this chapter.

Coupled flexural-torsional vibrations were applied to non symmetrical beams and presented by Timoshenko and Weaver (1989). A large number of studies have been performed in the past with regard to this and many papers have been published including vibrations of bridges. Since this project deals with coupled torsional-lateral vibrations in rotors the studies done on beams and structures are not discussed herein.

The effects of coupled torsional-lateral vibrations have been largely studied in geared rotor systems. In an experimental study of gearbox vibrations Mitchell and Mellen (1975) found that due to a cross coupling effect lateral vibrations of one remote shaft was transmitted to another shaft in a gear coupled system. However, when trying to analyze the data through a mathematical model based on an uncoupled system they failed to provide an irrefutable physical interpretation of real phenomena. They hypothesized the possibility of a coupled torsional-lateral vibration effecting the gear system, and stated that a complete study of a coupled torsional-lateral eigenvalues, eigenvector and response analysis of gears should be done to understand this system. They warned the equipment users that until a complete coupled torsional-lateral analysis technique is developed that they should critically review their applications of turbo-machinery when they are experiencing unexplainable high vibration peaks on shafts or suspect of being transmitted and amplified from other remote shafts in gear coupled systems.

Subsequent to the presentation of Mitchell and Mellen (1975), Iida and Tamura (1978) investigated the coupled torsional-flexural vibrations of a spur gear system. Although, noise and vibrations in spur gear systems had been a problem of concern in the past, and

investigations have been carried out prior to these studies, in all those studies the lateral and torsional responses were treated as uncoupled and the shafts were considered as rigid. In their study Iida and Tamura (1978) concentrated on free and forced vibrations in the spur geared system by taking into consideration that the flexural and torsional vibrations are coupled, and the gear wheels are geometrically eccentric and the wheels are unbalanced.

The model considered was a single set of spur gear system connected to a motor driving a dynamo. The nonlinear coupled equations of motion of the system were analyzed numerically, and the eigenvalues and eigenvectors were developed. The model considered both meshed and unmeshed conditions. Unmeshed condition refers to calculating the eigenvalues and eigenvectors for each shaft independently. The results revealed that the critical speeds in the case of a meshed gear system is different from that of the unmeshed system, and this is affected by the coupled torsional-flexural vibrations under meshed condition of the gears. The study concluded that in a system where gears are mounted on a flexible shaft, the torsional and flexural vibrations are coupled and the coupling affects the natural frequencies of the system.

In a NASA publication Wachel and Szenazi (1980) describe a field experience of an unstable lateral vibration occurring together with torsional oscillations in a geared rotor system. In this paper the authors did not describe the coupling mechanism, but pointed out the possibility of a coupled torsional-lateral vibration affecting the rotor dynamics of the system.

The previous model was based on a single pair spur gear system. The authors, Iida and Tamura (1984) extended their studies to analyze the dynamic characteristics of a two pair gear system. The equations of motion for flexural vibrations coupled with torsional vibrations of the shaft were derived and numerically analyzed for this system. The study concluded that the natural frequencies and mode shapes of a system which contain counter shafts are affected by the mesh angle and the coupled torsional-lateral vibration forces in the system.

In the past, when performing stability analyses of rotors only the lateral responses of the system were considered, and affects of torsional oscillations were not accounted in the calculations. Even in geared rotors the lateral vibrations and stability analyses of both shafts were carried out separately and independently. However, particular in the geared systems, the torsional and lateral vibrations of both rotors are coupled by gears. After it became clear that in geared rotor systems the dynamic characteristics of rotors are affected by coupled torsional-lateral vibrations, and also field experience indicated that torsional oscillations caused instability in lateral vibrations in a geared rotor system, a study of stability behavior of rotors due to coupled torsional-lateral vibrations became important.

The influence of torsional-lateral coupling on stability behavior of geared rotor systems were investigated by Schwibinger and Nordmann (1987). In their model a gas turbine driving a generator through a spur gear was considered.

In gear systems a strong torsional-lateral coupling exists naturally due to the mechanism of power transmission. The torsional moments fed into the gears are transmitted through the tooth forces and transverse forces and bending moments are resulted. In addition, provided that both wheels maintain contact during operation, the torsional and lateral displacements of the gear wheels are coupled kinematically. Because the torsional and bending displacements are coupled in the gears, the torsional oscillations of the gear rotors are excited by the lateral motion and vice versa. It is clear from this consideration that the stability behavior is affected by this energy exchange between the torsional and the lateral motions in the system.

In the first part of their study Schwibinger and Nordmann (1987) concluded results similar to those of Iida and Tamura (1975), where eigenfrequencies are effected by the coupled torsional-lateral vibrations in gears. They considered oil film bearings in their model when compared to knife-edge bearing supports considered in the initial model by Iida and Tamura (1975) and found that the eigenfrequencies varied with the speed. The changes in the natural frequencies between coupled and uncoupled modes of torsional and lateral vibrations were in the range of 5% to 15%. In some modes the eigenfrequencies changed only little and they almost coincided with solutions of the rigidly supported system. Nevertheless, in some other modes, for coupled and uncoupled torsional-lateral systems, the eigenfrequencies differed substantially. Particularly the second eigenfrequency of the coupled system was about 15% lower than that of the uncoupled system.

The coupling between torsional and lateral not only affects the eigenfrequencies and modes, but also affects the damping constants and the stability threshold speed of the rotors. As learned in classical rotor dynamic analysis in the uncoupled systems all the damping constants for bending modes are positive up to the threshold speed, and beyond the threshold speed they become negative and the rotor gets unstable. Threshold speed is referred to as the speed the rotor become unstable. However, if the damping constant becomes negative at a lower speed, because of the coupled torsional-lateral vibrations, one could expect that the rotor becomes unstable at a much lower speed than predicted, through uncoupled vibration modes. Thus it is important to know that the instability onset speed of coupled and uncoupled torsional-lateral systems are not the same. The coupling mechanism in gears may essentially lower the threshold speed of the system. Instability of the rotor will occur at a lower speed than anticipated.

If the torsional and bending vibrations are considered coupled in gears, the eigenvalues will be sensitive to torsional and bending parameters of the shafts. The effect of coupling on the stability of geared rotor systems can therefore be studied by concentrating on the following.

- How do modifications of torsional and bending system parameters change the stability threshold in geared rotor systems ?
- How do changes of torsional and bending system parameters affect the damping constants and the eigenvalues?

In the second part of their analysis Schwibinger and Nordmann (1987) studied the stability behavior of the geared rotor system, considering that the torsional and lateral vibrations are coupled. This included the stability and sensitivity analysis of a coupled geared rotor system. Their model revealed that the stability behavior is influenced by the bending parameters of one shaft and the torsional parameters of the other. Through this model they showed that ignoring the coupling between torsional and lateral modes of gears may lead to serious errors, especially in predictions of stability onset speed, critical speeds and the natural modes. The difference in solutions between coupled and uncoupled modes indicated that the torsional-lateral coupling must not be neglected when analyzing stability behavior of geared rotors. Since the results and predictions of this investigation were based on a theoretical model of a geared rotor system, verification of analytical results through an experimental analysis became apparent.

Although, it was known that a coupling between torsional and lateral vibrations can exist in rotors, they were always considered as weakly nonlinear. This in particular was due to very low imbalance and torsional forces exciting in the rotor systems. However, Vandenput and Belmans (1985) showed that in induction motors large torsional forces could occur due to voltage faults, short circuits, starting and braking torque disturbances. Such high torsional forces coupled with lateral vibrations in imbalance rotors can produce high coupled torsional vibrations in the systems. The influence of torsional vibrations on lateral oscillations of induction motor rotors were presented by Vandenput, Geysen and Belmans (1985).

The model considered was a single rotor system supported on knife-edge bearings. The rotor with mass imbalance was excited with external torque. The three degrees of freedom system involved with coupled torsional-lateral vibrations was solved by a small parameter technique. The analysis revealed that the torsional vibration will induce a vibration in the lateral mode and modulate the lateral vibration due to imbalance of the rotor. The coupled torsional vibration will occur at a frequency equal to imbalance excited frequency $\pm$ torsional excited frequency of the system. This finding was demonstrated with a prototype experimental model.

The problem of dynamic gear tooth loading has mainly been treated in the past as one of the purely rotational or torsional vibrations. After the investigations of dynamic characteristics and stability behavior of geared rotor systems, influenced by torsional and lateral coupling, the study of dynamic loading of gears due to coupled torsional-lateral vibrations became of interest. Dynamic gear tooth loading due to coupled torsional-lateral vibration in a geared rotor hydrodynamic bearing system was studied by Kishor and Gupta (1989). The study revealed that the coupled torsional-lateral vibrations affect the dynamic loading of gear teeth as well as bearing oil film. The journal vibration amplitudes and frequency are dependent of the amplitude and frequency of the gear excitation forces.

In the previous studies of gear vibrations the response frequency of the coupled torsional-lateral vibration was never emphasized. The author's experience in vibrations of gears has always shown modulation of tooth mesh frequency at the rotational frequencies of

drive or driven shafts. However, with the evidence of coupled torsional-lateral vibration and their influence on gears unveils the fact that these modulated frequencies are due to the coupling between torsional and lateral vibrations present in them.

Subsequent to the studies on the influence of coupled torsional-lateral vibrations in gears many studies were performed to improve the gear modeling accuracy. With respect to this an improved branch method for gear-coupled systems was presented by Kuang and Tsai (1991). *Multi-frequency transfer matrix method and branch transfer matrix* technique were applied to analyze the system. The model considered the coupling effects of lateral and torsional vibrations, wobble angle and unbalance of disks, the mass of the shaft, bearing and constant mesh stiffness.

The dynamic behavior of a geared rotor bearing system with coupled torsional-lateral motion was later investigated using a Hybrid Method, which is a combination of finite element and generalized polynomial expansion method. "A study on the dynamic characteristics of geared rotor-bearing system with hybrid method" was presented by Nelson and Chang (1994). This analysis method provided higher computational efficiency than any other method used without any loss of accuracy. The conclusions in the study were similar to those in the previous investigations, where gear mesh parameters significantly affected the system dynamic behavior especially when torsional-lateral coupling was considered in the system.

Current rotor dynamic analysis tools treat the lateral deformation associated with shaft bending and torsional deformation associated with shaft twisting, but they are statically and dynamically decoupled systems. On the other hand, studies of dynamics of geared systems are usually focused on the torsional vibration aspects only. Although this is a justifiable assumption in many applications, requirements for higher operating speed, higher power transmission and lighter geared rotor-bearing systems have resulted in cases where the coupling between torsional and lateral vibrations are of important consideration. Ignoring this coupling has led to inaccurate and misleading dynamic predictions.

Since the influence of coupled torsional-lateral vibrations on dynamic characteristics of geared shafts were brought to light many investigations were carried out to find the effect of this coupling on various gear systems. Some of the models already investigated are gear shafts supported on knife-edge type bearings and on hydrodynamic bearing. Subsequent to these studies the effect of coupled torsional lateral vibrations on a gear-pair system supported by squeeze film dampers were investigated and presented by Nelson and Natsiavas (1993). A model of a single pair gear system supported by Squeeze Film Dampers was excited by mass unbalance and external torque. The major objective of this study was to provide a better understanding of coupled torsional-lateral vibrations of geared shafts supported by squeeze film dampers. The model confirmed that the gear mesh stiffness substantially influenced the natural frequencies and modes of the system and the mesh damping reduced the amplitude of vibrations on both torsional and lateral modes. The results with and without the mesh coupling showed a substantial

difference in readings. The squeeze film dampers lowered the amplitudes of system response while the non-linearity introduced from squeeze film dampers resulted in irregular aperiodic response of the system.

The effects of coupled torsional-lateral vibrations on geared rotors were broadly analyzed mainly because they at large influence the dynamic characteristics of gears. The meshing causes the torsional oscillations to be coupled with the lateral vibrations in the gear system.

2.1 Chapter Summary

Although a number of studies were done with the focus on the influence of coupled torsional-lateral vibrations on gears, only few have been performed to analyze the effect of this vibration on rotor disk assemblies. This was due to the fact that high torsional forces were never experienced in the past in high speed centrifugal machines, and also the coupled torsional-lateral vibrations were thought as weakly nonlinear. This project is an extension of the previous study done by Belmans and Vanderput (1985) mentioned on page 19. The model was extended to analyze the response behavior of a two-disk rotor system, and the analytical data were compared with experimental field data on a motor pump assembly. Unlike the gear systems, the dynamic characteristics such as eigenvalues and eigenvectors are not significantly changed in rotor disk assemblies. However, the presence of mass imbalance can cause coupled torsional-lateral vibrations of rotors and excite them at the lateral natural frequencies of the system.

Chapter 3

Analysis Model 1 – Single Disk Rotor System

To analyze the effects of coupled torsional-lateral vibrations in rotor disk assemblies two rotor models were examined in this project. The first model is of a single disk rotor assembly, symmetrically supported on a pair of rigid bearings. The derivation of the equations of motion of the system, lateral response at steady speed and torque, and torsional oscillations due to mass imbalance in the disk are presented in this chapter.

Figure 3.1 shows the sketch of the rotor disk assembly. A rigid disk mounted on a uniform mass-less shaft mounted on two rigid bearings is shown in the sketch. The center of mass of the disk is offset by eccentricity 'e' from its geometric centroid (spin axis of the shaft). The system is defined by two Cartesian coordinates and one angular coordinate. Thus it has three degrees of freedom.

The three equations of motion of the system were derived by using Lagrangian dynamics method. These equations of motion, shown on Page 31, are coupled and nonlinear.

The lateral response of the system when the disk is subjected to constant torque and constant speed are analyzed in Section 3.3. Finally the torsional oscillations due to mass imbalance are shown.

3.1 Lagrange's Equation

Lagrange's equation, in its fundamental form for generalized coordinates q_i, is

$$\frac{d}{dt}\frac{\partial(K.E.)}{\partial \dot{q}_i} - \frac{\partial(K.E.)}{\partial q_i} + \frac{\partial(P.E.)}{\partial q_i} + \frac{\partial(D.E.)}{\partial \dot{q}_i} = Q_i$$

Where K.E. = Kinetic Energy of the system

P.E. = Potential Energy of the system

D.E. = Dissipation Energy of the system

Q_i = Generalized external force acting on the system

For a conservative system, Lagrange's equation can be written as

$$\frac{d}{dt}\frac{\partial L}{\partial \dot{q}_i} - \frac{\partial L}{\partial q_i} = 0$$

Where L = K.E. – P.E. is called the Lagrangian

Lagrange's equation can be applied to any number of equations involving many degrees of freedom in a system when the basic energy expressions containing the kinetic and potential energy of the systems are known.

3.2 Model 1 - Single Disk Rotor System

Assumption: Stiffness in directions X and Y are the same.

Rotor eccentricity weight = G = mg

Damping in directions X and Y are the same.

Bearings are rigid.

Figure 3.1: Eccentric disk mounted on a mass-less shaft

The rotor is eccentric. Center of mass of the rotor is at distance 'e' from the center of rotation of the shaft. The rotor rotates around the center of the shaft with the center of mass displaced by 'e' while the shaft whirls.

Motion of the rotor as a three-degrees-of-freedom system is considered. The location of the center of the rotor and center of the shaft at any particular time can be represented by

three coordinates, two rectilinear and one polar (angular). They are measured in linear directions x', y' and rotation φ, where φ is the angle of rotation of the disk.

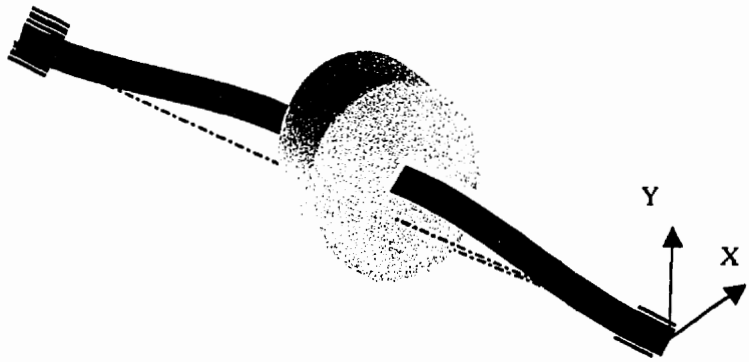

Figure 3.2: Single disk rotor supported on rigid bearings

The three independent coordinates (x', y', φ) are;

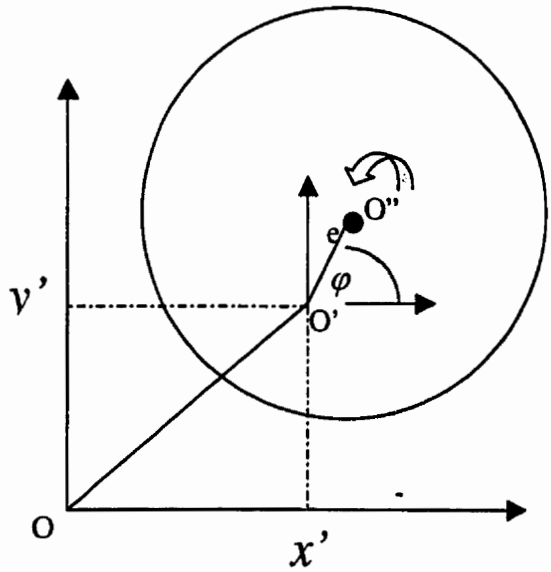

Figure 3.3: Single disk rotor coordinate system

Where O is on the axis of rotation of the shaft, which lies on the line connecting the bearing centers. The point O' is on the center axis of the shaft, and O" is the center of mass of the disk. The disk rotates around center of the shaft O' and the shaft rotates around the O. At any given time the center of the shaft is displaced by x' *and* y' from the point O and the shaft has rotated through the angle φ. The displacement of the center of the mass of the disk from point O in Cartesian coordinates are given by X *and* Y where the values of X *and* Y are given by

$$X = x' + e\,Cos\,\varphi \qquad\qquad Y = y' + e\,Sin\varphi \qquad\qquad (3.0)$$

The displacement of the shaft and displacement of the center of the mass of the disk can be represented by coordinates x', y' *and* φ or coordinates X, Y *and* φ. We can select either of the sets as generalized coordinates in the Lagrange's equation to derive the basic equations of motion to include both the rotational and lateral motions in the system.

In this study the X, Y and φ were selected as the generalized coordinates of the system. The energy equations of the system are written as follows.

Kinetic Energy

$$K.E. = T = \frac{1}{2} m(\dot{X}^2 + \dot{Y}^2) + \frac{1}{2} I\dot{\varphi}^2 \cdots\cdots\cdots\cdots (3.1)$$

Potential Energy

$$P.E. = \Pi = \frac{1}{2} kx'^2 + \frac{1}{2} ky'^2 + mgY \cdots\cdots\cdots\cdots (3.2)$$

Dissipation of Energy

$$D.E = \nabla = \frac{1}{2}c\dot{x}'^2 + \frac{1}{2}c\dot{y}'^2 \cdots\cdots\cdots\cdots (3.3)$$

Lagrange's equation is applied for generalized coordinates X, Y and φ

$$\frac{d}{dt}\frac{\partial(K.E.)}{\partial \dot{q}_i} - \frac{\partial(K.E.)}{\partial q_i} + \frac{\partial(P.E.)}{\partial q_i} + \frac{\partial(D.E.)}{\partial \dot{q}_i} = Q_i$$

Q_i = Applied Torque – Resistance Torque = Γ

Lagrange's equation for the X coordinate can be written as

$$\frac{d}{dt}\frac{\partial(T)}{\partial \dot{X}} - \frac{\partial(T)}{\partial X} + \frac{\partial(\Pi)}{\partial X} + \frac{\partial(\nabla)}{\partial \dot{X}} = 0 \cdots\cdots\cdots\cdots\cdots\cdots (3.4)$$

Using Eq. *(3.1)* for Kinetic Energy

$$\frac{d}{dt}\left(\frac{\partial T}{\partial \dot{X}}\right) = m\ddot{X} \quad and \quad \frac{\partial T}{\partial X} = 0 \cdots\cdots\cdots\cdots (3.5)$$

Using Eq. *(3.2)* for the Potential Energy

$$\frac{\partial \Pi}{\partial x'} = \frac{1}{2}k.2x' \quad and \frac{\partial x'}{\partial X} = 1$$

$$\frac{\partial \Pi}{\partial X} = \frac{\partial \Pi}{\partial x'}\frac{\partial x'}{\partial X}$$

$$\therefore \frac{\partial \Pi}{\partial X} = kx' \cdots\cdots\cdots\cdots (3.6)$$

Dissipation of Energy

$$\nabla = \frac{1}{2}c\dot{x}'^2 + \frac{1}{2}c\dot{y}'^2 \quad and\ x' = X - eCos\varphi$$

$$\frac{\partial \nabla}{\partial \dot{x}'} = \frac{1}{2}c.2\dot{x}' \quad and\ \frac{\partial \dot{x}'}{\partial \dot{X}} = 1$$

$$\frac{\partial \nabla}{\partial \dot{X}} = \frac{\partial \nabla}{\partial \dot{x}'}\frac{\partial \dot{x}'}{\partial \dot{X}} = c\dot{x}' \cdots\cdots\cdots\cdots (3.7)$$

Substituting Eqs. *(3.5), (3.6)* and *(3.7)* in Lagrange's Eq. *(3.4)* for *X* coordinates

The equation of motion for the *X* direction

$$m\ddot{X} + c\dot{x}' + kx' = 0 \cdots\cdots (3.8)$$

Since $X = x' + e.Cos\varphi$

$$\dot{X} = \dot{x}' - e.Sin\varphi.\dot{\varphi}$$

$$\ddot{X} = \ddot{x}' - e.Cos\varphi.\dot{\varphi}^2 - e.Sin\varphi.\ddot{\varphi}$$

Substituting in Eq. *(3.8)*

$$m\ddot{x}' + c\dot{x}' + kx' = me\dot{\varphi}^2 Cos\varphi + me\ddot{\varphi}\, Sin\varphi \cdots\cdots\cdots (3.9)$$

Similarly the Lagrange's equation for '*Y*' coordinate is

$$m\ddot{y}' + c\dot{y}' + ky' + mg = me\dot{\varphi}^2.Sin\varphi - me\ddot{\varphi}.Cos\varphi \cdots\cdots\cdots\cdots (3.10)$$

and the Lagrange's equation for coordinate φ is given by

$$I\ddot{\varphi} + kex' Sin\varphi - key' Cos\varphi + ce\dot{x}' Sin\varphi - ce\dot{y}' Cos\varphi = \Gamma \cdots\cdots\cdots\cdots (3.11)$$

The three equations of motion derived in *(3.9), (3.10)* and *(3.11)* can be written in the form

$$m\ddot{x}'+c\dot{x}'+kx' = me\dot{\varphi}^2 Cos\varphi + me\ddot{\varphi} Sin\varphi \cdots\cdots\cdots (3.9)$$

$$m\ddot{y}'+c\dot{y}'+ky'+mg = me\dot{\varphi}^2 . Sin\varphi - me\ddot{\varphi} . Cos\varphi \cdots\cdots (3.10)$$

$$I\ddot{\varphi} + (kx'+c\dot{x}')e Sin\varphi - (ky'+c\dot{y}')e Cos\varphi = \Gamma \cdots\cdots\cdots\cdots\cdots\cdots (3.11)$$

The equations are coupled and non-linear. If a time variation of angle $\varphi(t)$ were known a simple equation could be obtained. As it is seen, the coupling and the nonlinear term are due to the eccentricity 'e' of the disk.

3.3 Lateral Response

In the case of constant angular velocity $\dot{\varphi} = \Omega$ (= constant) is considered, the Eqs. *(3.9)* and *(3.10)* are reduced to the following ones:

$$m\ddot{x}'+c\dot{x}'+kx' = me\Omega^2 Cos\Omega t \quad \cdots\cdots\cdots (3.12)$$

$$m\ddot{y}'+c\dot{y}'+ky' = me\Omega^2 . Sin\Omega t - mg \cdots\cdots (3.13)$$

This is similar to the case of unbalance excitation applied to the system. The particular solution for this type is given in many texts. (See for example "Mechanical Vibrations" by S.S. Rao Page 146).

The solution of Eqs. *(3.12)* and *(3.13)* is.

$$x'(t) = r\, Cos(\Omega t - \in) \cdots\cdots\cdots\cdots (3.14)$$

$$y'(t) = r\, Sin(\Omega t - \in) - y'_s \cdots\cdots\cdots\cdots (3.15)$$

$$Where \quad r = \frac{me\Omega^2}{\sqrt{(k - m\Omega^2) + (c\Omega)^2}} \cdots\cdots\cdots\cdots (3.16)$$

$$\in = \tan^{-1} \frac{c\Omega}{k - m\Omega^2} \quad and \quad y'_s = \frac{G}{k} \cdots\cdots\cdots\cdots (3.17)$$

The amplitude 'r' describes the bending of the shaft. The term y'_s gives the static displacement of the shaft due to rotor weight. The phase angle $\in$ is due to damping in the system.

The graphical representation of the shaft center motion can be shown as follows.

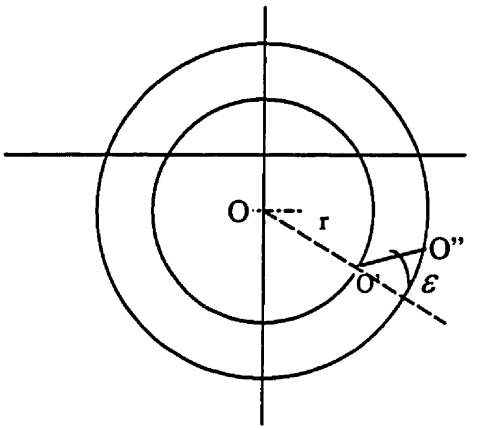

Figure 3.4 : Disk center motion

The shaft center O' is moving with angular velocity Ω in a circle of radius r and center O , the point of static equilibrium. The displacement 'r' and ε remains constant.

Let us introduce a new variable

$$\alpha = \Omega t - \epsilon \cdots\cdots\cdots\cdots (3.18)$$

Then by substituting it in Eqs. *(3.14)* and *(3.15)* we obtain

$$x' = r\,Cos\alpha \cdots\cdots\cdots\cdots (3.19)$$

and

$$y' = r\,Sin\alpha - y'_s \cdots\cdots\cdots (3.20)$$

Now Eqs (*3.12*) & (*3.13*), using x' and y' from Eqs. (*3.19*) and (*3.20*),

can be written in terms of 'r 'and 'α 'coordinates

$$mr\Omega^2\,Cos\alpha + c\Omega r\,Sin\alpha - kr\,Cos\alpha \quad + me\Omega^2\,Cos\Omega t \quad = 0 \cdots\cdots\cdots (3.21)$$

$$mr\Omega^2\,Sin\alpha + c\Omega r\,Cos\alpha - kr\,Sin\alpha + ky'_s + me\Omega^2\,Sin\Omega t - G \quad = 0 \cdots\cdots\cdots (3.22)$$

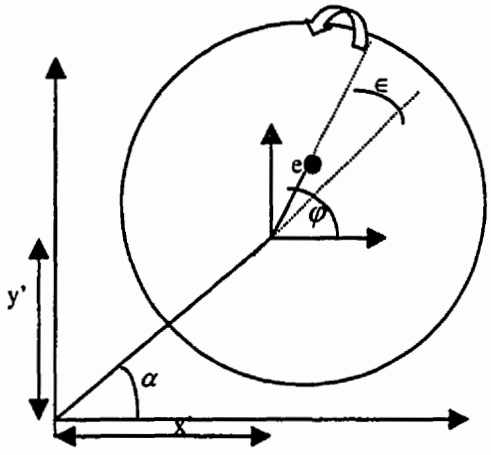

Figure 3.5 : Polar and Cartesian Coordinates

These equations are further simplified by multiplying Eq. *(3.21)* by $Sin\alpha$ and Eq. *(3.22)* by $Cos\alpha$ and then subtracting and summing up the results. The final equations then take the form

$$me\Omega^2 Sin \in = c\Omega r \cdots\cdots (3.23)$$

$$me\Omega^2 Cos \in + mr\Omega^2 = kr \cdots\cdots (3.24)$$

By substituting $x' = r\,Cos\alpha$, and $y' = r\,Sin\alpha - y'_s$ in Eq. *(3.11)* it is obtained

$$kre\,Sin \in - cre\,Cos \in + ky'_s e\,Cos\varphi = \Gamma(t)$$

Recalling that $ky'_s = mg$, and $\varphi = \Omega t$, the latter is reduced to

$$kre\,Sin \in - cre\,Cos \in + mg.e\,Cos(\Omega t) = \Gamma(t) \cdots\cdots\cdots (3.25)$$

In Eq. *(3.25)* the first two terms on the left hand side are constant terms. These constant terms occur due to damping.

If there is no damping $Sin \in$ ***will always be zero.***

The third term on the left hand side is an oscillatory term. This oscillating part originates from the unbalance weight of the disk. For a vertical shaft this term will be zero. For a well balanced rotor with a small eccentricity, the oscillating torque will be very small compared to the driving torque.

Thus required torque consists of to parts; a constant part and a oscillating part with frequency Ω

3.4 Conclusion

A single disk rotor system with an eccentric mass 'm' rotating at frequency Ω generates an unbalance force of $me\Omega^2$. This force causes the system to oscillate in rectilinear directions. In addition to this a torsional forces of magnitude 'mge' oscillating with frequency Ω is generated.

CHAPTER 4

ANALYSIS MODEL II – TWO DISK ROTOR SYSTEM

Analysis of a two-disk rotor model is presented in this Chapter. Two unbalanced disks of masses m_1 and m_2 mounted on a mass-less shaft are considered for this model. The center of masses of the disks are offset by eccentricities e_1 and e_2 from the center axis of the shaft. When the rotor is rotated, as explained in the single disk rotor system, the shaft bends and whirls around the axis of bearing centers. When an external torsional force is applied to a disk, the torsional oscillations of the eccentric mass are coupled with the lateral vibrations of the system and induce a coupled torsional-lateral vibration on the rotor assembly. The two-disk rotor model differs from the single disk rotor model because the relative twist between the two disks causing an additional oscillating torque on the rotor system.

4.1 Two Disk Rotor Model

Figure 4.1 shows the model of the two-disk-rotor system. The disks are fixed on a mass-less shaft supported on two rigid bearings. The center of masses of the disks are offset by eccentricities e_1 and e_2. The system is defined by six independent coordinates. Similar to the single disk rotor assembly, each disk is defined by two Cartesian and one angular coordinate.

Assumptions: Stiffness in both X and Y directions are the same.

The weights of rotors are $G_1=m_1g$ and $G_2=m_2g$

Damping in both directions X and Y are the same.

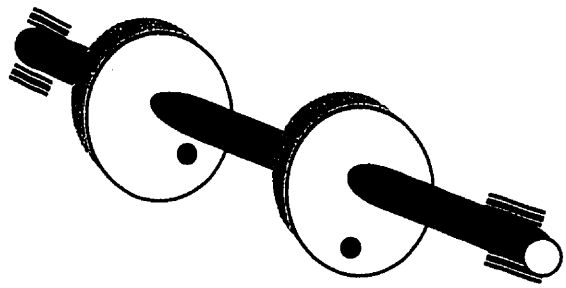

Figure 4.1: Two eccentric disks mounted on a mass less shaft

Figures 4.2 and 4.3 shows the deflection of the shaft and the coordinate systems used for defining the configuration. When the rotor rotates the shaft bends and rotates around the axis of bearing centers. The rectilinear and angular coordinates used for defining the system are described below.

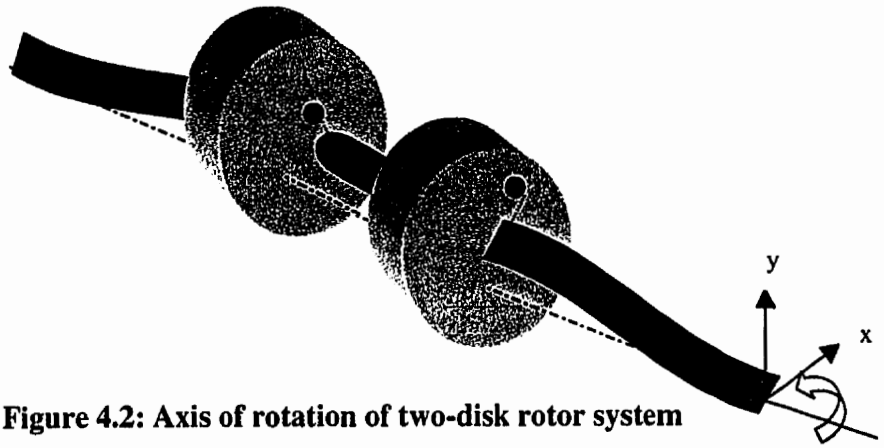

Figure 4.2: Axis of rotation of two-disk rotor system

Generalized Cartesian coordinates considered are as follows.

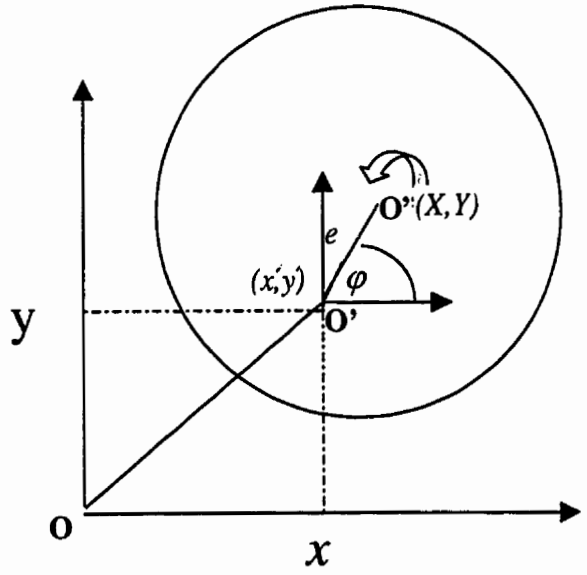

Figure 4.3: Cartesian coordinates of two-disk rotor system

O is the axis of rotation of the shaft, O' is the axis of rotation of the disk, and O" is the mass center of the disk. The coordinates of O' are (x',y') and the coordinates of O" are (X,Y). The angle of rotation of the center of mass of the disk is φ. Considering the Cartesian coordinate system, the generalized coordinates for the two disks can be defined from x'_1, y'_1, φ_1 and x'_2, y'_2, φ_2 or from X_1, Y_1, φ_1 and X_2, Y_2, φ_2 coordinates for disks 1 and 2 respectively.

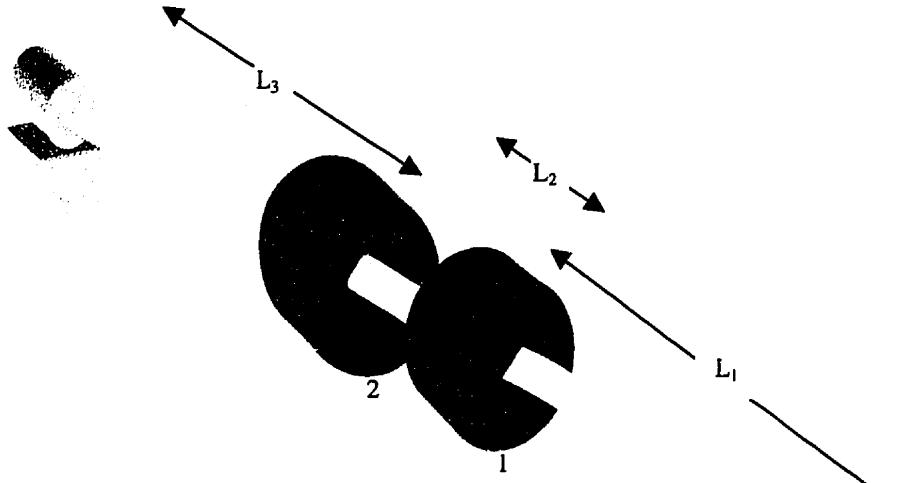

Figure 4.4: **Generalize coordinates and dimensions of two-disk rotor system**

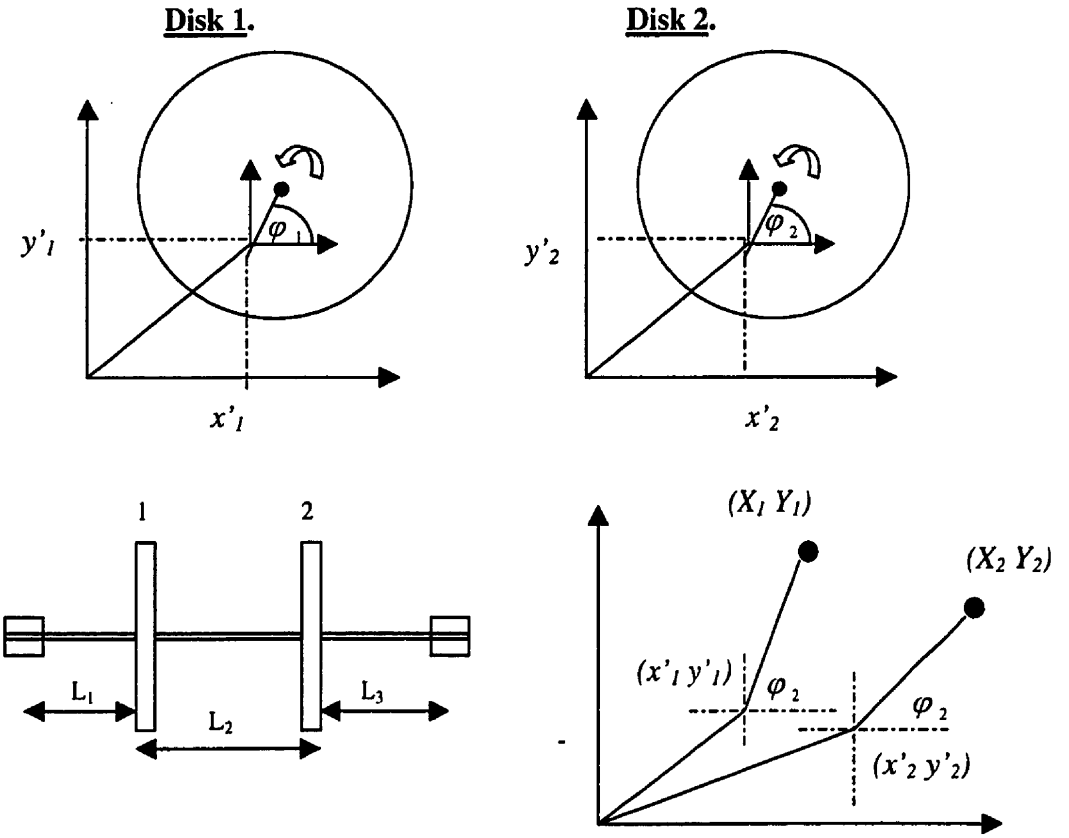

$$X_1 = x'_1 + e_1 Cos\varphi_1 \qquad X_2 = x'_2 + e_2 Cos\varphi_2$$

$$Y_1 = y'_1 + e_1 Sin\varphi_1 \qquad Y_2 = y'_2 + e_2 Sin\varphi_2$$

Applying Lagrange's equation

$$\frac{d}{dt}\frac{\partial(K.E.)}{\partial \dot{q}_i} - \frac{\partial(K.E.)}{\partial q_i} + \frac{\partial(P.E.)}{\partial q_i} + \frac{\partial(D.E.)}{\partial \dot{q}_i} = Q_i$$

Let $T = K.E.$, $\Pi = P.E.$ *and* $\nabla = D.E.$

$\Im$ = *Torsional Siffness of the shaft.*

Lagrange's equation is given by

$$\frac{d}{dt}\left(\frac{\partial T}{\partial \dot{q}_i}\right) - \left(\frac{\partial T}{\partial q_i}\right) + \frac{\partial \Pi}{\partial q_i} + \frac{\partial \nabla}{\partial q_i} = Q_i$$

The motion of the two disks is described in generalized coordinates

X_1, Y_1, φ_1 and X_2, Y_2, φ_2

Kinetic Energy

$$K.E. = T = \frac{1}{2}m_1(\dot{X}_1^2 + \dot{Y}_1^2) + \frac{1}{2}I_1\dot{\varphi}_1^2 + \frac{1}{2}m_2(\dot{X}_2^2 + \dot{Y}_2^2) + \frac{1}{2}I_2\dot{\varphi}_2^2 \cdots\cdots\cdots\cdots (4.1)$$

Potential Energy

$$P.E. = \Pi = \frac{1}{2}F_{1x}x'_1 + \frac{1}{2}F_{1y}y'_1 + m_1gY_1 + \frac{1}{2}F_{2x}x'_2 + \frac{1}{2}F_{2y}y'_2 + m_2gY_2 + \frac{1}{2}\Im(\varphi_2 - \varphi_1)^2 \cdots\cdots\cdots (4.2)$$

The forces associated with shaft displacements are

$$F_{1x} = k_{11}x'_1 + k_{12}x'_2 \cdots\cdots\cdots\cdots (4.3)$$

$$F_{2x} = k_{21}x'_1 + k_{22}x'_2 \cdots\cdots\cdots\cdots (4.4)$$

$$F_{1y} = k_{11}y'_1 + k_{12}y'_2 \cdots\cdots\cdots\cdots (4.5)$$

$$F_{2y} = k_{21}y'_1 + k_{22}y'_2 \cdots\cdots\cdots\cdots (4.6)$$

Where k_{11}, k_{12} etc. are shaft stiffness at corresponding disk locations.

Substitution of Eqs. 3, 4, 5 and 6 in Eq.2 gives

$$\Pi = \frac{1}{2}[k_{11}x'_1+k_{12}x'_2]x'_1+\frac{1}{2}[k_{11}y'_1+k_{12}y'_2]y'_1+m_1gY_1$$

$$+\frac{1}{2}[k_{21}x'_1+k_{22}x'_2]x'_2+\frac{1}{2}[k_{21}y'_1+k_{22}y'_2]y'_2+m_2gY_2+\frac{1}{2}\Im(\varphi_2-\varphi_1)^2 \cdots\cdots\cdots\cdots (4.7)$$

Dissipation Energy

$$D.E. = \nabla = \frac{1}{2}c\dot{x}'^2_1+\frac{1}{2}c\dot{y}'^2_1+\frac{1}{2}c\dot{x}'^2_2+\frac{1}{2}c\dot{y}'^2_2$$

Taking into account that

$$x'_1 = X_1 - e_1 Cos\varphi_1, \quad y'_1 = Y_1 - e_1 Sin\varphi_1$$

and $\quad x'_2 = X_2 - e_2 Cos\varphi_2, \quad y'_2 = Y_2 - e_2 Sin\varphi_2$

we have

$$\dot{x}'_1 = \dot{X}_1 + e_1 Sin\varphi_1.\dot{\varphi}_1, \quad \dot{y}'_1 = \dot{Y}_1 - e_1 Cos\varphi_1.\dot{\varphi}_1 \cdots\cdots\cdots\cdots (4.8)$$

$$\dot{x}'_2 = \dot{X}_2 + e_2 Sin\varphi_2.\dot{\varphi}_2, \quad \dot{y}'_2 = \dot{Y}_2 - e_2 Cos\varphi_2.\dot{\varphi}_2 \cdots\cdots\cdots\cdots (4.9)$$

Solving with respect to x_1 coordinate gives

$$m_1(\ddot{x}'_1 - e_1 Sin\varphi_1.\ddot{\varphi}_1 - e_1 Cos\varphi_1.\dot{\varphi}_1^2) + c\dot{x}'_1 + k_{11}x'_1 + k_{12}x'_2 = 0$$

$$m_1\ddot{x}'_1 + c\dot{x}'_1 + k_{11}x'_1 + k_{12}x'_2 = m_1e_1\ddot{\varphi}_1 Sin\varphi_1 + m_1e_1\dot{\varphi}_1^2 Cos\varphi_1 \cdots\cdots\cdots\cdots (4.10)$$

And the coordinate y'_1 is

$$m_1\ddot{y}'_1+c\dot{y}'_1+k_{11}y'_1+k_{12}y'_2+m_1g=-m_1e_1\ddot{\varphi}_1\,Cos\varphi_1+m_1e_1\dot{\varphi}_1^2\,Sin\varphi_1\cdots\cdots\cdots\cdots\cdots\cdots(4.12)$$

Lagrange' s equation for generalized φ_1 coordinate is given by

$$\frac{d}{dt}(\frac{\partial T}{\partial\dot{\varphi}_1})-\frac{\partial T}{\partial\varphi_1}+\frac{\partial\Pi}{\partial\varphi_1}+\frac{\partial\nabla}{\partial\varphi_1}=\Gamma_1\cdots\cdots\cdots(4.13)$$

Solving with respect to φ_1 coordinate

$$I_1\ddot{\varphi}_1+c\dot{x}'_1e_1Sin\varphi_1-c\dot{y}'_1e_1Cos\varphi_1+k_{11}x'_1e_1Sin\varphi_1$$
$$+k_{12}x'_2e_1Sin\varphi_1-k_{11}y'_1e_1Cos\varphi_1-k_{12}y'_2e_1Cos\varphi_1-\Im(\varphi_2-\varphi_1)=\Gamma_1(t)\cdots\cdots\cdots\cdots(4.14)$$

The equations of motions derived for disk 1 is given in (4.10), (4.12) and (4.14). Similar to these the equations of motions for disk 2 can be written as follows.

For the lateral motion of disk 2

$$m_2\ddot{x}'_2+c\dot{x}'_2+k_{22}x'_2+k_{21}x'_1=m_2e_2\ddot{\varphi}_2\,Sin\varphi_2+m_2e_2\dot{\varphi}_2^2\,Cos\varphi_2\cdots\cdots\cdots\cdots\cdots(4.15)$$

$$m_2\ddot{y}'_2+c\dot{y}'_2+k_{22}y'_2+k_{21}y'_1+m_2g=-m_2e_2\ddot{\varphi}_2\,Cos\varphi_2+m_2e_2\dot{\varphi}_2^2\,Sin\varphi_2\cdots\cdots\cdots\cdots(4.16)$$

For the torsional oscillations of disk 2

$$I_2\ddot{\varphi}_2+c\dot{x}'_2e_2Sin\varphi_2-c\dot{y}'_2e_2Cos\varphi_2+k_{22}x'_2e_2Sin\varphi_2$$
$$+k_{21}x'_1e_2Sin\varphi_2-k_{22}y'_2e_2Cos\varphi_1-k_{21}y'_1e_2Cos\varphi_2+\Im(\varphi_2-\varphi_1)=\Gamma_2(t)\cdots\cdots\cdots\cdots\cdots\cdots(4.17)$$

The six equations of motions for coupled torsional and lateral vibrations of two disk rotor system together below are;

$$m_1\ddot{x}'_1+c\dot{x}'_1+k_{11}x'_1+k_{12}x'_2=m_1e_1\ddot{\varphi}_1\,Sin\varphi_1+m_1e_1\dot{\varphi}_1^2\,Cos\varphi_1\cdots\cdots\cdots\cdots(4.10)$$

$$m_1\ddot{y}'_1+c\dot{y}'_1+k_{11}y'_1+k_{12}y'_2+m_1g=-m_1e_1\ddot{\varphi}_1\,Cos\varphi_1+m_1e_1\dot{\varphi}_1^2\,Sin\varphi_1\cdots\cdots\cdots\cdots(4.12)$$

$$\begin{aligned}&I_1\ddot{\varphi}_1+c\dot{x}'_1\,e_1Sin\varphi_1-c\dot{y}'_1\,e_1Cos\varphi_1+k_{11}x'_1\,e_1Sin\varphi_1\\&+k_{12}x'_2\,e_1Sin\varphi_1-k_{11}y'_1\,e_1Cos\varphi_1-k_{12}y'_2\,e_1Cos\varphi_1-\Im(\varphi_2-\varphi_1)=\Gamma_1(t)\cdots\cdots\cdots\cdots(4.14)\end{aligned}$$

$$m_2\ddot{x}'_2+c\dot{x}'_2+k_{22}x'_2+k_{21}x'_1=m_2e_2\ddot{\varphi}_2\,Sin\varphi_2+m_2e_2\dot{\varphi}_2^2\,Cos\varphi_2\cdots\cdots\cdots\cdots(4.15)$$

$$m_2\ddot{y}'_2+c\dot{y}'_2+k_{22}y'_2+k_{21}y'_1+m_2g=-m_2e_2\ddot{\varphi}_2\,Cos\varphi_2+m_2e_2\dot{\varphi}_2^2\,Sin\varphi_2\cdots\cdots\cdots\cdots(4.16)$$

$$\begin{aligned}&I_2\ddot{\varphi}_2+c\dot{x}'_2\,e_2Sin\varphi_2-c\dot{y}'_2\,e_2Cos\varphi_2+k_{22}x'_2\,e_2Sin\varphi_2\\&+k_{21}x'_1\,e_2Sin\varphi_2-k_{22}y'_2\,e_2Cos\varphi_1-k_{21}y'_1\,e_2Cos\varphi_2+\Im(\varphi_2-\varphi_1)=\Gamma_2(t)\cdots\cdots\cdots\cdots(4.17)\end{aligned}$$

As it is seen from the above equations they are coupled and non-linear. Even if a known function of $\varphi(t)$ is used the lateral oscillations will have a static coupling. Thus in order to solve this non-linear coupled system a numerical solution method was applied.

The equations were formed into a 6 x 6 matrix. The input parameters of the matrix are defined as;

m_1 = Mass of disk 1

m_2 = Mass of disk 2

I_1 = Polar Moment of Inertia of disk 1

I_2 = Polar Moment of Inertia of disk 2

e_1 = Eccentricity of mass center of disk 1

e_2 = Eccentricity of mass center of disk 2

c = Internal damping coefficient of rotor shaft

$k_{11}, k_{12}, k_{21}, k_{22}$ = Lateral shaft stiffnesses at disk locations (direct and cross)

They are calculated from the flexibility matrix as follows.

$$\begin{bmatrix} k_{11} & k_{12} \\ k_{21} & k_{22} \end{bmatrix} = \begin{bmatrix} \alpha_{11} & \alpha_{12} \\ \alpha_{21} & \alpha_{22} \end{bmatrix}^{-1}$$

$$\alpha_{11} = \frac{l_1^2(l_2+l_3)^2}{3EIL}, \quad \alpha_{22} = \frac{l_3^2(l_1+l_2)^2}{3EIL}, \quad \alpha_{21} = \frac{l_1 l_3(L^2 - l_1^2 + l_3^2)}{6EIL}$$

Refer to figure 4.1

l_1 = distance from first bearing support to the first disk

l_2 = distance between two disks

l_3 = distance from second disk to the second bearing support

L = Total distance of the shaft $= l_1 + l_2 + l_3$

E = Modulus of Elasticity

I = Moment of Inertia of the shaft = $\dfrac{\pi \times rotor\ diameter^4}{64}$

$\Im$ = Torsional stiffness of shaft = $\dfrac{\pi \times \text{modulus of rigidity} \times \text{shaft diameter}^4}{32 \times \text{shaft length}}$

$$\begin{bmatrix} m_1 & 0 & -m_1 e_1 Sin\varphi_1 & 0 & 0 & 0 \\ 0 & m_1 & m_1 e_1 Cos\varphi_1 & 0 & 0 & 0 \\ 0 & 0 & I_1 & 0 & 0 & 0 \\ 0 & 0 & 0 & m_2 & 0 & -m_2 e_2 Sin\varphi_2 \\ 0 & 0 & 0 & 0 & m_2 & m_2 e_2 Cos\varphi_2 \\ 0 & 0 & 0 & 0 & 0 & I_2 \end{bmatrix} \begin{bmatrix} \ddot{x}'_1 \\ \ddot{y}'_1 \\ \ddot{\varphi}_1 \\ \ddot{x}'_2 \\ \ddot{y}'_2 \\ \ddot{\varphi}_2 \end{bmatrix} +$$

$$c \begin{bmatrix} 1 & 0 & 0 & 0 & 0 & 0 \\ 0 & 1 & 0 & 0 & 0 & 0 \\ e_1 Sin\varphi_1 & -e_1 Cos\varphi_1 & 0 & 0 & 0 & 0 \\ 0 & 0 & 0 & 1 & 0 & 0 \\ 0 & 0 & 0 & 0 & 1 & 0 \\ 0 & 0 & 0 & e_2 Sin\varphi_2 & -e_2 Cos\varphi_2 & 0 \end{bmatrix} \begin{bmatrix} \dot{x}'_1 \\ \dot{y}'_1 \\ \dot{\varphi}_1 \\ \dot{x}'_2 \\ \dot{y}'_2 \\ \dot{\varphi}_2 \end{bmatrix} +$$

$$\begin{bmatrix} k_{11} & 0 & 0 & k_{12} & 0 & 0 \\ 0 & k_{11} & 0 & 0 & k_{12} & 0 \\ k_{11} e_1 Sin\varphi_1 & -k_{11} e_1 Cos\varphi_1 & \Im & k_{12} e_1 Sin\varphi_1 & -k_{12} e_1 Cos\varphi_1 & -\Im \\ k_{21} & 0 & 0 & k_{22} & 0 & 0 \\ 0 & k_{21} & 0 & 0 & k_{22} & 0 \\ k_{21} e_2 Sin\varphi_2 & -k_{21} e_2 Cos\varphi_2 & -\Im & k_{22} e_2 Sin\varphi_2 & -k_{22} e_2 Cos\varphi_2 & \Im \end{bmatrix} \begin{bmatrix} x'_1 \\ y'_1 \\ \varphi_1 \\ x'_2 \\ y'_2 \\ \varphi_2 \end{bmatrix}$$

$$= \begin{bmatrix} m_1 e_1 \dot{\varphi}_1^2 Cos\varphi_1 \\ m_1 e_1 \varphi_1^2 Sin\varphi_1 - m_1 g \\ \Gamma_1(t) \\ m_2 e_2 \dot{\varphi}_2^2 Cos\varphi_2 \\ m_2 e_2 \dot{\varphi}_2^2 Sin\varphi_2 - m_2 g \\ \Gamma_2(t) \end{bmatrix}$$

4.2 Method of Solution

The matrix form of the six equations of motion is shown on page 46. To solve these nonlinear coupled equations a solver program from Numerical Recipies was used.

The numerical solver program was based on the Newmark integration scheme. A complete detail of the program is found in the reference text, (Wilson 1994). The program was provided by Rotor Bearing Technology and Software Inc. in USA.

The output of the solver program computes a time base response of lateral and torsional oscillations of the shaft. These output data are then plotted to represent the time waveform of torsional and lateral vibrations of the shaft. The time waveform is then converted to a spectra by Fourier transformation.

To plot the time waveform and frequency spectra of lateral and torsional vibrations a plotter program from Advanced Rotating Machinery Dynamic Software was used. Prior authorization to use the plotter program was obtained from Rotor Bearing Technology and Software Inc. in Pennsylvania.

The analysis was based on two parts. In the first part the frequency response of lateral and torsional vibrations were computed for different rotational speeds and torsional excitations of the rotor. The time waveform and spectra for each case was plotted and the coupled torsional-lateral vibration frequencies were tabulated.

The objective of the second part of the study was to determine the response behavior of coupled torsional-lateral vibration at natural frequencies of the rotor. When the lateral and torsional are de-coupled the natural frequencies of the system were initially computed from the Mathematica program. Then the rotational speed of the rotor was held constant and the frequency of the torsional vibration was increased until the coupled torsional-lateral vibrations coincide at the natural frequency of the rotor. The amplitudes of the coupled torsional-lateral vibrations were tabulated for all torsional excitations. This analysis was performed for two different cases.

4.3 Two disk rotor model dimensional data

Rotor dimensions as per figure 4.4

Rotor Length = L = 1.0 meter

$l_1 = l_3 = 0.3$ meters; $l_2 = 0.4$ meters;

Diameters of disk 1 = disk 2 = 0.769 meters = 30.0 inches

Thickness of disk 1 = disk 2 = 0.038 meters = 1.5 inches

Diameter of shaft = 0.154 meters = 6.0 inches

Material properties of shaft and disk; Density = 7.68 x 10^3 kg/m^3

Modulus of Elasticity = 2 x 10^11 Pa

Modulus of rigidity = 72 x 10^9 Pa

The concentrated masses of the two disks and the lateral and torsional stiffness of the shaft are computed from the 'Mathematica Program'.

A copy of this program with details is given in Appendix C1.

The computed mass elastic properties are as follows.

Mass of disk 1 = mass of disk 2 = 138.723 Kg

Polar moment of inertia:

Disk 1= Disk 2 =10.2544 Kg-m^2

Lateral Shaft Stiffness

$k_{11} = k_{22} = 1.25264 \times 10^9$

$k_{12} = k_{21} = -1.0481 \times 10^9$

Torsional Stiffness

$\Im = 3.97572 \times 10^6$

These values were input into the Numerical solver program and the analysis was performed in two parts. The first part of the analysis was to determine the response frequencies of the coupled torsional-lateral vibrations. The second part was to analyze the coupled torsional-lateral vibrations at natural frequencies of the system.

4.4 PART 1 – ANALYSIS OF RESPONSE FREQUENCIES OF COUPLED TORSIONAL-LATERAL VIBRATIONS.

The first part of the analysis was to determine the response frequencies of coupled torsional-lateral vibrations of the two-disk-rotor assembly. At a selected steady rotational speed the torsional excitation frequency of the rotor was varied and the response amplitude of the lateral vibrations was computed as a time depended displacement or velocity function and graphed as a time waveform plot. The Fast Fourier Transformation spectrum of the time waveform was then processed and plotted. The frequencies of the vibration components were tabulated in table 4.1. Ten case studies were performed to verify the data.

4.5 INPUT TEST DATA AND RESULTS

	Disk 1	Disk 2
Mass:	138.723 Kg	138.723 Kg
Polar Moment of Inertia:	10.2544 Kg-m^2	10.2544 Kg-m^2
Eccentricity of mass center:	0.0038 m	0.0038 m

$$\text{Lateral Stiffness} = \begin{bmatrix} 1.25264 \times 10^{9} & -1.0481 \times 10^{9} \\ -1.0481 \times 10^{9} & 1.25264 \times 10^{9} \end{bmatrix}$$

$$\text{Torsional Stiffness} = 3.97572 \times 10^{6}$$

Torque Amplitude = 30,000 N-M

The computer input data sheets and the plotted waveforms and spectra of the test results for all case studies are attached in Appendix A pages 80 through 91.

Case 1: Rotational Speed = 2000 rpm = 33.3 Hz

Torsional Excitation Frequency = 62.8 rad/sec = 10 Hz

Coupled Lateral-Torsional Vibration Frequencies = 23.3 and 43.3 Hz

Reference lateral vibration response plot is in Appendix A, page 82

Case 2: Rotational Speed = 2000 rpm = 33.3 Hz

Torsional Excitation Frequency = 94.2 rad/sec = 15 Hz

Coupled Lateral-Torsional Vibration Frequencies = 18.3 and 48.3 Hz

Reference lateral vibration response plot is in Appendix A, page 83.

Case 3: Rotational Speed = 2000 rpm = 33.3 Hz

Torsional Excitation Frequency = 251.2 rad/sec = 40 Hz

Coupled Lateral-Torsional Vibration Frequency = 73.3 Hz

Reference lateral vibration response plot is in Appendix A, page 84.

Case 4: Rotational Speed = 2000 rpm = 33.3 Hz

Torsional Excitation Frequency = 314.0 rad/sec = 50 Hz

Coupled Lateral-Torsional Vibration Frequency = 83.3 Hz

Reference lateral vibration response plot is in Appendix A, page 85.

Case 5: Rotational Speed = 2000 rpm = 33.3 Hz

Torsional Excitation Frequency = 376.8 rad/sec = 60 Hz

Coupled Lateral-Torsional Vibration Frequency = 93.3 Hz

Reference lateral vibration response plot is in Appendix A, page 86.

Case 6: Rotational Speed = 3000 rpm = 50.0 Hz

Torsional Excitation Frequency = 62.8 rad/sec = 10 Hz

Coupled Lateral-Torsional Vibration Frequencies = 40 and 60 Hz

Reference lateral vibration response plot is in Appendix A, page 87.

Case 7: Rotational Speed = 3000 rpm = 50.0 Hz

Torsional Excitation Frequency = 125.6 rad/sec = 20 Hz

Coupled Lateral-Torsional Frequency = 30.0 and 70 Hz

Reference lateral vibration response plot is in Appendix A, page 88.

Case 8: Rotational Speed = 3000 rpm = 50.0 Hz

Torsional Excitation Frequency = 376.8 rad/sec = 60 Hz

Coupled Lateral-Torsional Frequency = 110.0 Hz

Reference lateral vibration response plot is in Appendix A, page 89.

Case 9: Rotational Speed = 3000 rpm = 50.0 Hz

Torsional Excitation Frequency = 439.6 rad/sec = 70 Hz

Coupled Lateral-Torsional Frequency = 120.0 Hz

Reference lateral vibration response plot is in Appendix A, page 90.

Case 10: Rotational Speed = 3000 rpm = 50.0 Hz

Torsional Excitation Frequency = 502.4 rad/sec = 80 Hz

Coupled Lateral-Torsional Vibration Frequency = 130.0 Hz

Reference lateral vibration response plot is in Appendix A, page 91.

The data are tabulated as follows.

Table 4.1

Rotational Speed in Hz	**Torsional Excitation frequency in Hz**	**Lateral vibration response frequencies Hz**		
		1	2	3
33.3 Hz	10.0 Hz	23.3 Hz	33.3 Hz	43.3 Hz
33.3 Hz	15.0 Hz	18.3 Hz	33.3 Hz	48.3 Hz
33.3 Hz	40.0 Hz	-	33.3 Hz	73.3 Hz
33.3 Hz	50.0 Hz	-	33.3 Hz	83.3 Hz
33.3 Hz	60.0 Hz	-	33.3 Hz	93.3 Hz
50.0 Hz	10.0 Hz	40.0 Hz	50.0 Hz	60.0 Hz
50.0 Hz	20.0 Hz	30.0 Hz	50.0 Hz	70.0 Hz
50.0 Hz	60.0 Hz	-	50.0 Hz	110.0 Hz
50.0 Hz	70.0 Hz	-	50.0 Hz	120.0 Hz
50.0 Hz	80.0 Hz	-	50.0 Hz	130 Hz.

The column 1 and 2 in the above table are the frequencies of the forcing functions. The column 1 gives the frequency of the lateral excitation force caused by the imbalance of the rotor, and the frequencies of the torsional excitation force are tabulated in column 2. Column 3, 4 and 5 are response frequencies of the lateral vibration components. Column 4 gives the response due to the imbalance excitation of the rotor. Frequencies at column 3 and 5 are due to the modulation of imbalance excited vibrations at torsional excitation frequency of the rotor. This shows that if a lateral vibration is occurring at ω_r and a

torsional oscillation is occurring at ω_t the coupled torsional-lateral vibrations will occur at frequencies $\omega_r \pm \omega_t$.

4.6 Part II – Response analysis of the coupled torsional-lateral vibrations at natural frequencies of the rotor

In the second part of the study the response amplitude of coupled torsional-lateral vibrations at the natural frequencies of the rotor was analyzed. In order to perform this the coupled torsional-lateral vibration frequency was varied through a frequency range around the natural frequency of the rotor. The amplitude of the coupled torsional-lateral vibration was tabulated.

The natural frequencies of the rotor were first computed from a program built from "Mathematica". Same dimensions of the model and mass and stiffness matrix obtained from the previous program were used. **The computed natural frequencies of this model are at 193.257 Hz and 648.156 Hz.** Details of the program are given in Appendix C2.

Two case studies were performed. First the rotational frequency of the rotor was held at 3000 rpm = 50 Hz, and to assess the effect of coupled torsional-lateral response in lateral mode, the frequency of the torsional oscillations were varied from 700 rad/sec to 1200 rad/sec. The amplitudes of the coupled vibration components occurred at the frequency $\omega_r + \omega_T$ were tabulated. The waveform and spectrum data of the computed results are attached in Appendix B1 and B2.

Case 11 : Rotor Speed = 3000 rpm = 50 Hz

Table 4.2

Rotor Speed ω_r	**Torsional Excitation Frequency** ω_T		**Coupled Torsional and Lateral vibration frequency** $\omega_r + \omega_T$	**Amplitude of coupled vibration frequency**	
	Rad/sec	**Hz**		**10^{-5} meters**	**mils**
50 Hz	700	111.465	161.465	.2	0.5
50 Hz	800	127.388	177.388	.36	0.9
50 Hz	850	135.350	185.350	.72	1.8
50 Hz	860	136.943	186.943	.8	2
50 Hz	870	138.535	188.535	1	2.5
50 Hz	875	139.331	189.331	.96	2.4
50 Hz	885	140.924	190.924	2.36	5.9
50 Hz	890	141.719	191.720	3.12	7.8
50 Hz	900	143.312	193.312	3.52	8.8
50 Hz	920	146.497	196.497	1.28	3.2
50 Hz	1000	159.236	209.236	.28	0.7
50 Hz	1100	175.159	225.159	.12	0.3
50 Hz	1200	191.083	241.083	.04	0.1

The graph of torsional excitation frequency vs the amplitude of the lateral coupled response frequency of Case 11. is shown on plot 4.1 page 56. The Y axis represent the amplitude of the coupled torsional-lateral vibration measured in lateral mode.

The torsional oscillation frequency was varied in the frequency range 111 Hz through 191 Hz to assess the affect of coupled torsional-lateral vibrations when passes through the 1st natural frequency of the rotor, at 193 Hz, as calculated from "Mathematica" program attached in Appendix C2.

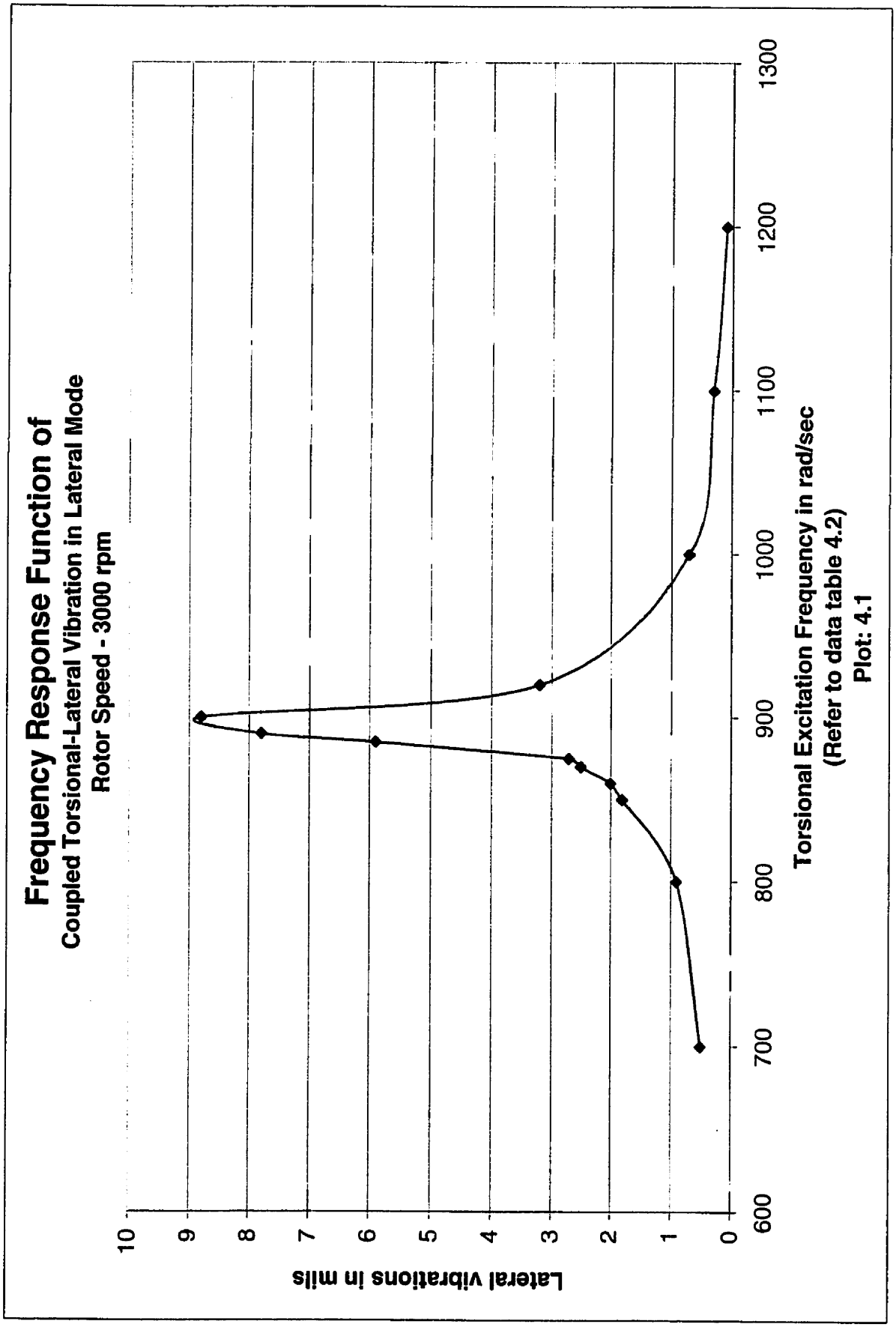
Frequency Response Function of
Coupled Torsional-Lateral Vibration in Lateral Mode
Rotor Speed - 3000 rpm
Lateral vibrations in mils
0
1
2
3
4
5
6
7
8
9
10
600
700
800
900
1000
1100
1200
1300
Torsional Excitation Frequency in rad/sec
(Refer to data table 4.2)
Plot: 4.1

The test similar to case 11 was repeated in case 12 at a higher rotational speed of the shaft.

Case 12.: Rotor Speed = 3600 rpm = 60 Hz

Table 4.3

Rotor Speed ω_r	Torsional Excitation Frequency ω_T		Coupled Torsional and Lateral vibration frequency $\omega_r + \omega_T$	Amplitude of coupled vibration frequency	
	Rad/sec	Hz		10^{-5} meters	mils
60 Hz	700	111.465	171.465	2.0	0.8
60 Hz	800	127.388	187.388	7.0	2.8
60 Hz	820	130.573	190.573	14.5	5.8
60 Hz	830	132.166	192.166	23.75	9.5
60 Hz	835	132.962	192.962	26.25	10.5
60 Hz	840	133.758	193.758	22.0	8.8
60 Hz	850	135.350	195.350	13.75	5.5
60 Hz	900	143.312	203.312	2.5	1.0
60 Hz	1000	159.236	219.236	1.25	0.5

The graph of torsional excitation frequency vs the amplitude of the lateral coupled response frequency of Case 12. is shown on plot 4.2 page 59. The Y axis represent the amplitude of the coupled torsional-lateral vibration measured in lateral mode.

4.7 CONCLUSION

1. When a rotor with mass imbalance rotating at speed ω_r is excited at a torsional frequency of ω_t a coupled torsional-lateral vibration will be induced in the system. The coupled torsional-lateral vibrations will occur at $\omega_r \pm \omega_t$. This vibration will be in addition to the lateral vibration of the rotor, due to imbalance of the disk at ω_r.

2. The coupled torsional-lateral oscillations will excite the rotor at their natural frequencies.

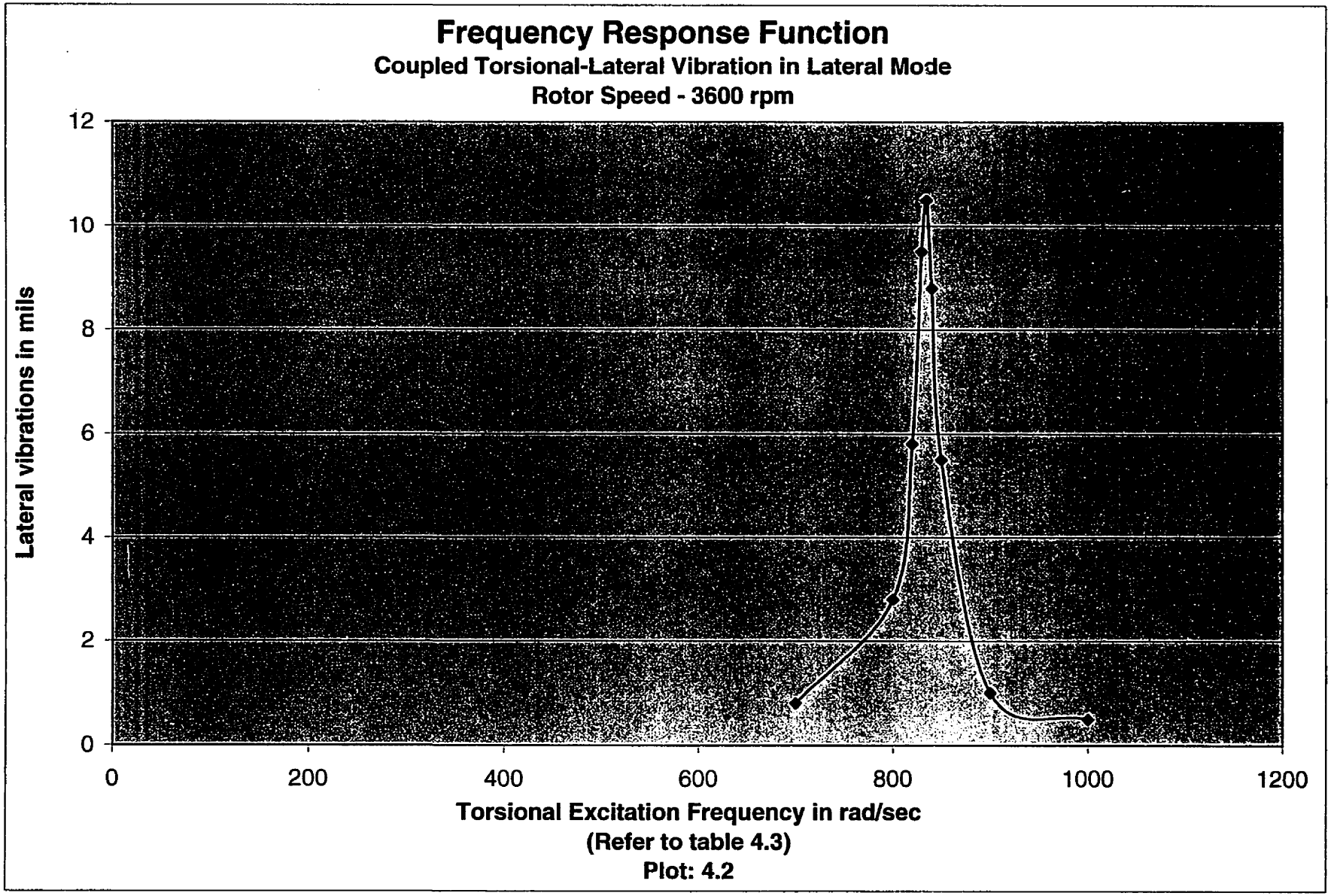
Frequency Response Function
Coupled Torsional-Lateral Vibration in Lateral Mode
Rotor Speed - 3600 rpm
Lateral vibrations in mils
12
10
8
6
4
2
0
0
200
400
600
800
1000
1200
Torsional Excitation Frequency in rad/sec
(Refer to table 4.3)
Plot: 4.2

CHAPTER 5

ANALYSIS OF EXPERIMENTAL DATA

In Chapters 4 and 5 single and two disk rotor systems were modeled and analyzed. Nonlinear, coupled equations of motion involving torsional and lateral vibrations of the systems were solved numerically. The lateral responses of shaft vibrations were computed and tabulated.

The analyses concluded that in imbalance rotors the torsional and lateral vibrations are coupled. When an unbalanced rotor is rotated at a frequency ω_r, and excited from a torsional oscillation at a frequency ω_t a coupled torsional-lateral vibration is induced at frequencies $\omega_r \pm \omega_t$. The coupled torsional-vibrations can excite the rotor at their natural frequencies and cause resonance.

In this chapter we will analyze the experimental data that were already acquired from an industry rotor and compare this data with the above findings. A two-stage pump rotor driven from a variable frequency drive motor was selected for this analysis.

Figure 6.1 on page 69 shows a rotor model of a two-stage Bingham pump impeller assembly. The pumps are used in major pipeline companies to pump raw and processed oil across Canada. The pump has two six-vane impellers and is center supported on journal bearings.

The pump is driven from a 4000 Horsepower induction motor, powered through an adjustable speed drive unit. The adjustable speed drive was a current source inverter type variable frequency drive unit. These two-adjustable speed drives operate by varying their excitation frequency supplied to the motor. During the process of frequency conversions high torsional oscillations are generated in these drives. There are many technical papers published with respect to this subject, for example refer to "Torsional vibrations resulting adjustable speed drive units" by David Sheppard (1988).

The selected data used in the project is from a pump in a major pipeline company in Alberta. When this pump was commissioned in January 1995 an unusual chattering noise was heard emanating from the coupling and the author was called upon to test and analyze the vibrations. A series of tests including casing and shaft axial vibrations, pressure pulsation, acoustic and current measurements of the pump were performed. The pump speed was ramped through the speed range from minimum speed 1440 rpm to 3960

rpm and the transient vibrations were captured. During the ramp up the coupling motion was frozen from a triggered strobe light, and this motion was filmed for further analysis.

All test data directed to a possible torsional resonance of the system. A conventional torsional test using strain gauge techniques were performed to verify the findings.

The tests confirmed that high torsional vibrations are generated from the variable frequency drive and excited the rotor at 6x rpm order of the pump. When the torsional forces coincide the 2nd torsional natural frequency of the rotor resonance occurred. The coupling chatter occurred during the torsional resonance of the rotor assembly.

The plots on pages 65 and 66 are torsional oscillation data, which include a detail waveform plot and a cascade plot of torsional vibrations of the system. The detail waveform plot gives a digitized real time waveform, of the measured vibrations, in a specified speed range. The cascade plot gives corresponding spectra at each time sample in the detail waveform.

The 6x rpm order oscillations exciting the rotor at the resonance frequency is shown on the plots. The confirmed that torsional resonance of the rotor is at frequency 270 Hz. The 6x rpm order is refer to as six times the running speed of the rotor.

The plots on pages 67 and 68 are cascade and detail waveform plots of bearing housing vibrations, acquired on the outboard end bearing of the pump. The cascade plot shows

occurrence of 1x rpm order vibrations due to slight mechanical imbalance, 2x line frequency electrical induce vibrations and 6x rpm order vane passing frequency vibrations of the pump. The 6x rpm order vibrations peaked at the frequency 321 Hz and this was a resonance condition.

The resonance around 320 Hz has been found in the past in many pumps of this configuration. They have been confirmed through tests, and sufficient data are available to prove their existence.

The most important fact that can be noted on the plot is excitation of the 7x rpm order vibration at 321 Hz. This was an unusual peak that excited this rotor assembly at the same resonance frequency of the pump. As the pump has six impellers only there are no other excitation forces occurring on the unit at this speed.

As mentioned earlier this pump rotor has severe torsional excitation from the variable frequency drive occurring at 6x rpm order of the rotor. The imbalance excited lateral vibrations are also occurring at 1x rpm of the pump rotor. The imbalance excited vibrations couple with the lateral vibrations, induced a coupled torsional-lateral vibrations on the unit, at 7x rpm order of the pump. This 7x rpm order coupled torsional-lateral vibration excited the rotor at 321 Hz, which was a known resonance frequency of the unit.

To verify the natural frequencies of the rotor assembly an analytical study of natural frequencies was performed. Advanced Rotating Machinery Dynamic software of Rotor Bearing Technology and Software Inc. was used to compute the damped natural frequencies of the system. A detail calculation of the model is attached in Appendix D1. The first three lowest damped natural frequencies and mode shapes are attached on pages 70 through 72. In the calculated model the damped natural frequency of the third mode occurred at 323.5 Hz. Refer to plot on page 72.

The pump rotor was a complex model and it had many degrees of freedom. The coupled torsional-lateral vibration excited the rotor at a higher frequency, i.e. at the third flex mode of the rotor. As in this study the coupled torsional-lateral vibration was analyzed through a simple two-degree-of freedom model we could not simulate the pump rotor through our program to analyze the qualitative properties of the experimental system.

The experimental data verified the findings that were concluded in Chapters 4 and 5. As the rotor imbalance was low the coupled torsional-lateral vibrations did not show at the other frequencies. However, the coupled torsional-lateral vibrations excited the rotor at a resonance frequency of the rotor.

The 7x rpm order refers to as seven times the running speed of the rotor.

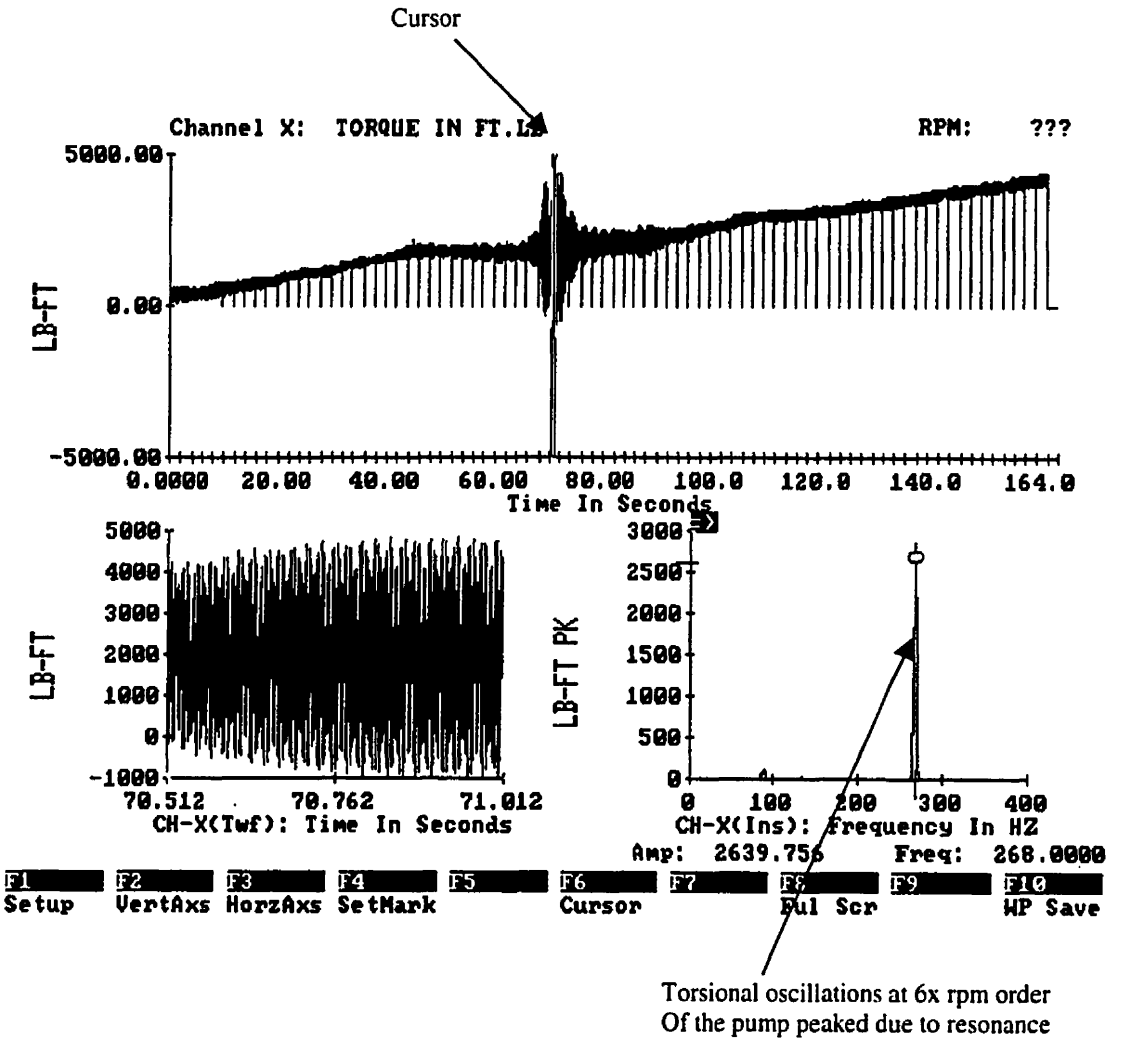

Plot 5.1 : Detail waveform plot of torsional oscillations

Upper: Detail waveform plot

Lower: Spectra and waveform at cursor location

Speed ramped up from 1440 rpm to 3690 rpm.

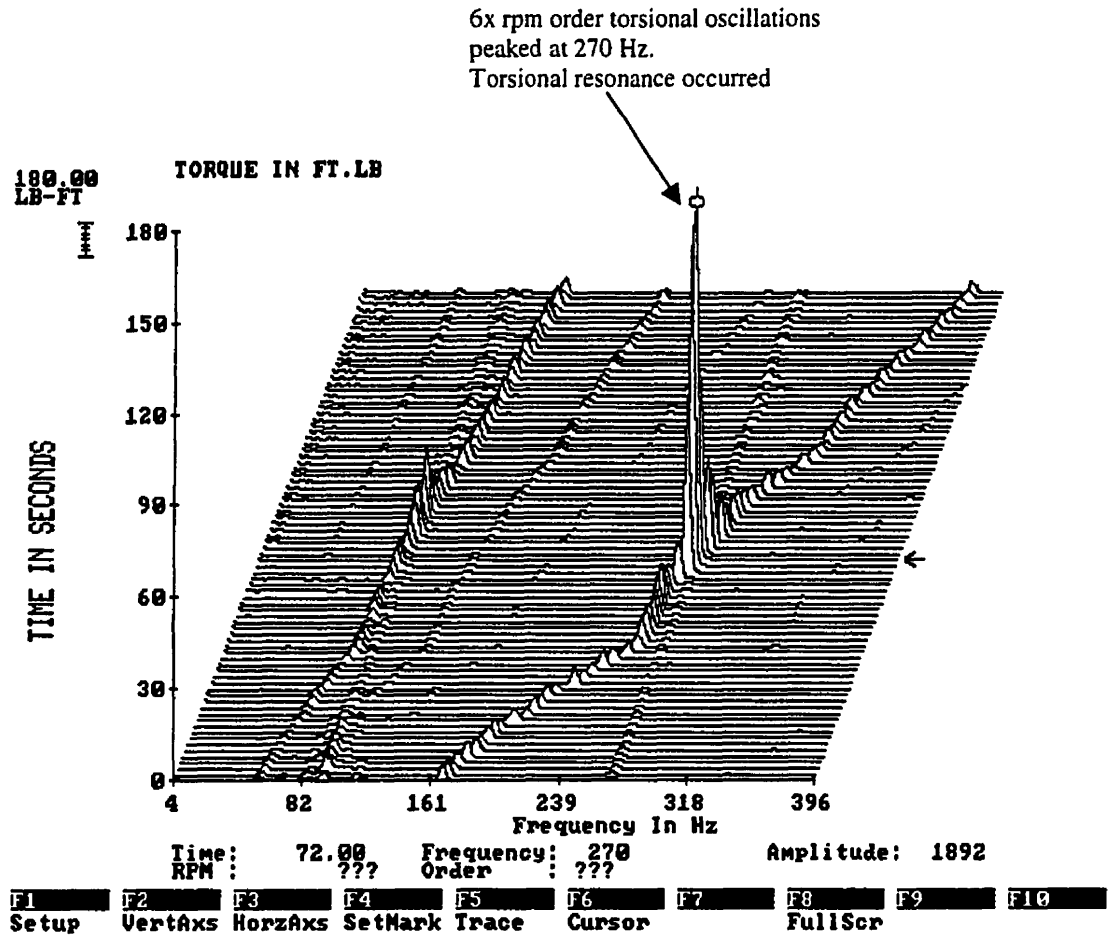

Plot 5.2 : Cascade plot of pump torsional oscillations

Torsional oscillations occurred at 6x rpm order of the pump and peaked at 270 Hz.

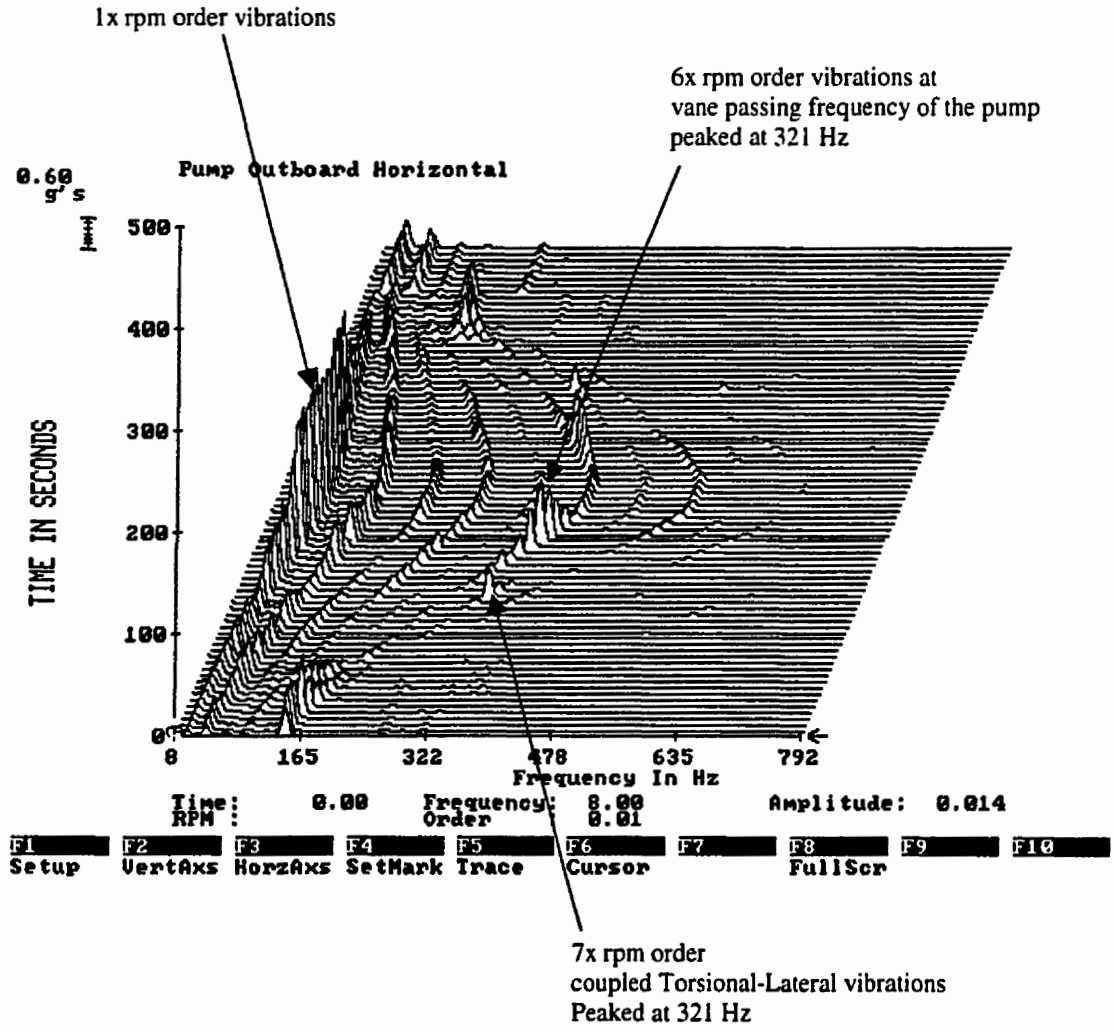

Plot 5.3 : Cascade Plot of Pump Outboard Horizontal Vibration

Note the increase of vane passing frequency vibration at 321 Hz due to resonance, and the 7x rpm order vibration peak also appeared only at 321 Hz. The torsional oscillations at 6x rpm order, coupled with the lateral vibration at 1x rpm order, induced a coupled torsional-lateral vibration at the 7x rpm order of the pump. There are no other 7x rpm order lateral vibration forces occurring in the pump as these are direct driven centrifugal units, and the hydraulic forces are at vane passing frequency, at 6x rpm order of the pump.

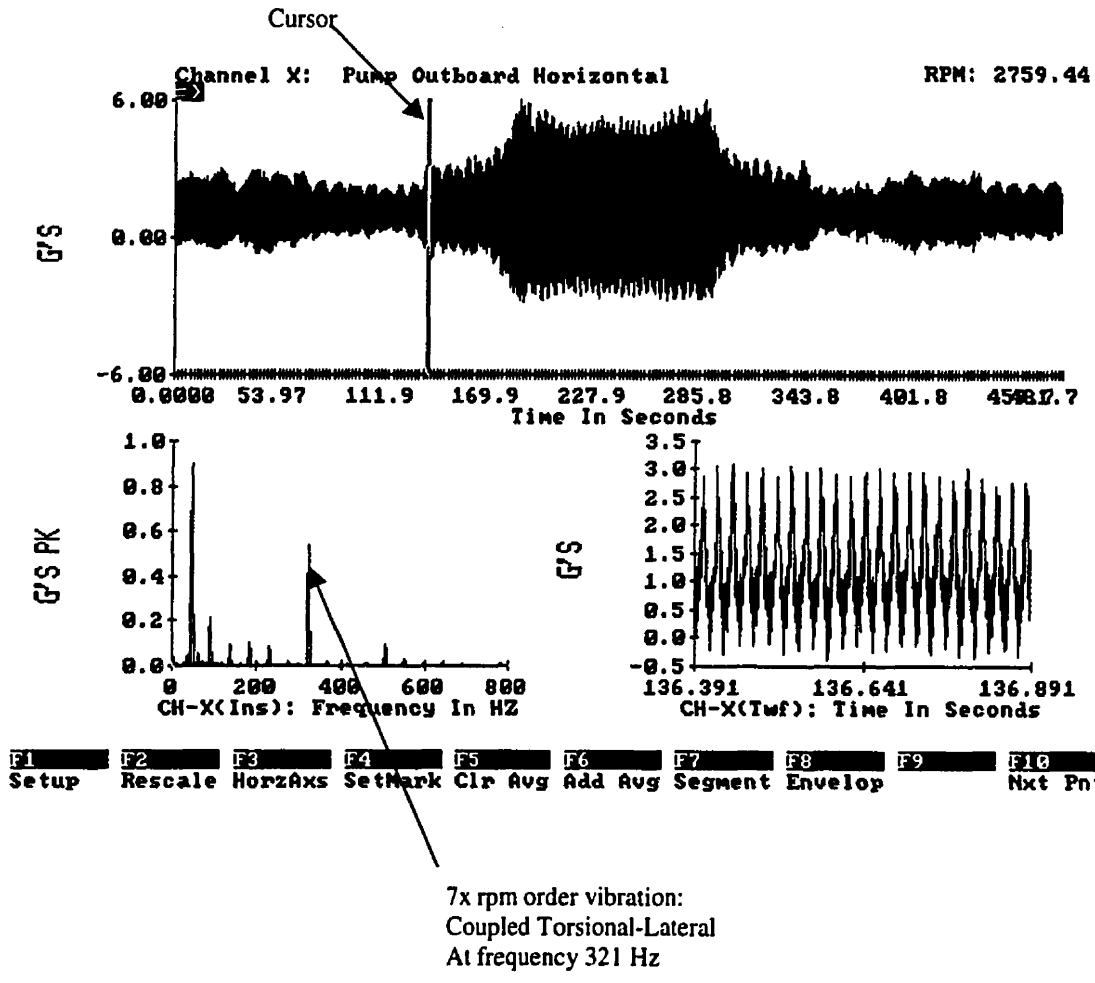

Plot 5.4 : Detail Waveform Plot of Pump Outboard Horizontal Vibration

Upper plot : A detail time waveform of pump vibration. Cursor located at speed 2759 rpm. The lower plots are spectrum and time waveform corresponds to the speed at cursor location, (i.e at speed 2759 rpm). At this speed the 7x rpm order vibration peak occurred at 321 Hz. This plot corresponds to the cascade plot on page 71. Speed ramped up from 1440 rpm to 3960 rpm.

'Nx rpm order' refers to N times the running speed of the unit.

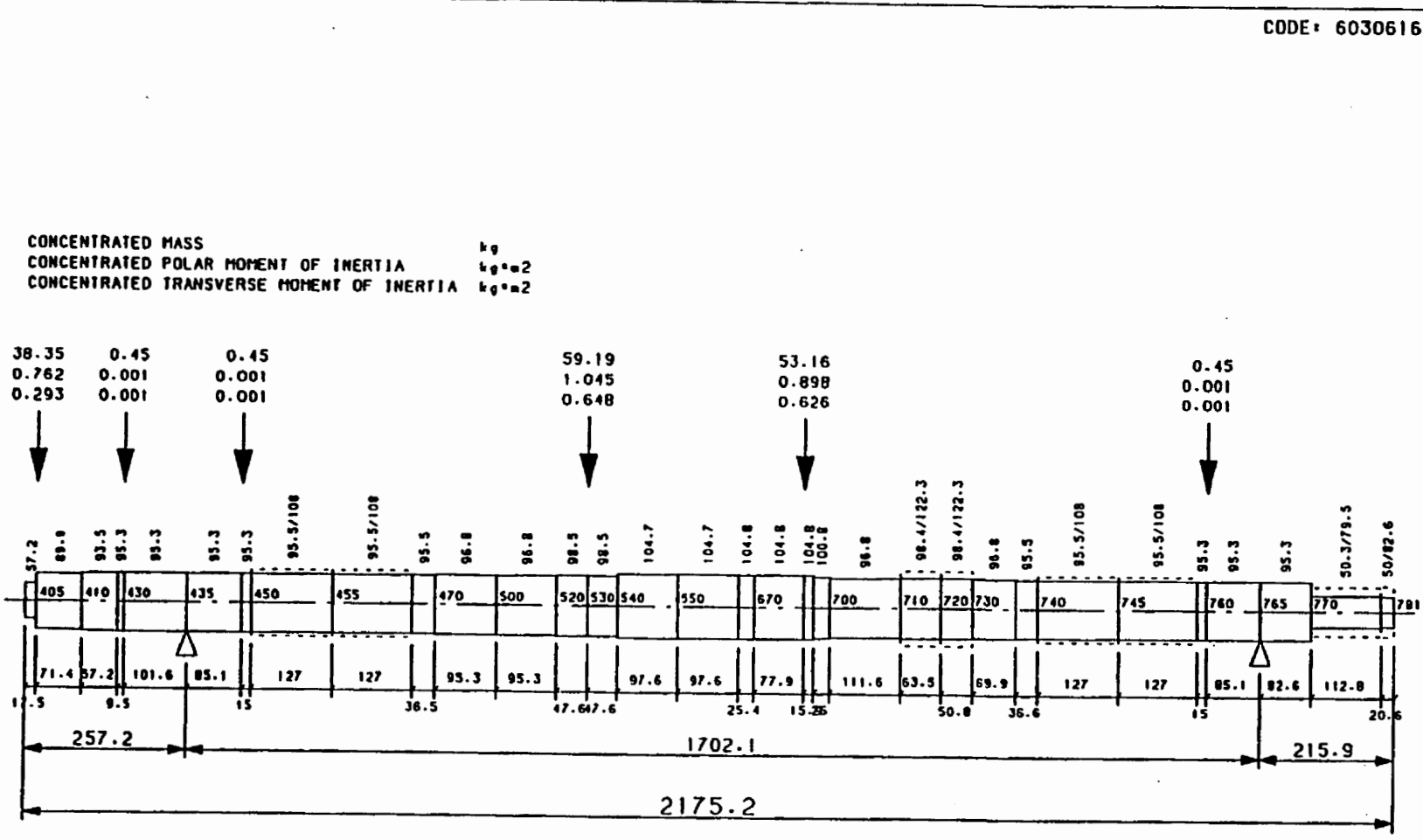

Plot 5.5: Dimensional Details of the Pump Rotor

ROTOR MASS = 2.872E+02kg
ROTOR POLAR MASS MOMENT = 2.886E+00kgm2

LATERAL ROTOR MODEL	SCALE 1 : 6.6	DATE: 06.03.96
1E725 Pump Type 12x12x15.5 MSD-D 2 Stg.		
SULZER BINGHAM PUMPS INC - PORTLAND, OREGON, USA		Fig A1

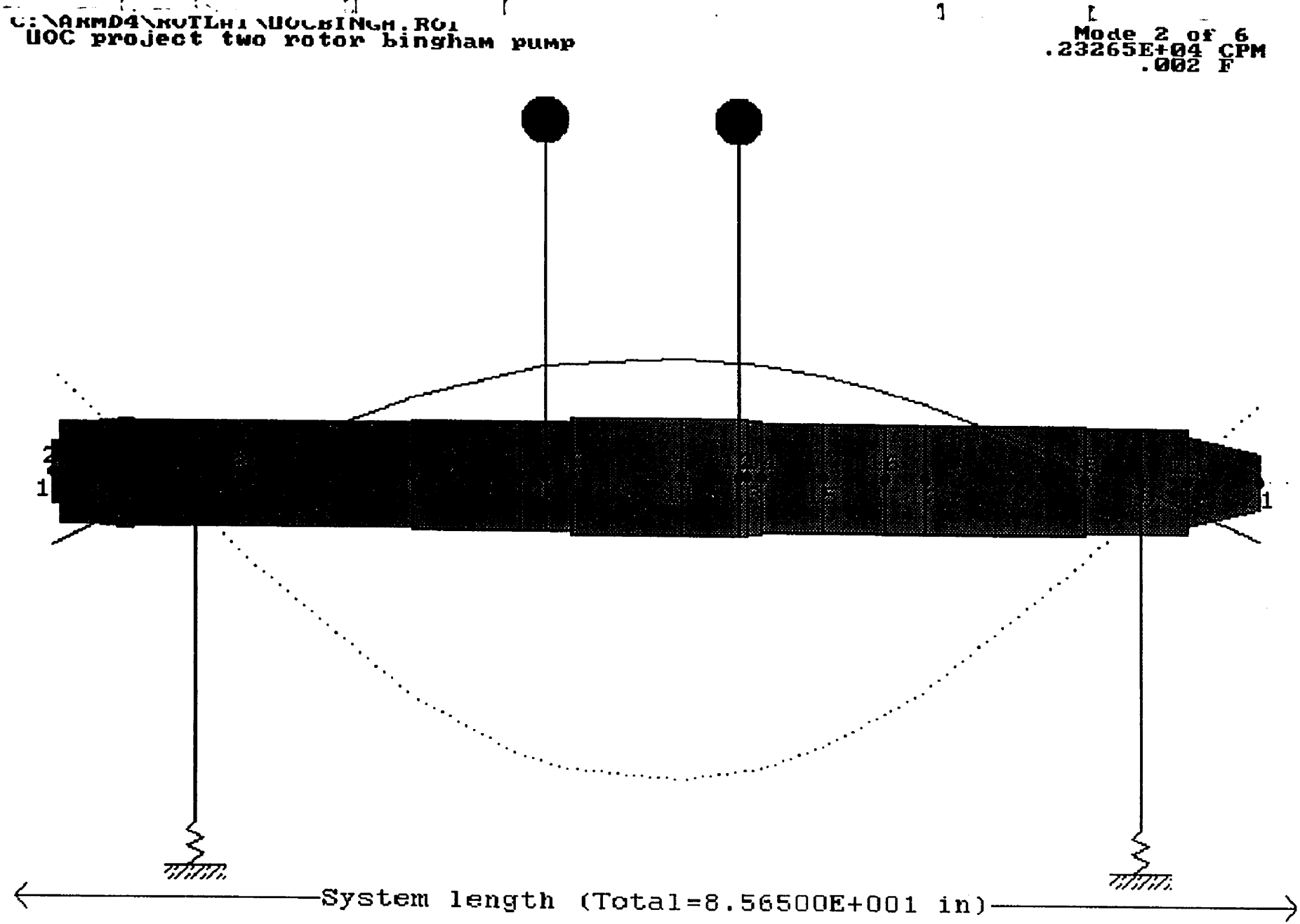

Plot 5.6: **First Bending Mode of the Pump Rotor**

At 38.7 Hz.

Plot 5.7: **Second Bending Mode of the Pump Rotor**

At 172.92 Hz.

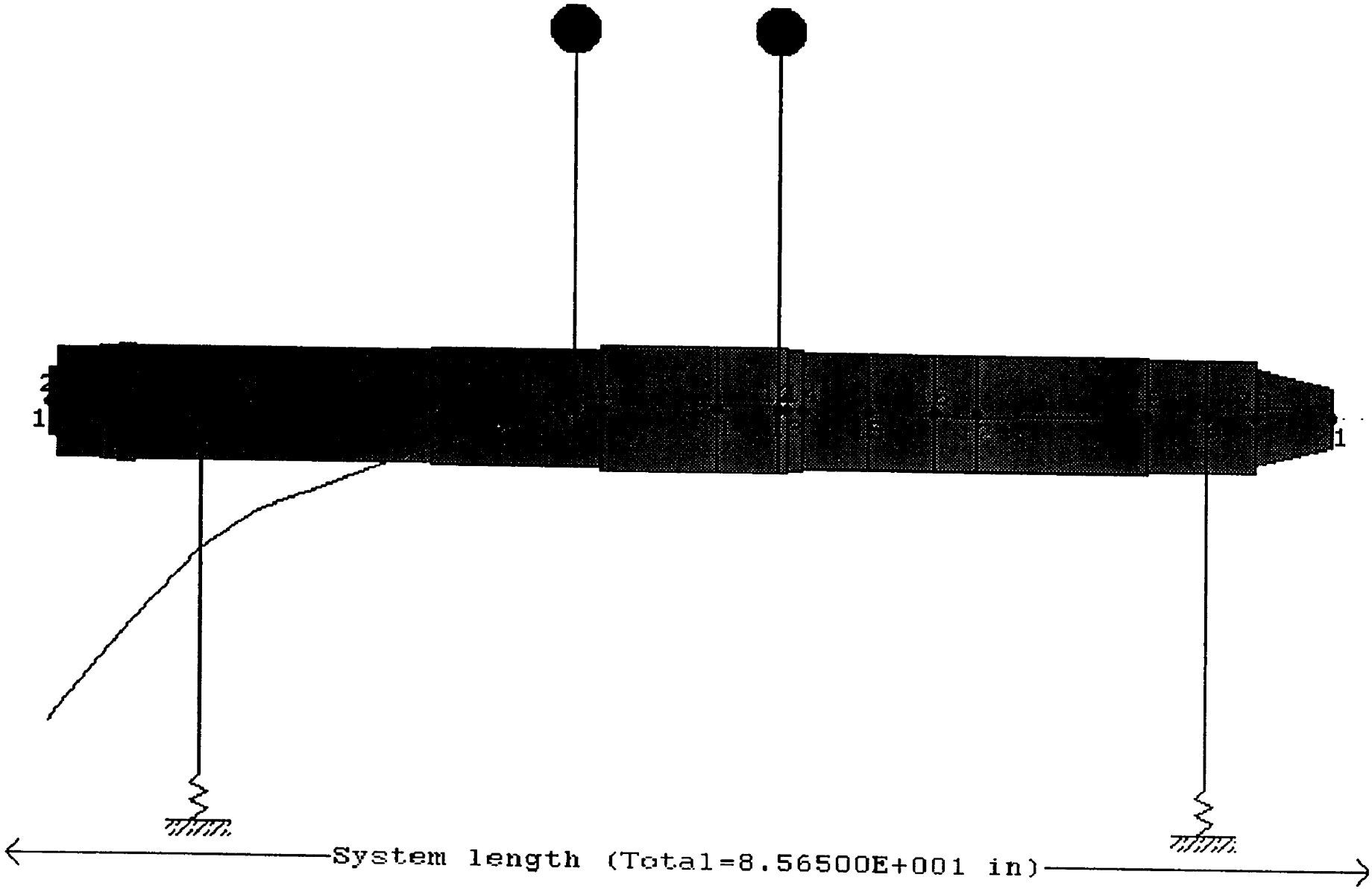

Plot 5.8: **Third Flexing Mode of the Pump Rotor**

At 323.5 Hz.

CHAPTER 6

CONCLUSIONS AND RECOMMENDATIONS

The influence of coupled torsional-lateral vibrations on rotor bearing assemblies was analyzed in this study. The results concluded through analytical modeling were verified by experimental data that were already performed on an industry rotor model. The response frequencies of the coupled torsional-lateral vibrations, the effect of coupled torsional-lateral vibration at lateral natural frequencies of the rotor were investigated, and the parameters that influence this coupling were studied.

When a rotor with a mass imbalance of 'me' is rotated at a speed of ω_r a lateral vibration of magnitude $me\omega_r^2$ is generated, where 'e' is the eccentricity of the imbalance mass 'm'. This imbalance excited lateral vibration occurs at the same rotational

frequency of the rotor. In addition, a torsional vibration of magnitude '*mge*' is also induced, due to this imbalance force, at the same rotational frequency of the rotor. The magnitude of the lateral vibration increases as a square of the speed, but the magnitude of the torsional vibration remains constant at all speeds. Thus the imbalance induced torsional vibrations of the system are weak compared to the lateral vibrations.

When this imbalance rotor is excited by an external torsional oscillation, the torsional oscillation will couple with the lateral vibration of the system and induce a coupled torsional-lateral vibration. The torsional oscillation will modulate the lateral vibration, and the induced coupled torsional-lateral vibration will occur at rotational frequency $\pm$ torsional frequency of the rotor.

When the frequency of the coupled torsional-lateral vibrations approach the lateral natural frequency of the rotor the vibration response of the system increases to a maximum. The induced coupled torsional-lateral vibrations excite the rotor due to resonance.

The magnitude of the coupled torsional-lateral vibrations depend on the eccentricity of the imbalance mass. Since in many rotors the imbalance mass is small, the magnitude of the coupled torsional-lateral vibration remains weak. The parameters that affect the coupled torsional-lateral vibrations in a rotor system are:

- Magnitude of the imbalance mass
- Magnitude of the torsional oscillation forces.

- Damping coefficient of the rotor disk assembly.

In geared rotor systems the torsional and lateral vibrations are coupled due to nature of their geometry. The torsional moments in gears are transmitted through tooth force. The transverse forces and bending moments are generated from these torsional moments.

In contrast to the geared rotor systems, in rotor disk assemblies, the torsional and lateral vibrations are coupled only if a large imbalance is present in the system, but still this coupling tends to be weak. However, if an external oscillating force of higher magnitude is applied to the rotor, the coupled torsional-lateral vibrations grow stronger and increase the response characteristics of the system. Thus when designing systems, particularly those being driven through variable frequency drive (VFD) motors, where torsional oscillations are present, special care should be taken to minimize the imbalance occurring in rotors.

In classical linear vibration analysis the affects of coupling between the torsional and lateral vibrations are ignored. Current rotor dynamic analysis tools also treat lateral deformations, associated with shaft bending, and torsional twisting as independent of each other and the systems are considered to be statically and dynamically decoupled. On the other hand, for rotors subjected to rotating unbalance or lateral forces, studies of dynamic response are performed by focusing on the lateral vibration aspect only. Similarly, the systems where torsional forces are considered predominant, torsional response analysis is carried out independently of lateral vibrations. This assumption may

appear reasonable in many applications. However, requirements for high speed, high power transmission and lighter rotors may require that the coupling between lateral and torsional oscillations is taken into account, since ignoring this coupling may lead to inaccurate and misleading dynamic predictions.

Bibliography

Corbo, M. A. & Malanoski, S.B., (1996) Practical Design Against Torsional Vibration, *25th Turbomachinery Symposium, Texas A&M University, Texas.*

Grgic, A., Heil, W., & Prenner, H., (1992) Large Converter-Fed Adjustable Speed AC Drives for Turbomachines, *Proceedings of the 21st Turbomachinery Symposium, Texas A&M University. P 103-112*

Hudson, J. H., (1992) Lateral Vibration Created by Torsional Coupling of a Centrifugal Compressor System Driven by a Current Source Driver for a Variable Speed Induction Motor, *Proceedings of the Twenty-first Turbomachinry Symposium, Turbomachinery Laoratory, Department of Meachanical Engineering, Texas A&M University, College Station, Texas (1992)*

Iida, H., Tamura, A. & Oonishi, M., (1984) Coupled Torsional-Lateral Vibration of a Shaft in a Geared Rotor System II, *Bulletin of JSME, Vol 28, No 245, December 1985.*

Iida, H., Tamura, A. & Yamada, Y., (1978) Coupled Torsional-Lateral Vibration of a Shaft in a Geared Rotor System I, *Bulletin of JSME, Vol 23, No 186, December 1980.*

Iwatsubo, T. & Nan, H., (1989) Coupled Lateral-Torsional Vibration of a Rotor System trained by Gears (10th Report. Noise Measurement by Sound Intensity Method), *Transaction of the Japan Society of Mechanical Engineers, Part C v n 518 Oct 1989, p 2527-2532, ISSN: 0387-5024.*

Kishor, B. & Gupta, S.K., (1989) On Dynamic Gear Tooth Loading Due to Coupled Torsional-Lateral Vibrations in a Geared Rotor Hydrodynamic Bearing System, *Publication n Journal of Tribology, January, 1989.*

Kramer, E., (1993) Dynamics of Rotors and Foundations, *Springer-Verlag, Berlin Heidelberg, New York (1993)*

Kuang, J. & Tsai, J.H., (1991) Improved Branch Method for Gear-Coupled Systems, *Journal of the Chinese Society of Mechanical Engineers, v 12 n 2 Apr 1991 p 177-187, ISSN: 0257-9731.*

Kuniyoshi, I., Yasuhiko, O., Akira, O. & Hideaki, M.,(1990) Field Telemetry of Blade-Rotor Coupled Torsional Vibration at Matuura Power Station No. 1 Unit, *Presentation at the Sixth Workshop on Rotordynamic Instability Problems in High Performance Turbomachinery, May 21-23, 1990, Texas A&M University, Texas.*

Mario, P. (1991) Structural Dynamics Theory and Computation, *Van Nostrand Reinhold, New York*

Mitchell, L.D. & Mellen, D.M., (1975) Torsional-Lateral Coupling in a Geared, High-Speed Rotor System, *presentation at Design Engineering Technical Conference, Washington D.C., September 17-19, 1975, Design Engineering Division, ASME paper 75-DTE-75*

Nelson, H.D., Natsiavas, S. & Chin-Shong, C., (1993) Coupled Lateral-Torsional Vibration of a Gear-Pair System Supported by a Squeeze Film Damper, *ASME Publication, Non-Linear Vibrations, DE-Vol 54.*

Nelson, H.D., Shiau, T.N., & Chou, Y.W., (1994) Study on the Dynamic Characteristics of Geared Rotor-Bearing System with Hybrid Method, *ASME (Paper)*

Proceedings of the international Gas Turbine and Aeroengine Congress and Exposition, June 13-16, 1994, Hague, Neth Publication by ASME New York, NY, USA, p 1-11, Paper; 94-GT-355, ISSN: 0402-1215.

Rao, S.S., (1990) Mechanical Vibrations, 2nd Edition, *Addison Wesley Publishing Company, New York (1990)*

Schwibinger, P. & Nordmann, R., (1987)The Influence of Torsional-Lateral Coupling on the Stability behavior of Geared Rotor Systems, *ASME Journal of Engineers for Gas Turbine and Power, September 1987.*

Sheppard, D. J., (1988) Torsional Vibation Resulting From Adjustable-Frequency AC Drives, *IEEE Transaction on Industry Applications, Vol. 24, No. 5, September/October 1988.*

Steidel, R.F (1989) An Introduction to Mechanical Vibrations, *John Wiley & Sons, New York (1989)*

Thompson, A. S., (1997) Advancements in Machinery Management using the Measurement of Rotor Torsional Response, *Presentation at ASME ASIA 97 Congress & Exhibition, Sep 30-Oct 1, 1997, Singapore, ASME Paper; 97-AA-128 ISSN: 0402-1215*

Thompson, W.T. (1988) Theory of Vibrations with Applications, *Prentice Hall, New Jersey, 3rd Edition*

Timoshenko, S.P., Weaver, W. & Young, D., (1990) Vibration Problems in Engineering, *John Wiley and Sons, New York (1990)*

Vance, J.M. & French, R.S., ((1984) Measurement of Torsional Vibration in Rotating Machinery, *Presentation at Design Engineering Technical Conference, Cambridge, Massachusetts, ASME Paper No 84-DTE-55, June 15, 1984.*

Vandenput, A., Geysen, W. & Belmans, R. (1985) Influence of Torsional Vibrations on Lateral Oscillations of Induction Motor Rotors, *IEEE Transactions of Power Apperatus and Systems, Vol PAS-104, No 7, July 1985.*

Wachel, J.C. & Szenasi, F.R., (1980) Field Verification of Latera-Torsional Coupling Effects on Rotor Instabilities in Centrifugal Compressors, *NASA Conference Publication No. 2147, 1980.*

Wachel, J.C. & Szenasi, F.R., (1993) Analysis of Torsional Vibartions in Rotating Machinery, *Proceedings of the 22nd Turbomachinery Symposium, Texas A&M University, p 126-151.*

Wilson, E.L., & Bathe, K., (1990) Numerical Methods in Finite Element Analysis, *Prentice Hall, New Jersey.*

Yaman, Y. (1996) Vibrations of Open-Section Channels: A Coupled Flexural and Torsional Wave Analysis, *Journal of Sound and vibration (1997),v 204 n 1, Jul 3, 1997 p131-158*

Appendix A

Computed lateral vibration response plots as per Case 1 through Case 10 of Chapter 4, Section 4.5. are attached in this appendix. As the response in both directions are symmetrical only one response plot per each Case Study is included.

```
Two Disk Test File
7 150000  0.00010 100000  10 2000.0  9.8
138.723  10.2544  138.723 10.2544
0.038   0.000
5000.
1.25264e9  -1.0481e9  -1.0481e9  1.25264e9  3.97572e6
30000.0   62.8    0.0
    0.0     0.0    0.0
```

Input Guide

```
LINE 1:TITLE (72 CHARACTERS)
LINE 2:NUMB. OF DEGREES OF FREEDOM (ALWAYS 7 = 6 + 1 RIGID BODY ROTATION)
       NUMB. OF TIME STEPS
       TIME STEP INCREMENT (DELTA T - SECONDS)
       NUMB. OF TIME STEPS TO SKIP BEFORE BEGINNING TO PRINT OUTPUT
       NUMB. OF TIME STEPS TO SKIP BETWEEN OUTPUT PRINTING (EVERY 10TH STEP)
       SHAFT SPEED (RPM)
       GRAVITY (M/S^2)
LINE 3:DISK #1 MASS (KG)
       DISK #1 POLAR INERTIA (KG-M^2)
       DISK #2 MASS (KG)
       DISK #2 POLAR INERTIA (KG-M^2)
LINE 4:DISK #1 ECC. FROM SHAFT CENTER TO CENTER OF MASS (M)
       DISK #2 ECC. FROM SHAFT CENTER TO CENTER OF MASS (M)
LINE 5:DAMPING FOR LATERAL BEAM BENDING

LINE 6:K11 LATERAL SHAFT STIFFNESS
       K12 LATERAL SHAFT STIFFNESS
       K21 LATERAL SHAFT STIFFNESS
       K22 LATERAL SHAFT STIFFNESS
       TAU TORSIONAL STIFFNESS
LINE 7:DISK #1 TORQUE AMPLITUDE (N-M)
       DISK #1 TORQUE FREQUENCY (RAD/SEC)
       DISK #1 TORQUE PHASE ANGLE (RAD)
       DISK #2 TORQUE AMPLITUDE (N-M)
       DISK #2 TORQUE FREQUENCY (RAD/SEC)
       DISK #2 TORQUE PHASE ANGLE (RAD)
```

Plot: A1

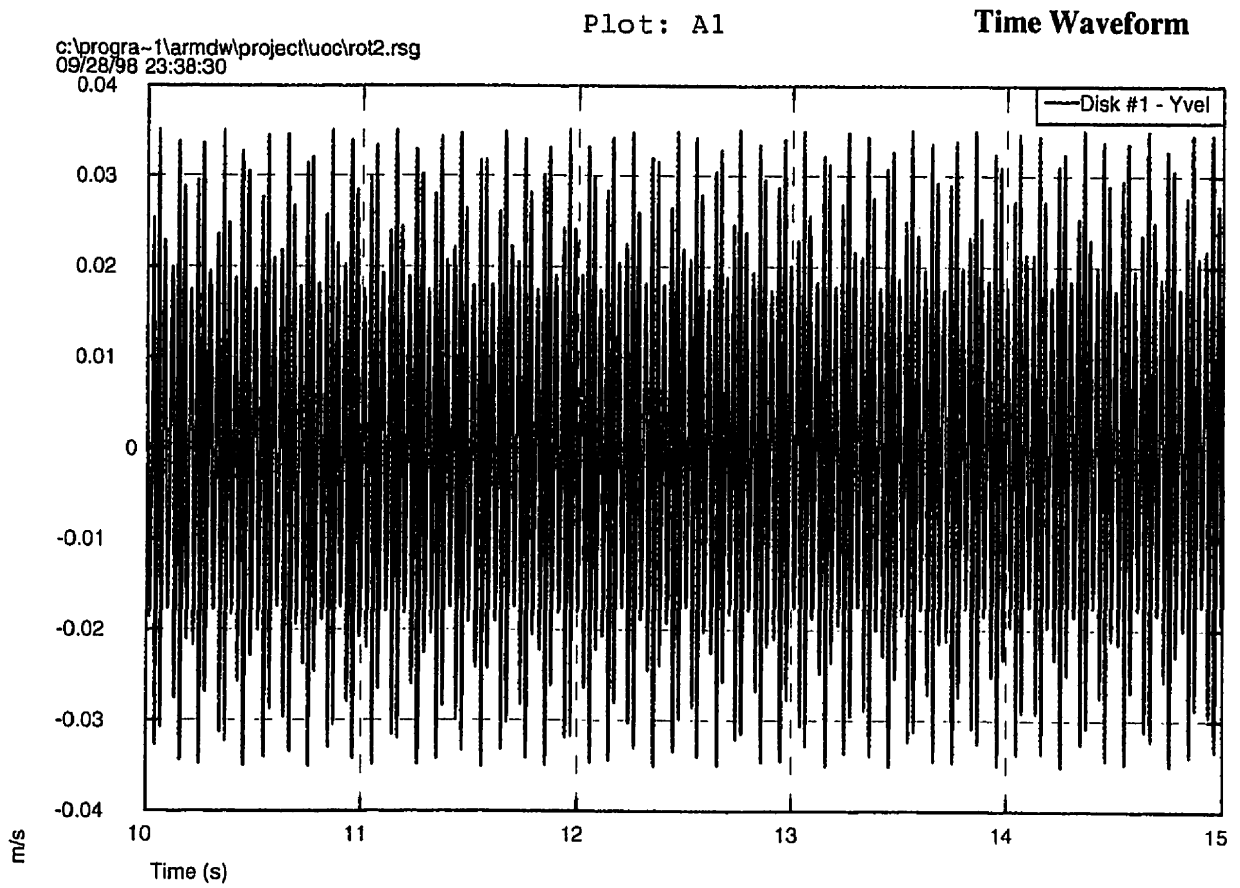
Time Waveform
c:\progra~1\armdw\project\uoc\rot2.rsg
09/28/98 23:38:30
Disk #1 - Yvel
0.04
0.03
0.02
0.01
0
-0.01
-0.02
-0.03
-0.04
m/s
10
11
12
13
14
15
Time (s)

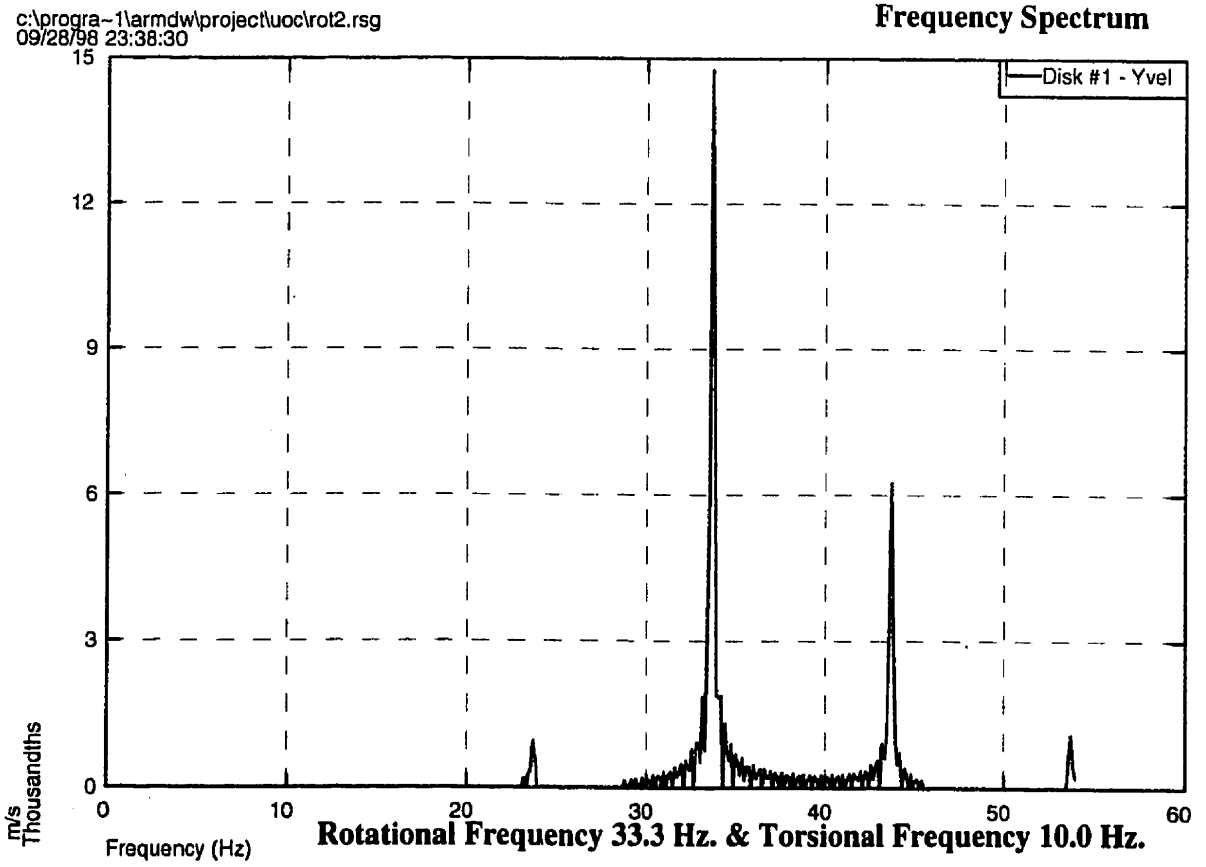
Frequency Spectrum
c:\progra~1\armdw\project\uoc\rot2.rsg
09/28/98 23:38:30
Disk #1 - Yvel
15
12
9
6
3
0
m/s
Thousandths
0
10
20
30
40
50
60
Frequency (Hz)
Rotational Frequency 33.3 Hz. & Torsional Frequency 10.0 Hz.

Plot: A2

Time Waveform

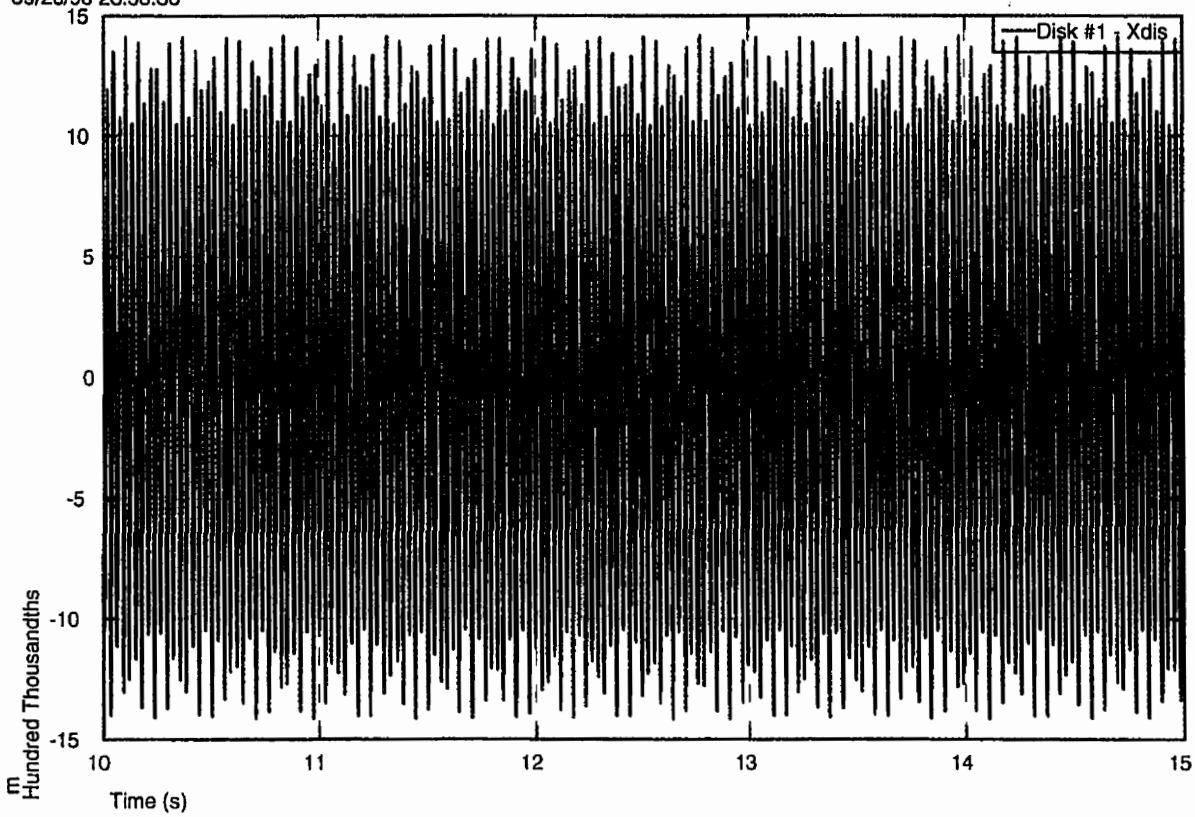

Frequency Spectrum

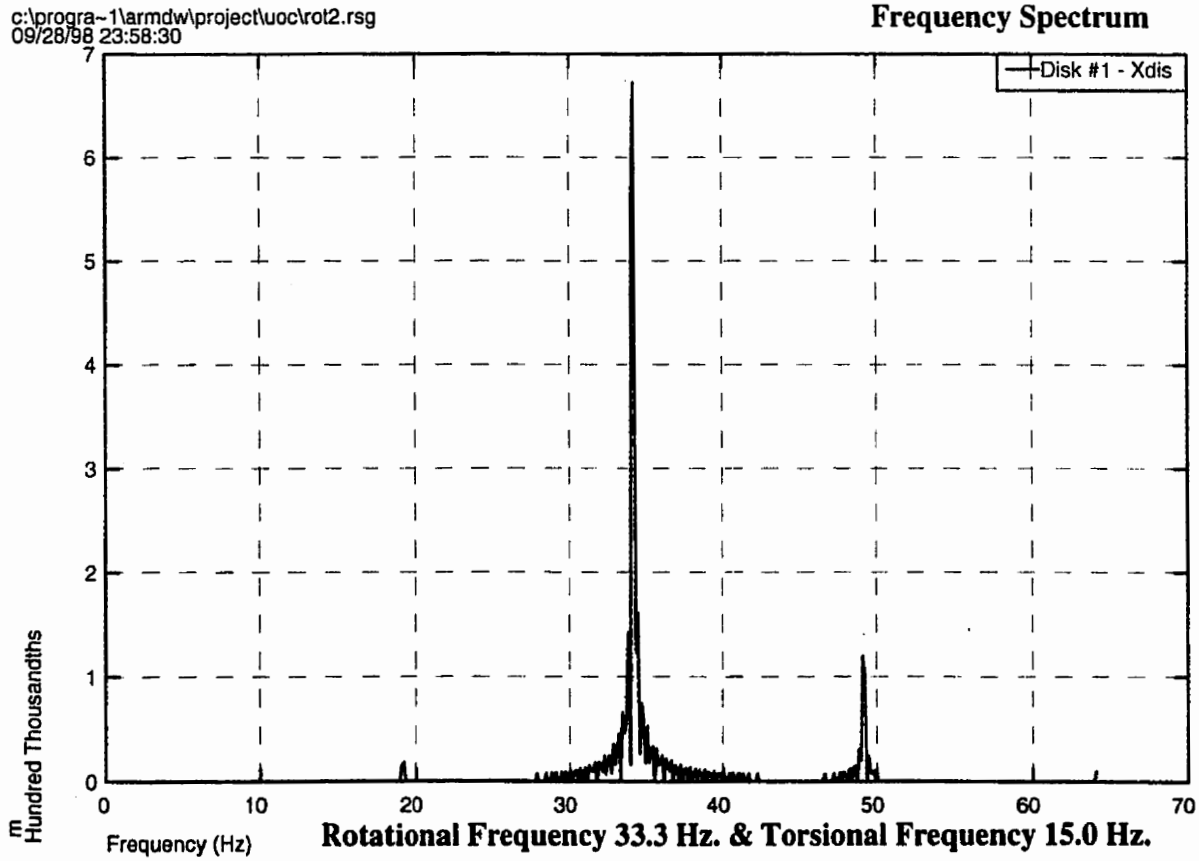

Rotational Frequency 33.3 Hz. & Torsional Frequency 15.0 Hz.

Plot: A3

Time Waveform

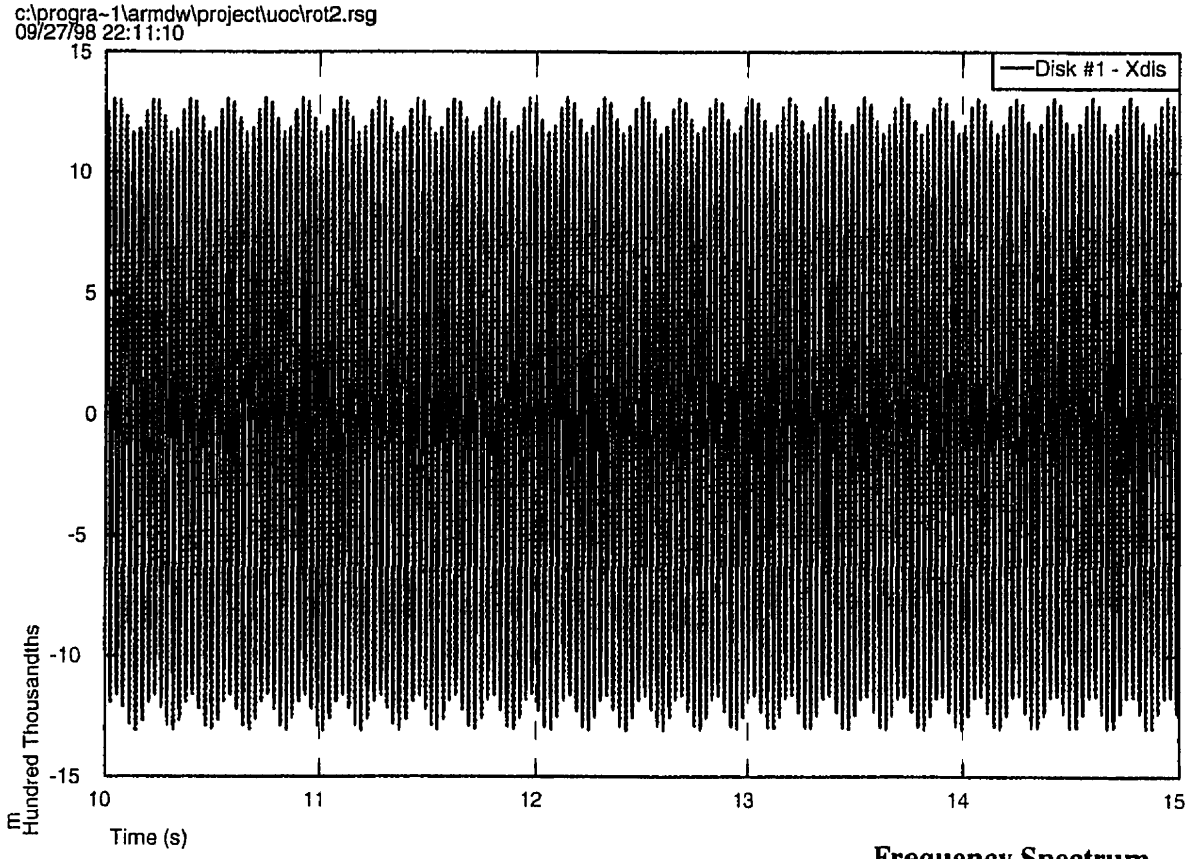

Frequency Spectrum

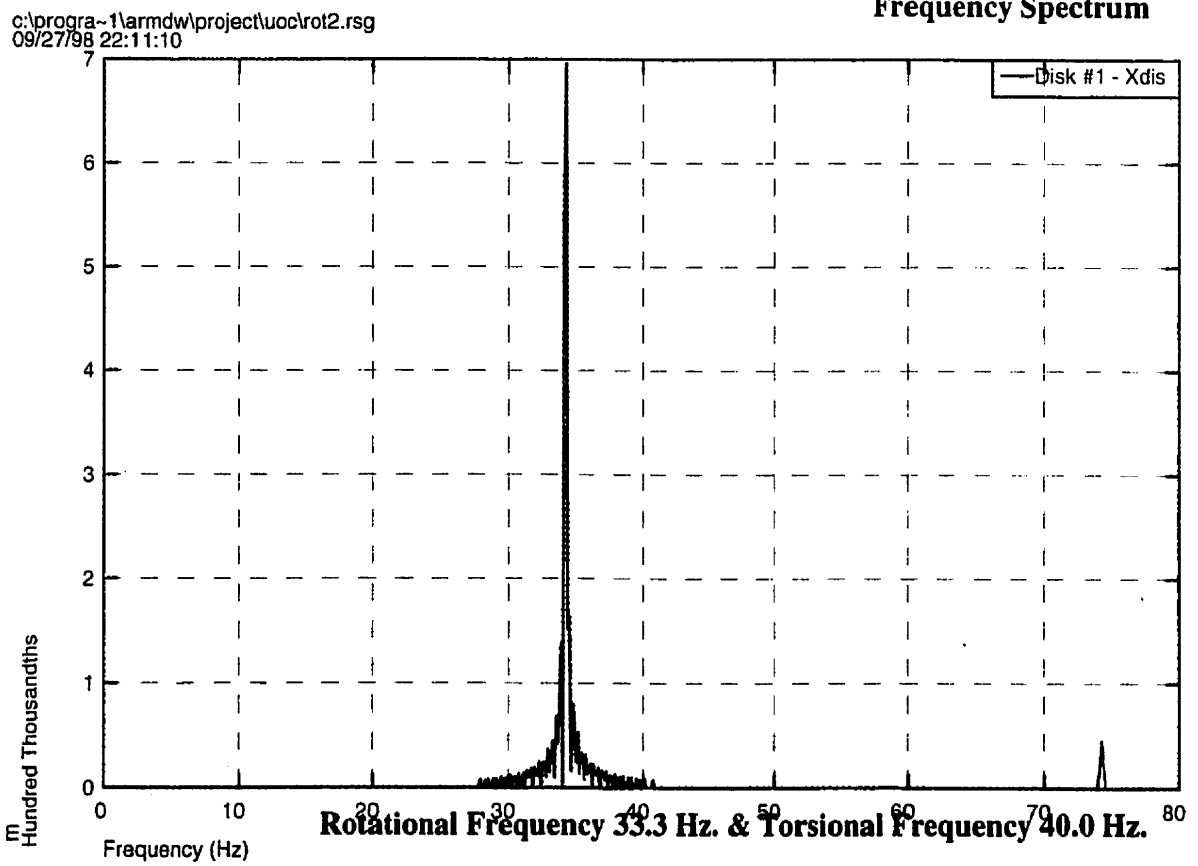

Rotational Frequency 33.3 Hz. & Torsional Frequency 40.0 Hz.

Plot: A4

Time Waveform

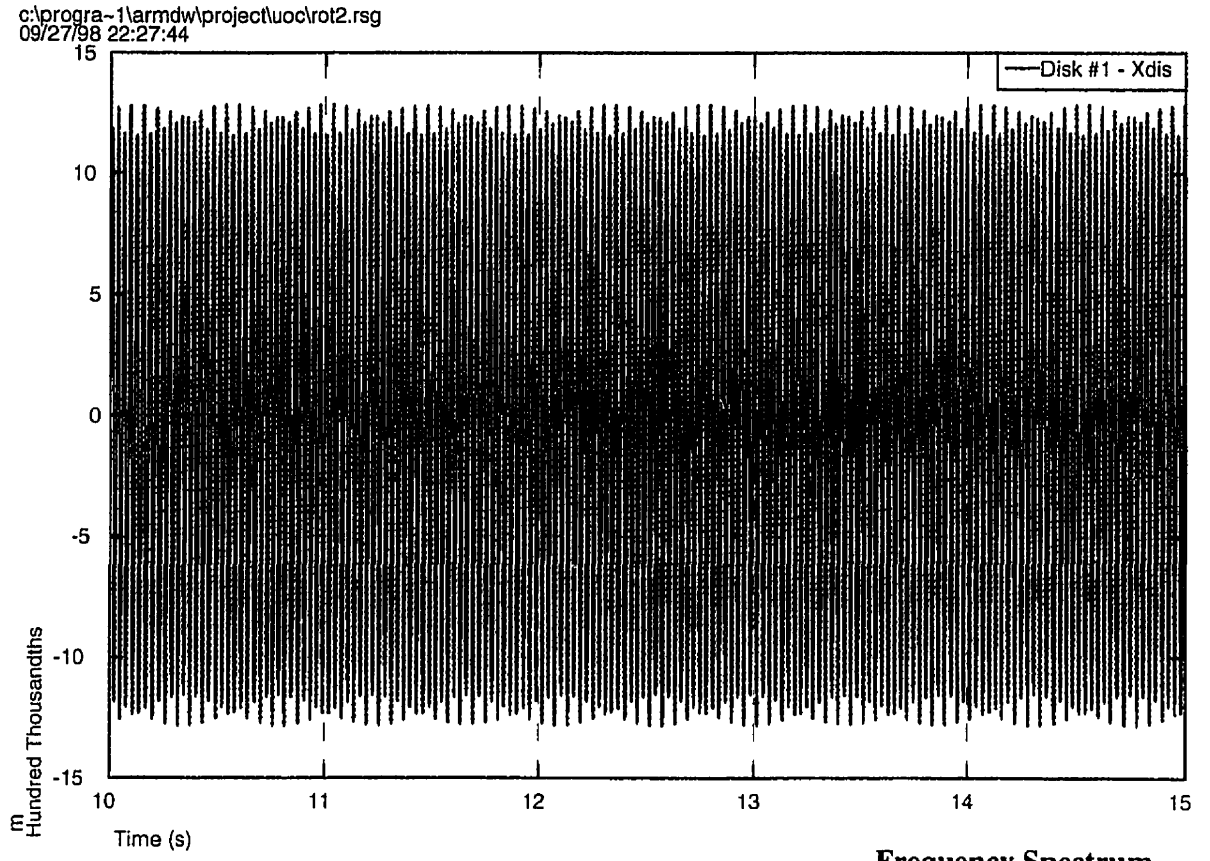

Frequency Spectrum

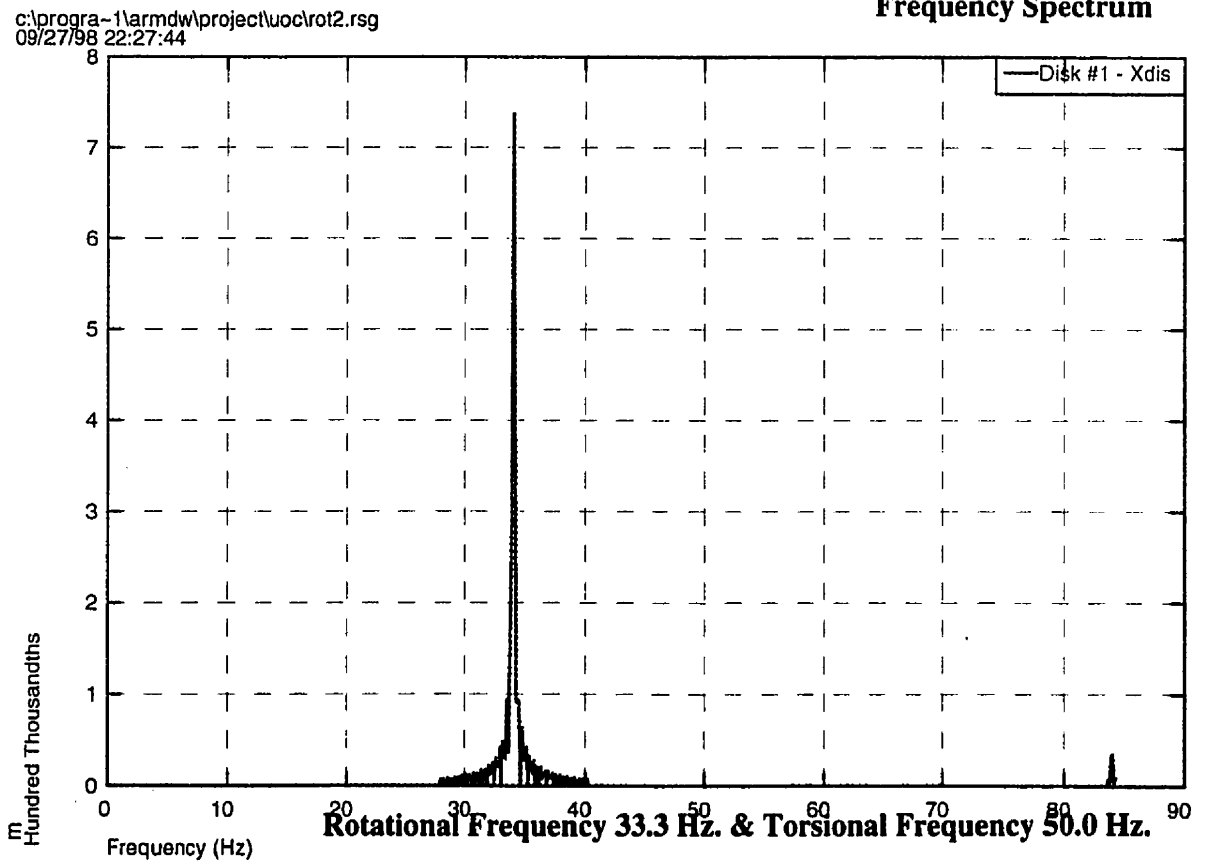

Rotational Frequency 33.3 Hz. & Torsional Frequency 50.0 Hz.

Time Waveform

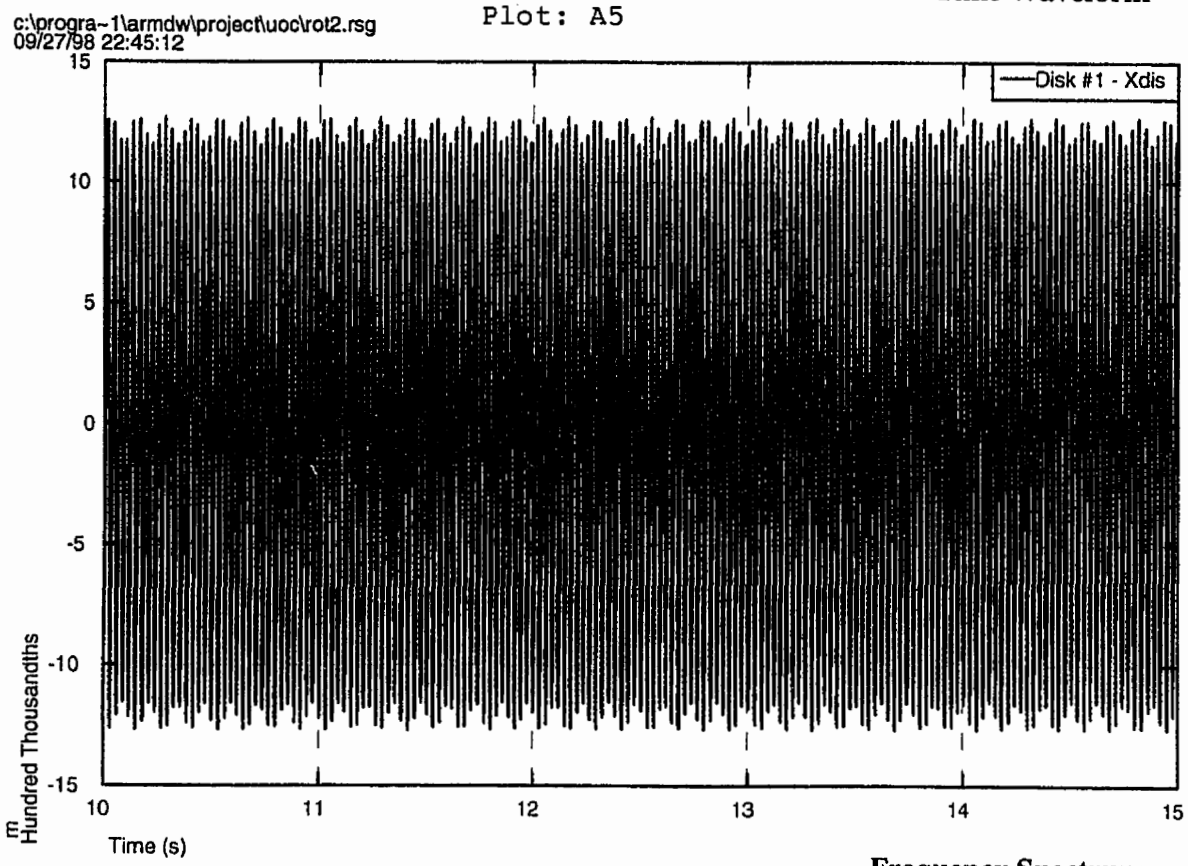

Frequency Spectrum

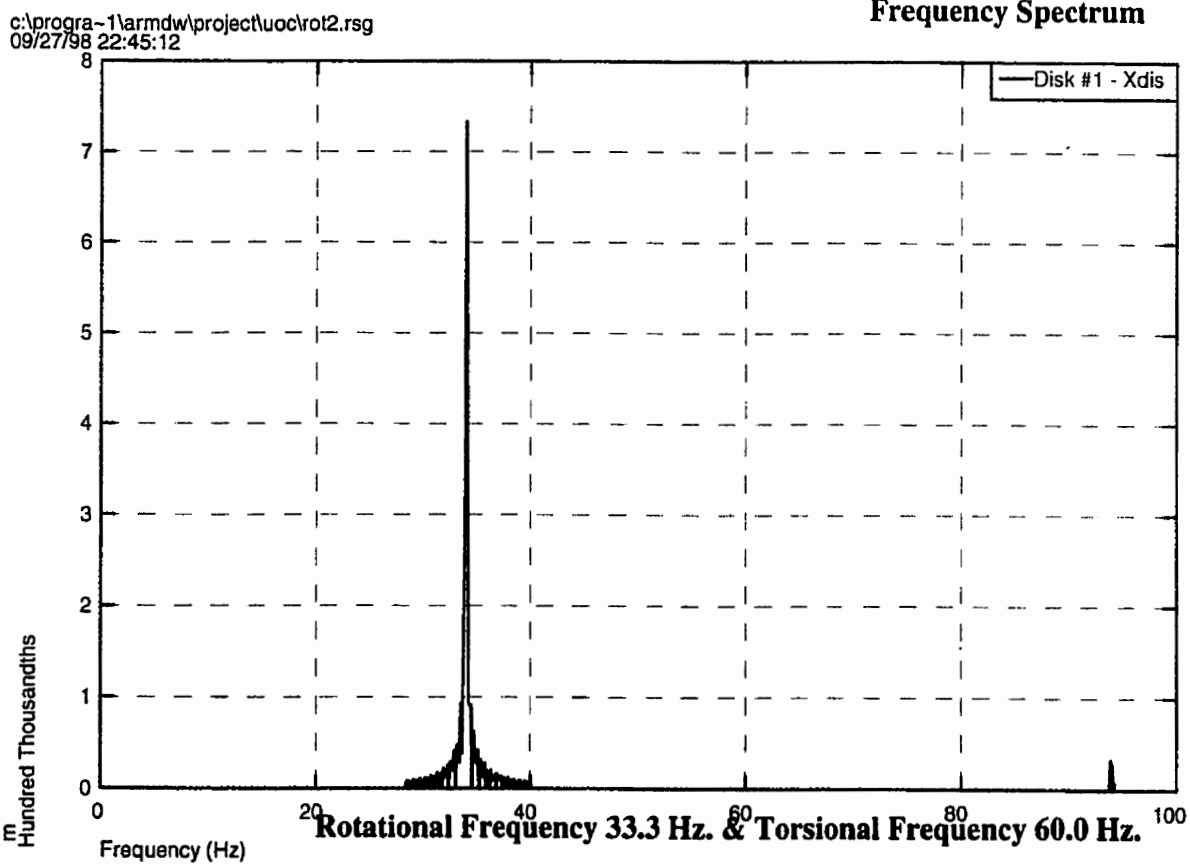

Rotational Frequency 33.3 Hz. & Torsional Frequency 60.0 Hz.

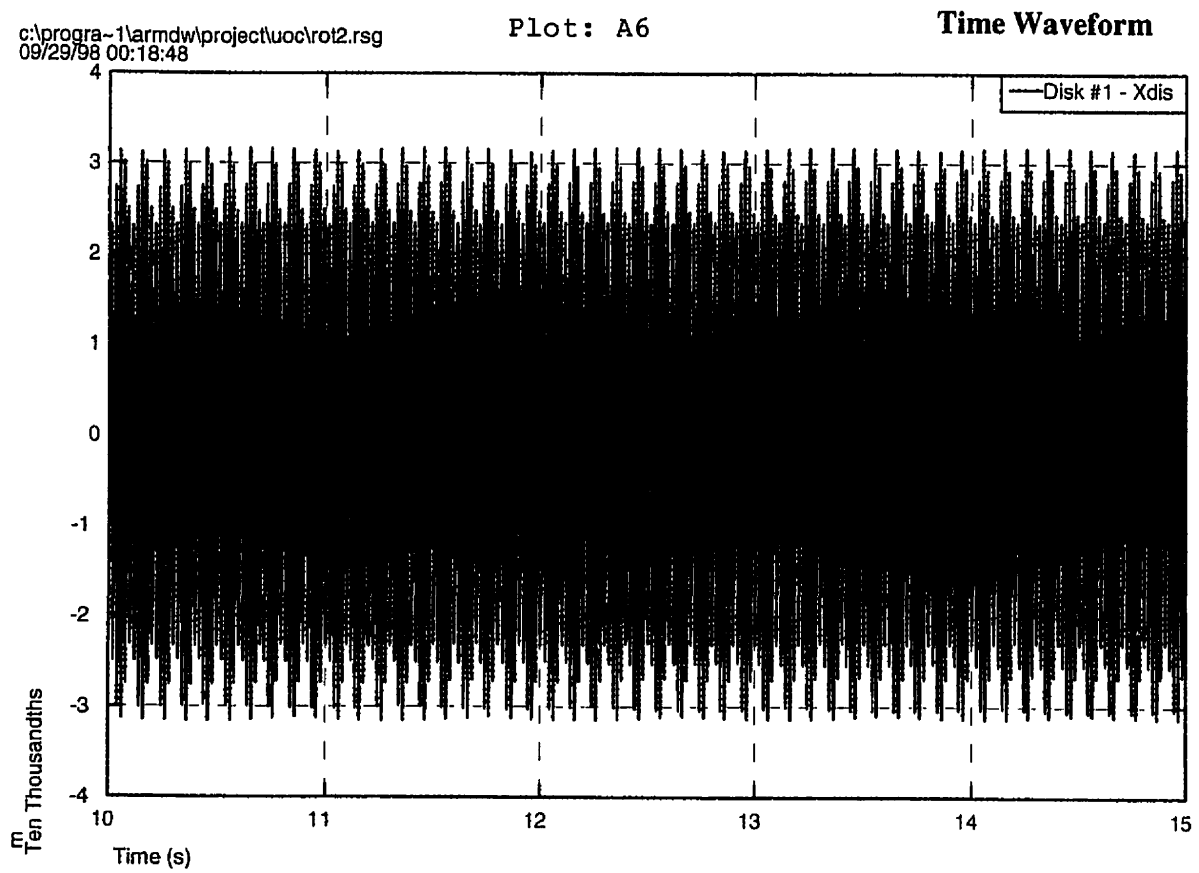
c:\progra~1\armdw\project\uoc\rot2.rsg
09/29/98 00:18:48
Plot: A6
Time Waveform
Disk #1 - Xdis
4
3
2
1
0
-1
-2
-3
-4
10
11
12
13
14
15
Ten Thousandths
Time (s)

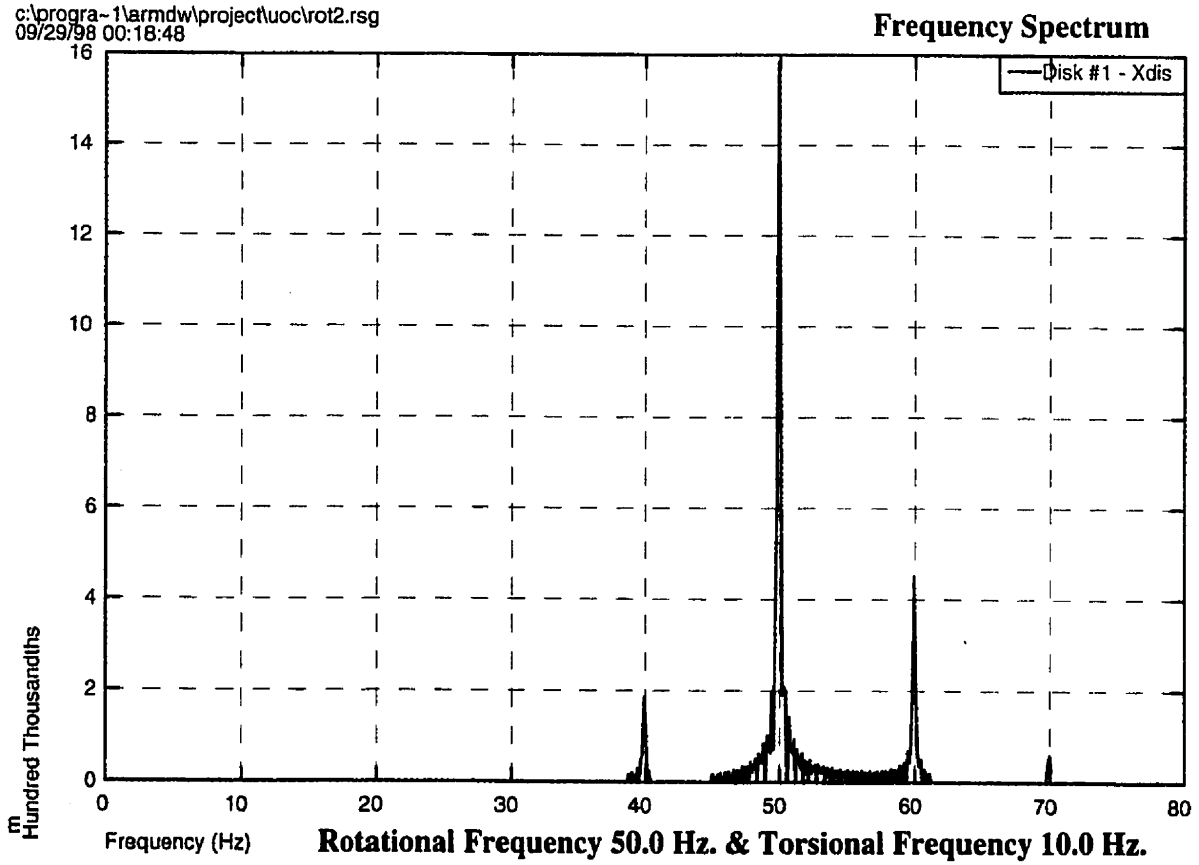
c:\progra~1\armdw\project\uoc\rot2.rsg
09/29/98 00:18:48
Frequency Spectrum
Disk #1 - Xdis
16
14
12
10
8
6
4
2
0
0
10
20
30
40
50
60
70
80
Hundred Thousandths
Frequency (Hz)
Rotational Frequency 50.0 Hz. & Torsional Frequency 10.0 Hz.

Plot: A7

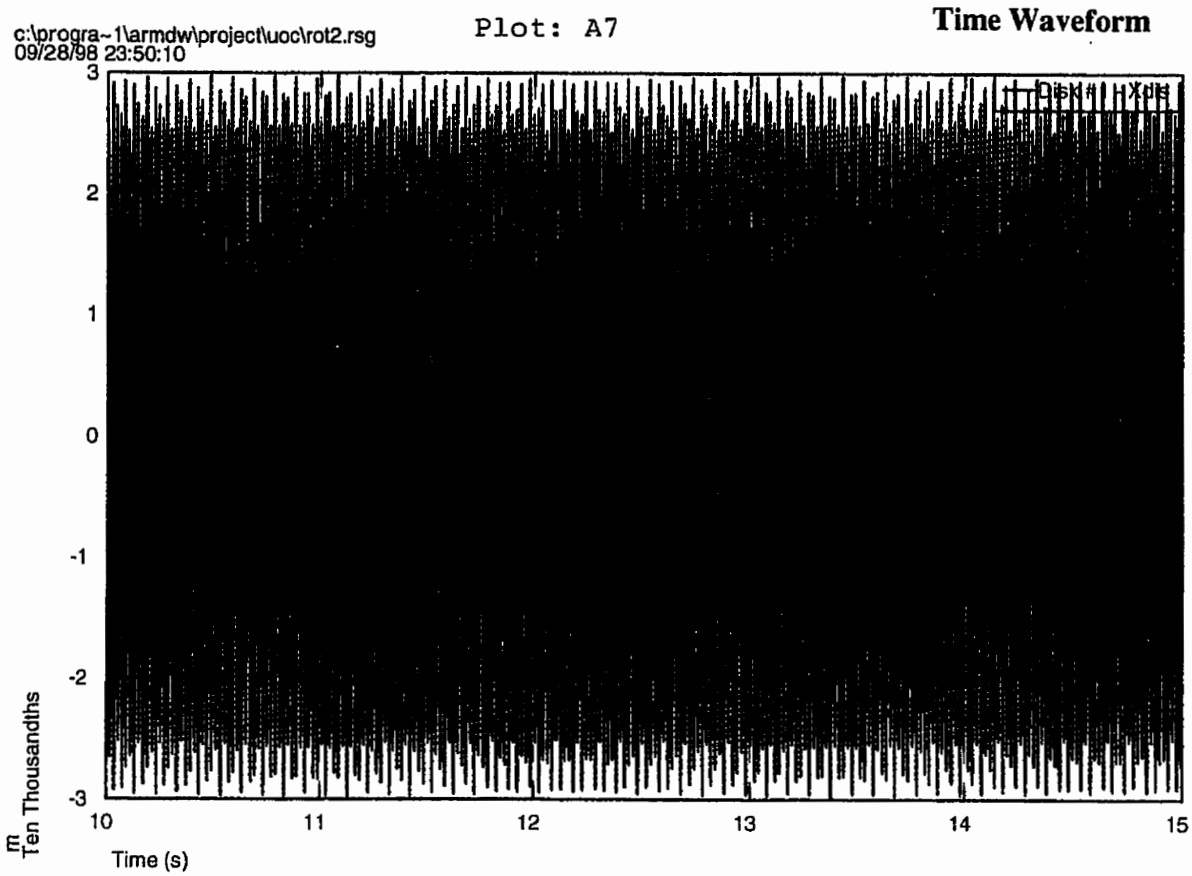
Time Waveform
c:\progra~1\armdw\project\uoc\rot2.rsg
09/28/98 23:50:10
Disk #1 - Xdis
3
2
1
0
-1
-2
-3
10
11
12
13
14
15
Ten Thousandths
Time (s)

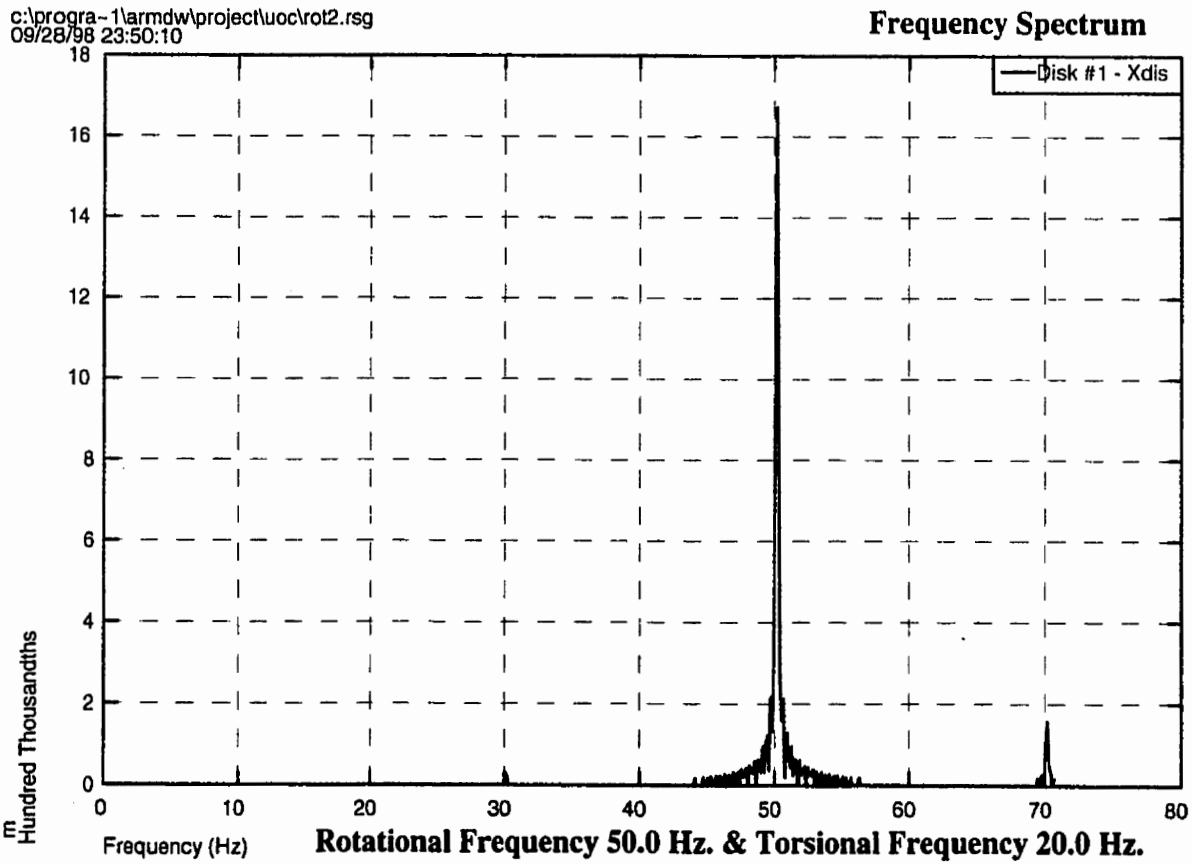
Frequency Spectrum
c:\progra~1\armdw\project\uoc\rot2.rsg
09/28/98 23:50:10
Disk #1 - Xdis
18
16
14
12
10
8
6
4
2
0
0
10
20
30
40
50
60
70
80
Hundred Thousandths
Frequency (Hz)
Rotational Frequency 50.0 Hz. & Torsional Frequency 20.0 Hz.

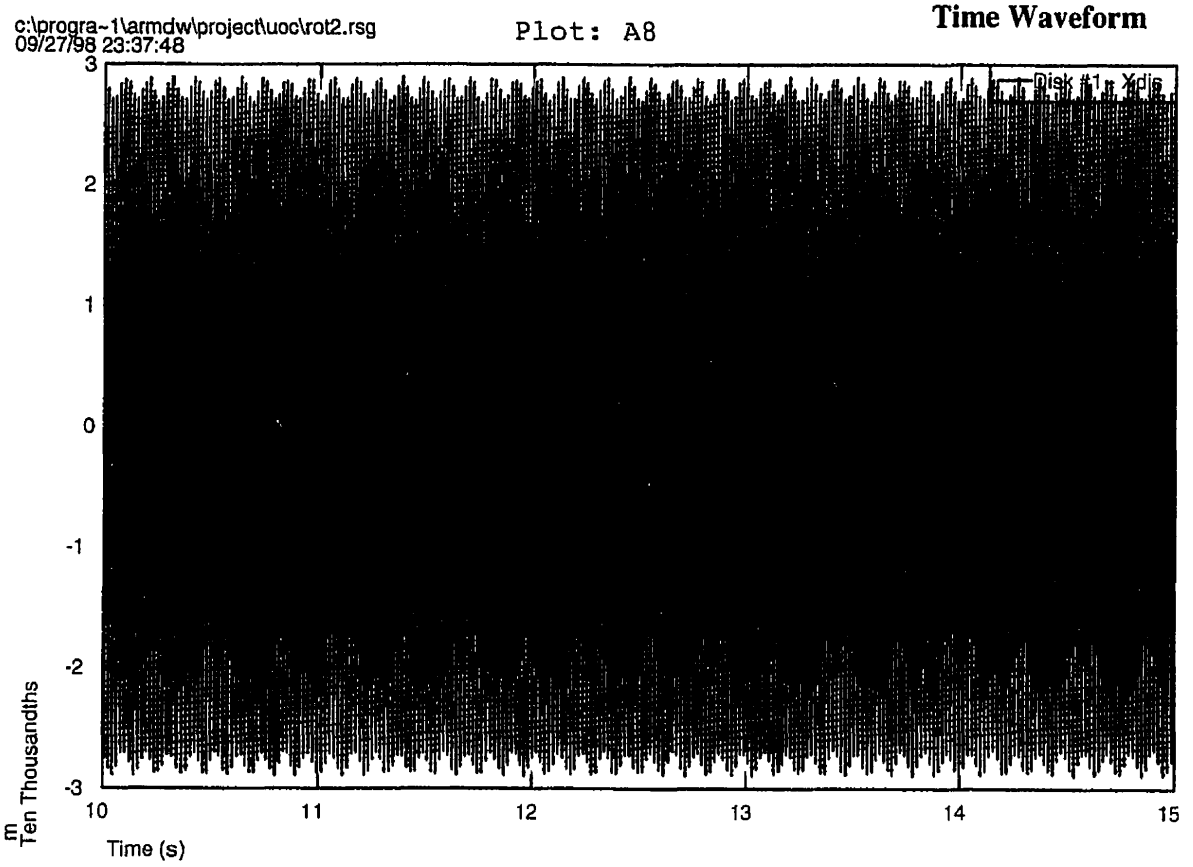

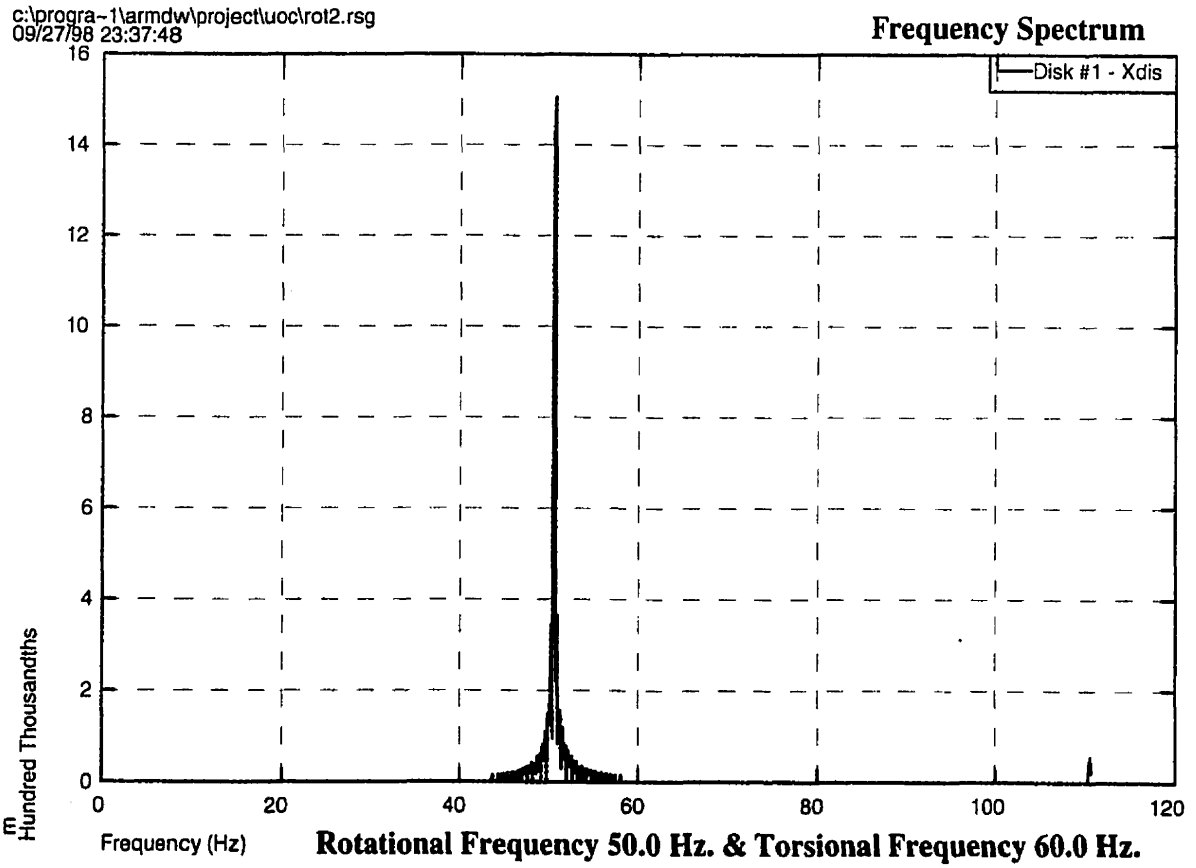

Rotational Frequency 50.0 Hz. & Torsional Frequency 60.0 Hz.

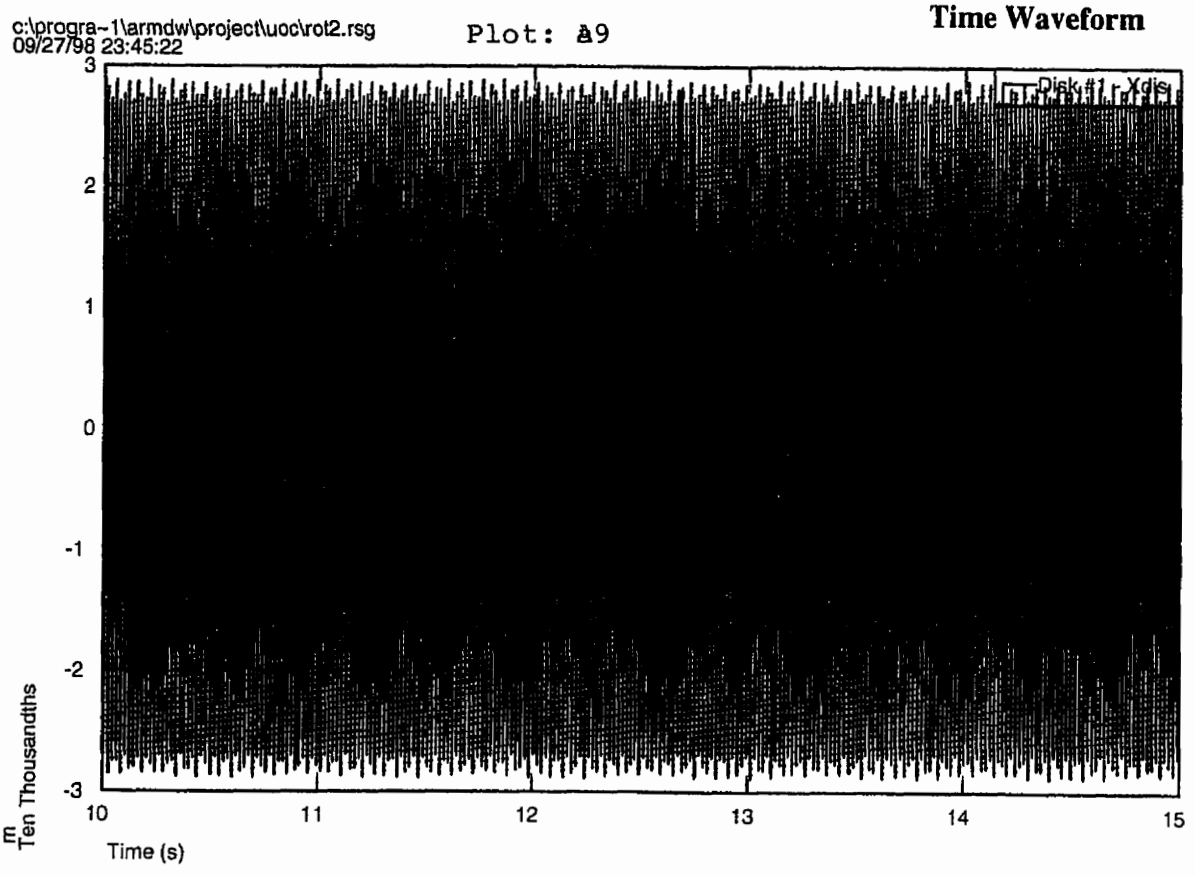

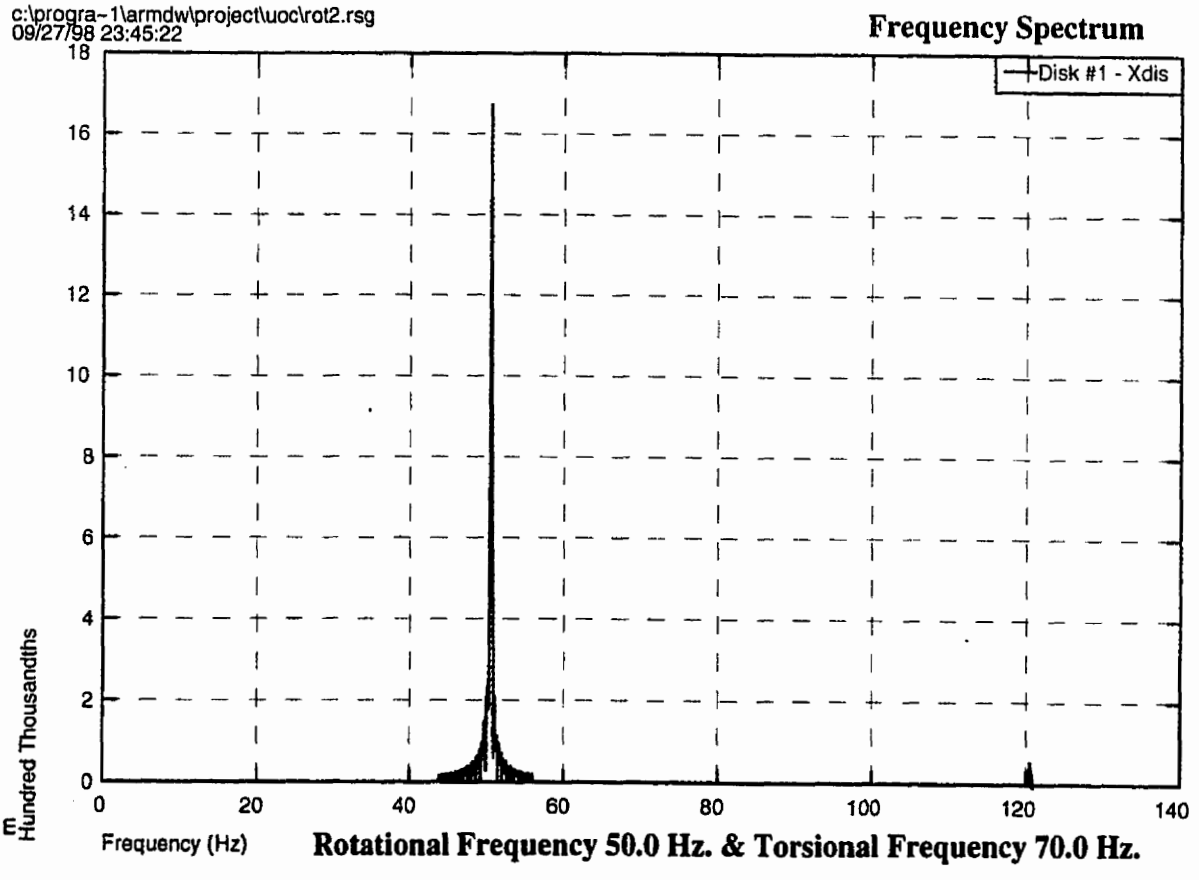

Rotational Frequency 50.0 Hz. & Torsional Frequency 70.0 Hz.

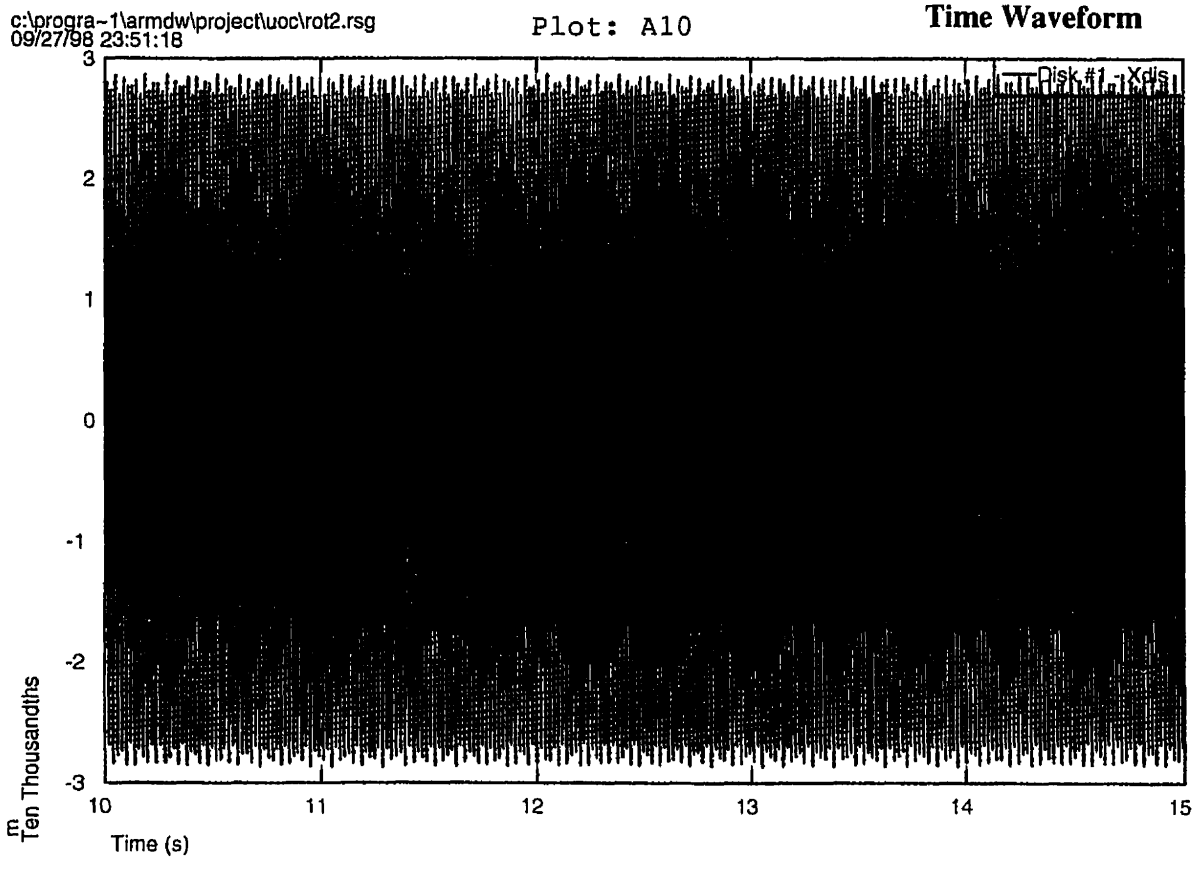

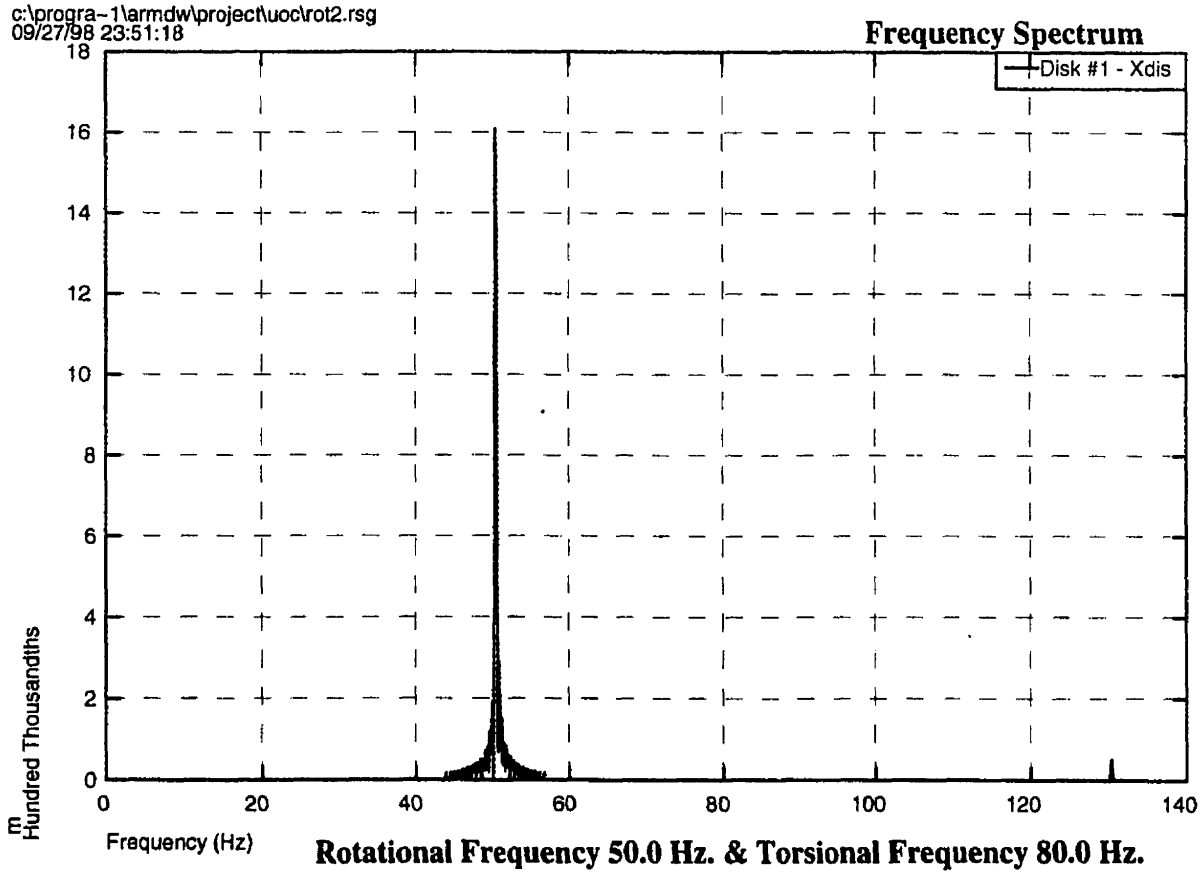

Rotational Frequency 50.0 Hz. & Torsional Frequency 80.0 Hz.

Appendix B1

Computed lateral vibration response plots as per Case 11 of Chapter 4, Section 4.6 are attached in this appendix.

```
Two Disk Test File
7 150000  0.00010 100000  10 3000.0  9.8
138.723  10.2544  138.723 10.2544
0.038   0.000
5000.
1.25264e9  -1.0481e9  -1.0481e9  1.25264e9  3.97572e6
30000.0   900.0    0.0
    0.0     0.0    0.0
```

Input Guide

```
LINE 1:TITLE (72 CHARACTERS)
LINE 2:NUMB. OF DEGREES OF FREEDOM (ALWAYS 7 = 6 + 1 RIGID BODY ROTATION)
       NUMB. OF TIME STEPS
       TIME STEP INCREMENT (DELTA T - SECONDS)
       NUMB. OF TIME STEPS TO SKIP BEFORE BEGINNING TO PRINT OUTPUT
       NUMB. OF TIME STEPS TO SKIP BETWEEN OUTPUT PRINTING (EVERY 10TH STEP)
       SHAFT SPEED (RPM)
       GRAVITY (M/S^2)
LINE 3:DISK #1 MASS (KG)
       DISK #1 POLAR INERTIA (KG-M^2)
       DISK #2 MASS (KG)
       DISK #2 POLAR INERTIA (KG-M^2)
LINE 4:DISK #1 ECC. FROM SHAFT CENTER TO CENTER OF MASS (M)
       DISK #2 ECC. FROM SHAFT CENTER TO CENTER OF MASS (M)
LINE 5:DAMPING FOR LATERAL BEAM BENDING

LINE 6:K11 LATERAL SHAFT STIFFNESS
       K12 LATERAL SHAFT STIFFNESS
       K21 LATERAL SHAFT STIFFNESS
       K22 LATERAL SHAFT STIFFNESS
       TAU TORSIONAL STIFFNESS
LINE 7:DISK #1 TORQUE AMPLITUDE (N-M)
       DISK #1 TORQUE FREQUENCY (RAD/SEC)
       DISK #1 TORQUE PHASE ANGLE (RAD)
       DISK #2 TORQUE AMPLITUDE (N-M)
       DISK #2 TORQUE FREQUENCY (RAD/SEC)
       DISK #2 TORQUE PHASE ANGLE (RAD)
```

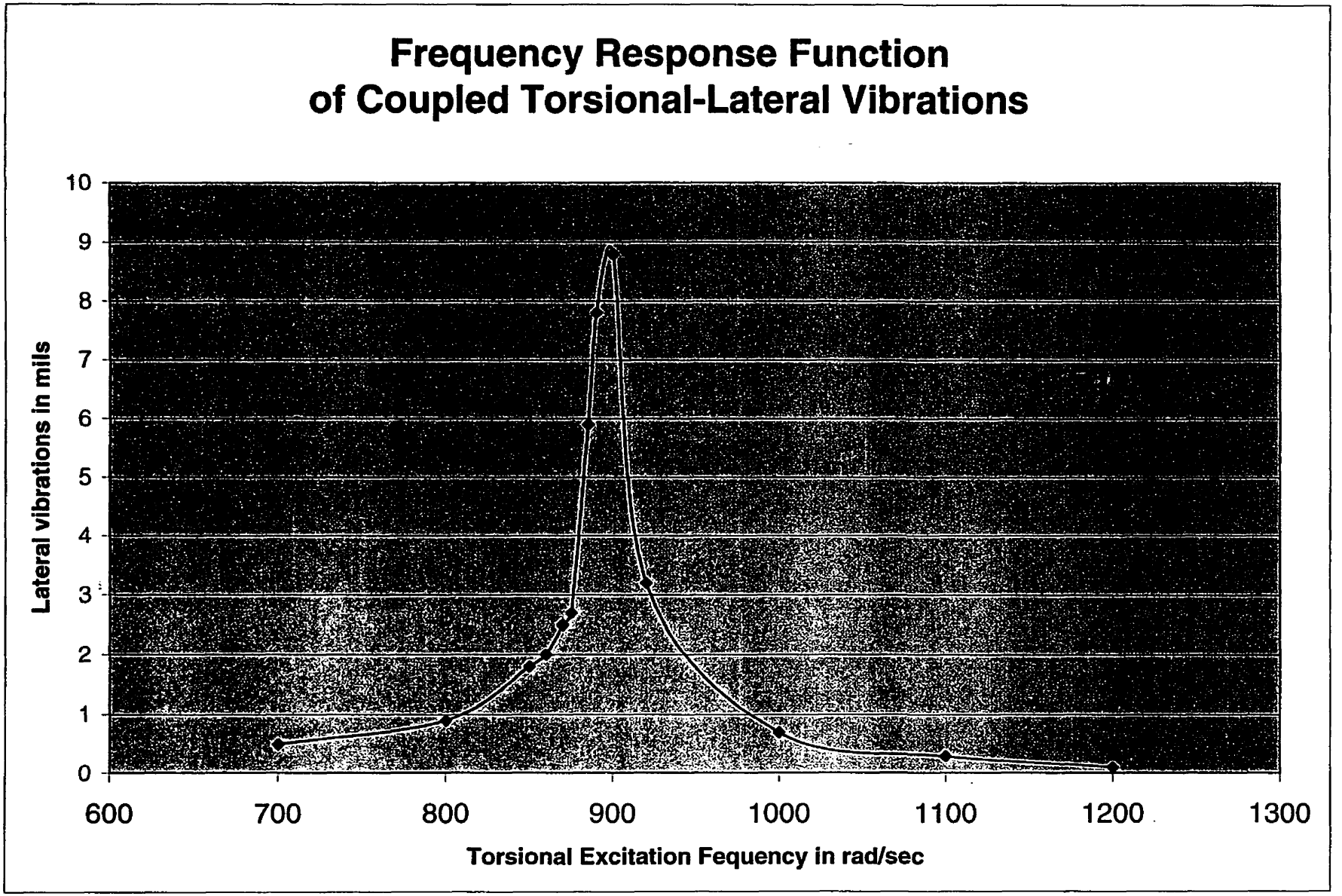
Frequency Response Function
of Coupled Torsional-Lateral Vibrations
Lateral vibrations in mils
10
9
8
7
6
5
4
3
2
1
0
600
700
800
900
1000
1100
1200
1300
Torsional Excitation Fequency in rad/sec

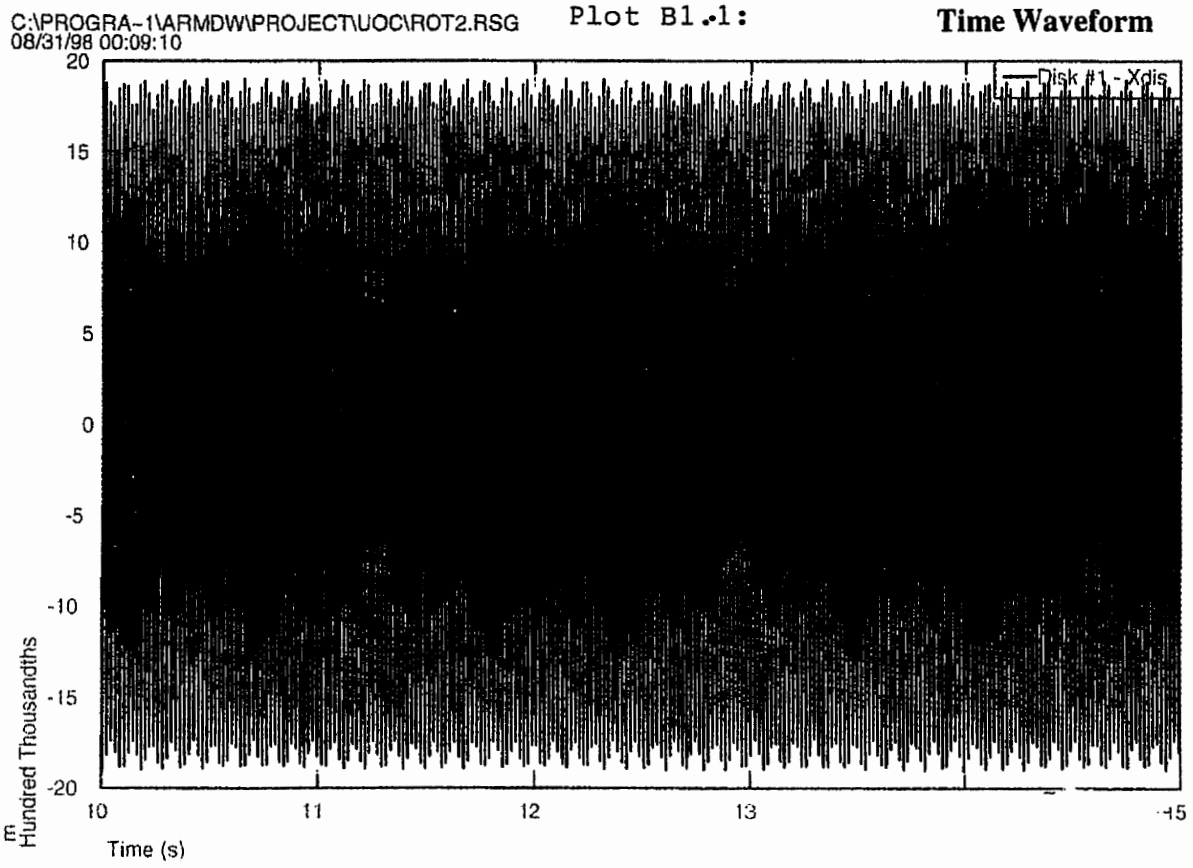

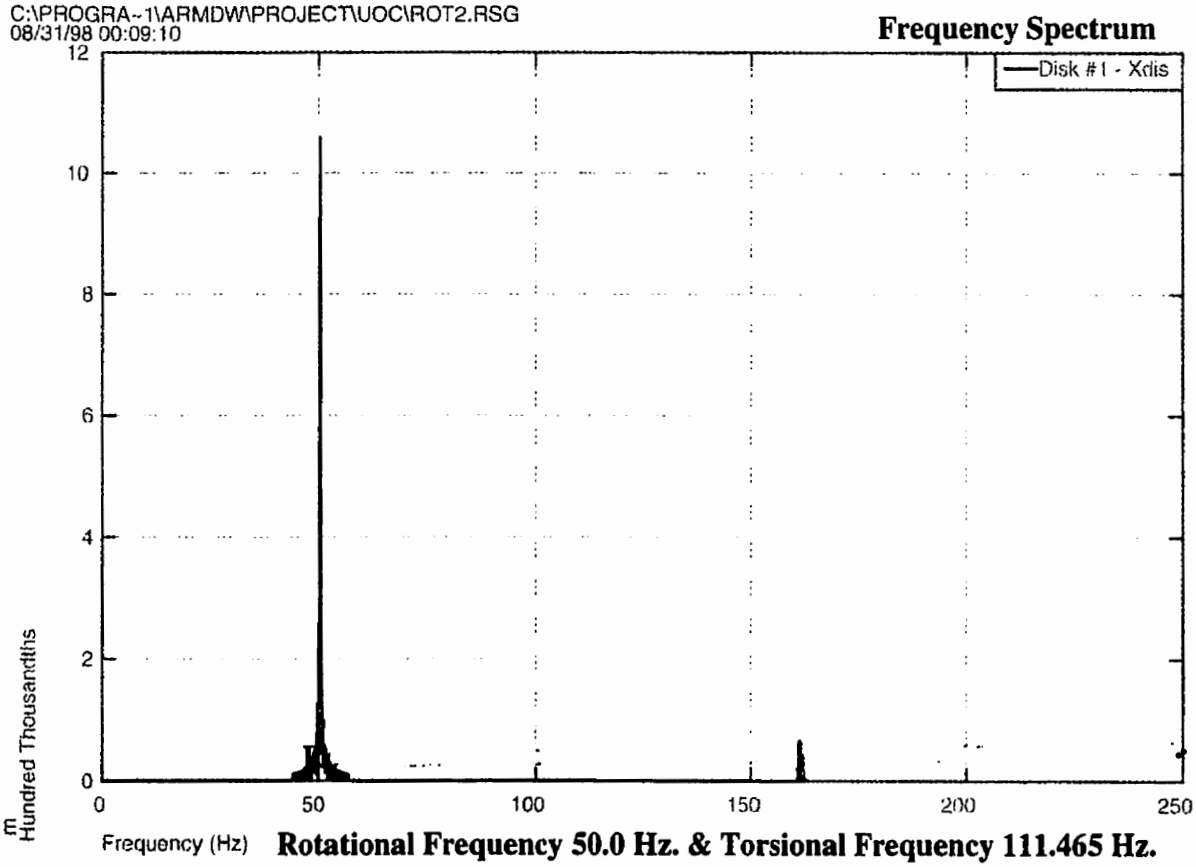

Rotational Frequency 50.0 Hz. & Torsional Frequency 111.465 Hz.

C:\PROGRA~1\ARMDW\PROJECT\UOC\ROT2.RSG
08/31/98 00:05:18

Plot B1.2

Time Waveform

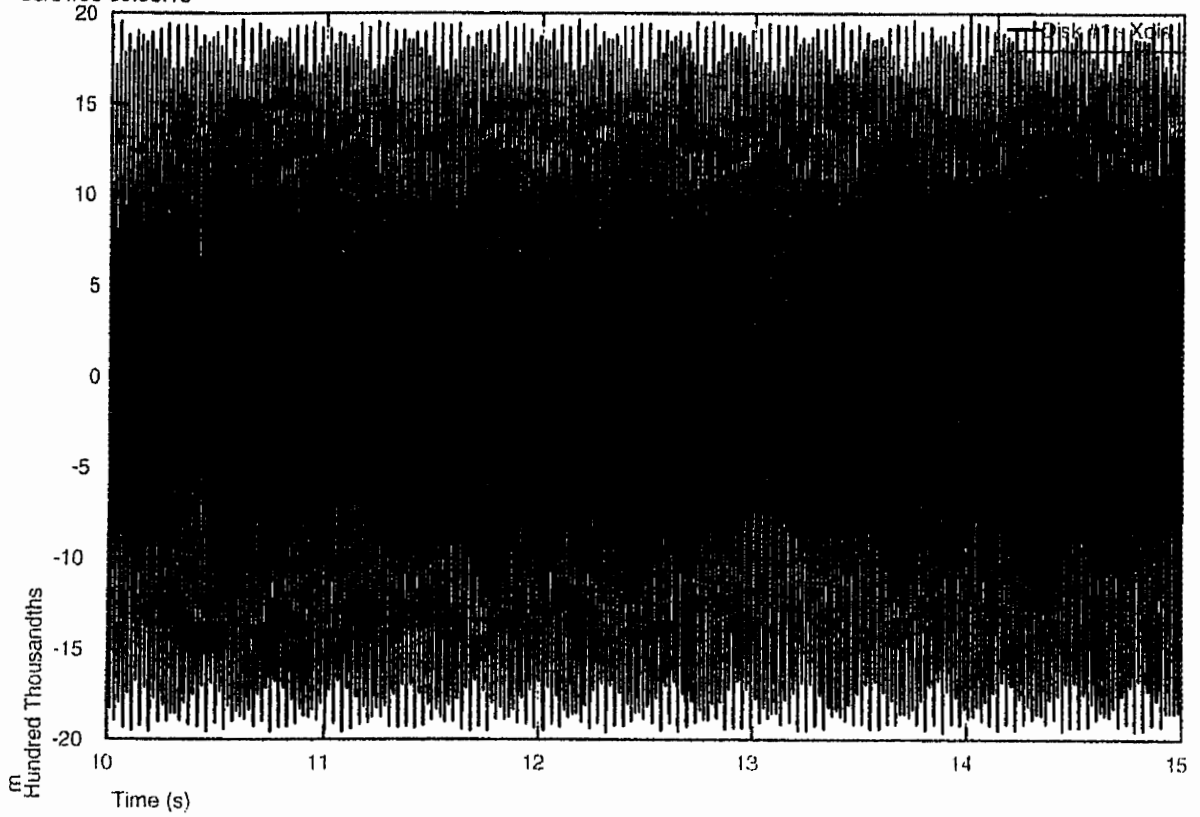

C:\PROGRA~1\ARMDW\PROJECT\UOC\ROT2.RSG
08/31/98 00:05:18

Frequency Spectrum

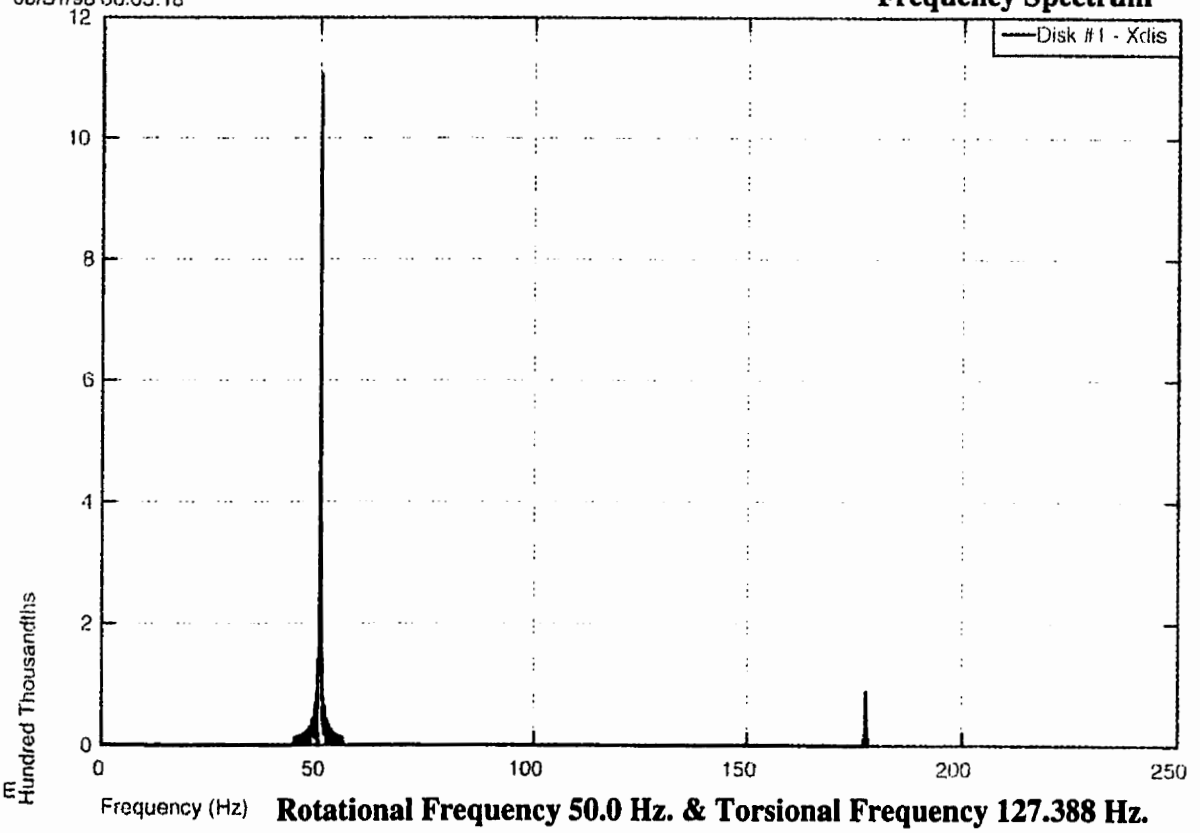

Rotational Frequency 50.0 Hz. & Torsional Frequency 127.388 Hz.

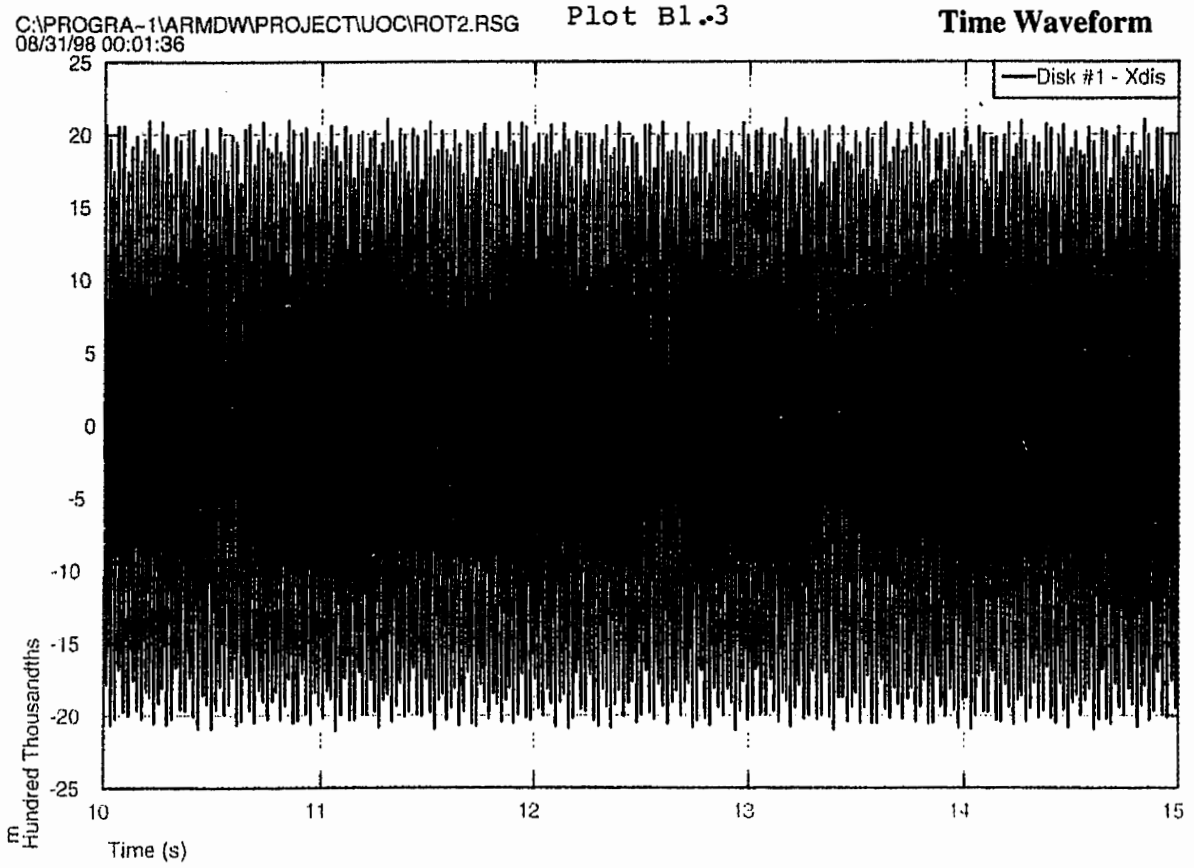

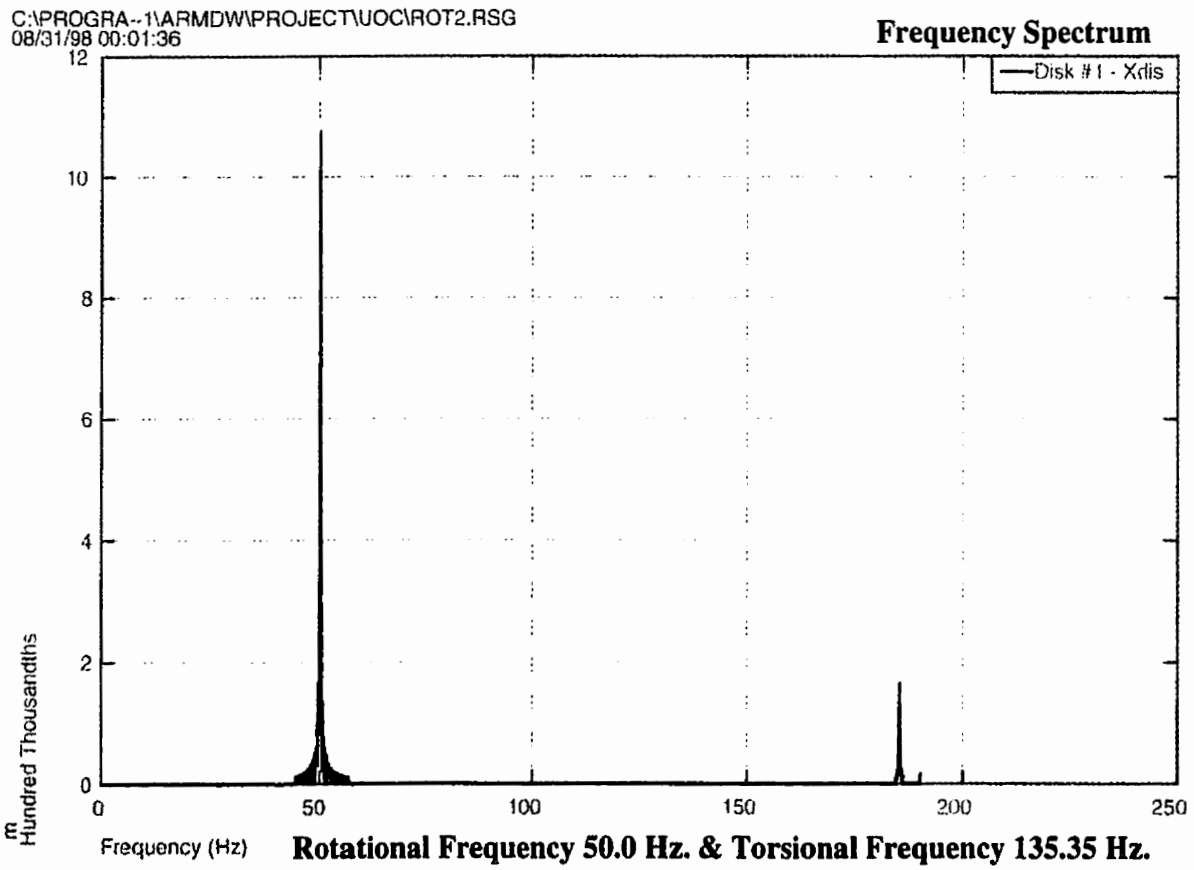

Rotational Frequency 50.0 Hz. & Torsional Frequency 135.35 Hz.

C:\PROGRA~1\ARMDW\PROJECT\UOC\ROT2.RSG
08/30/98 23:56:04

Plot B1.4

Time Waveform

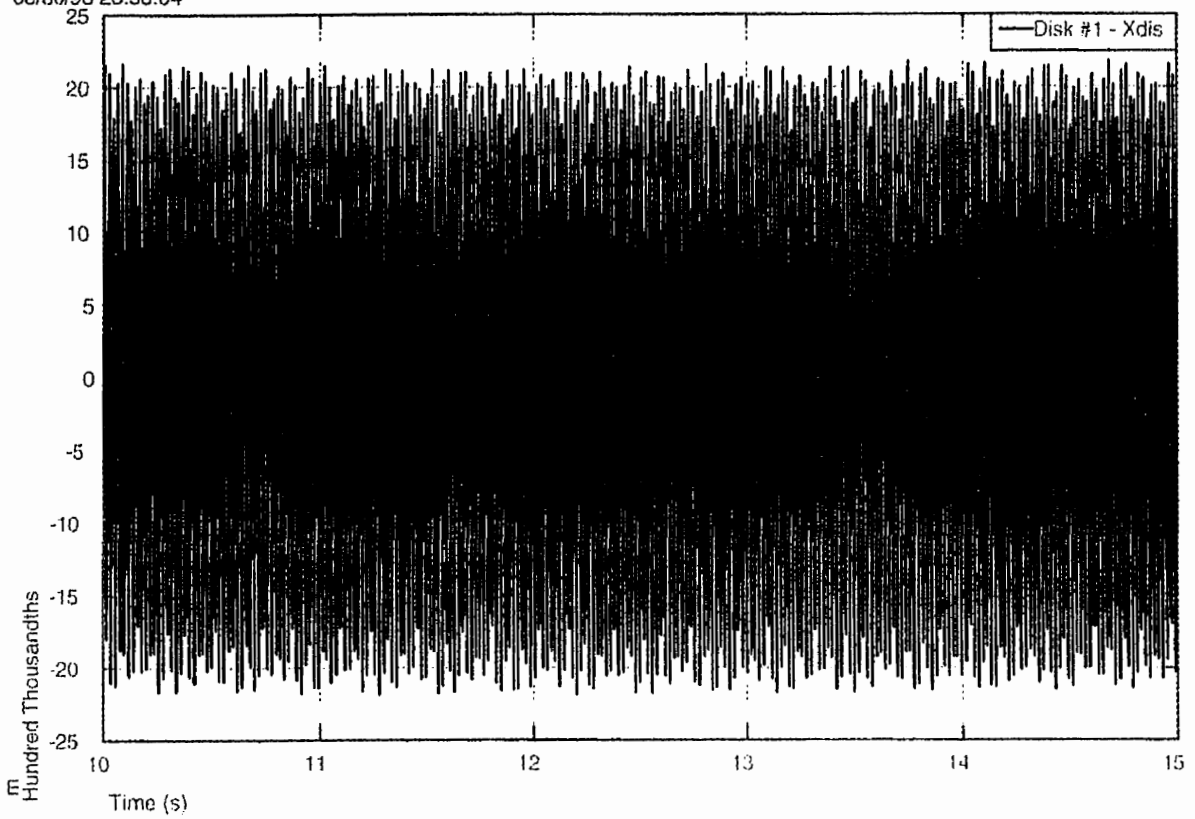

C:\PROGRA~1\ARMDW\PROJECT\UOC\ROT2.RSG
08/30/98 23:56:04

Frequency Spectrum

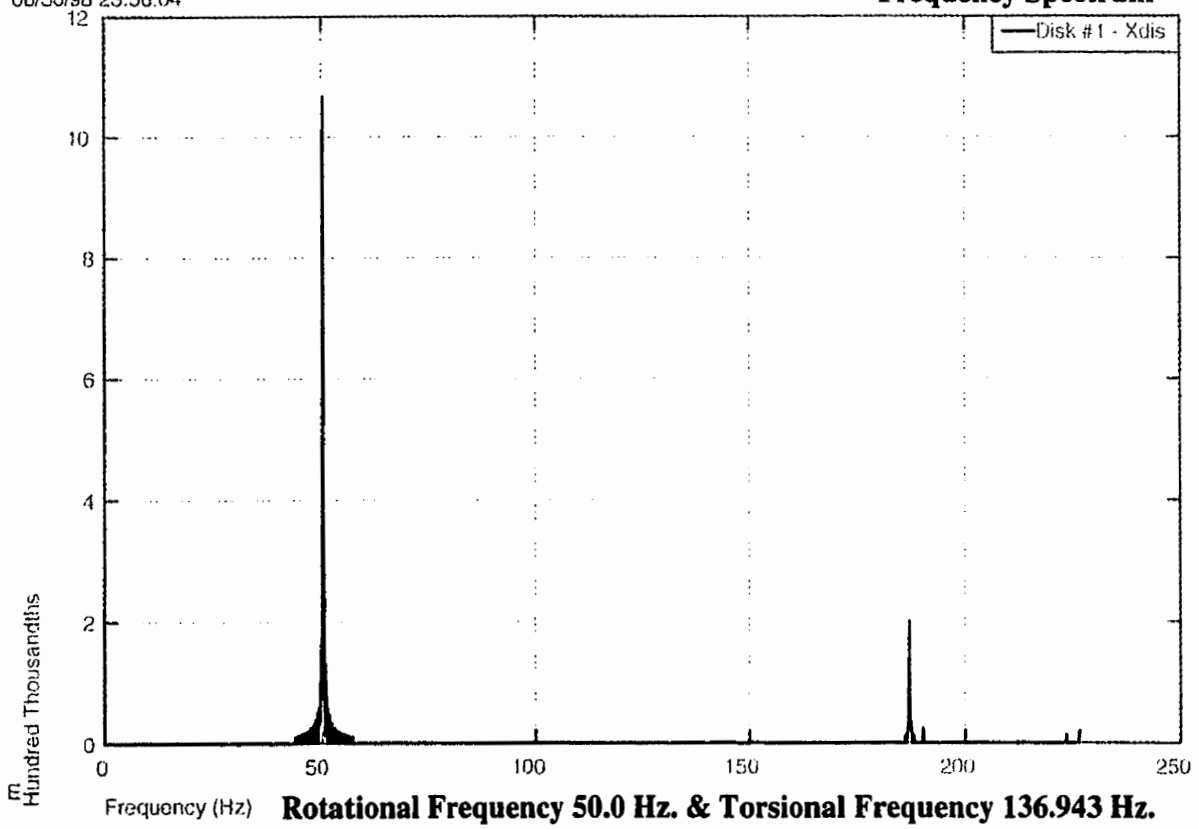

Rotational Frequency 50.0 Hz. & Torsional Frequency 136.943 Hz.

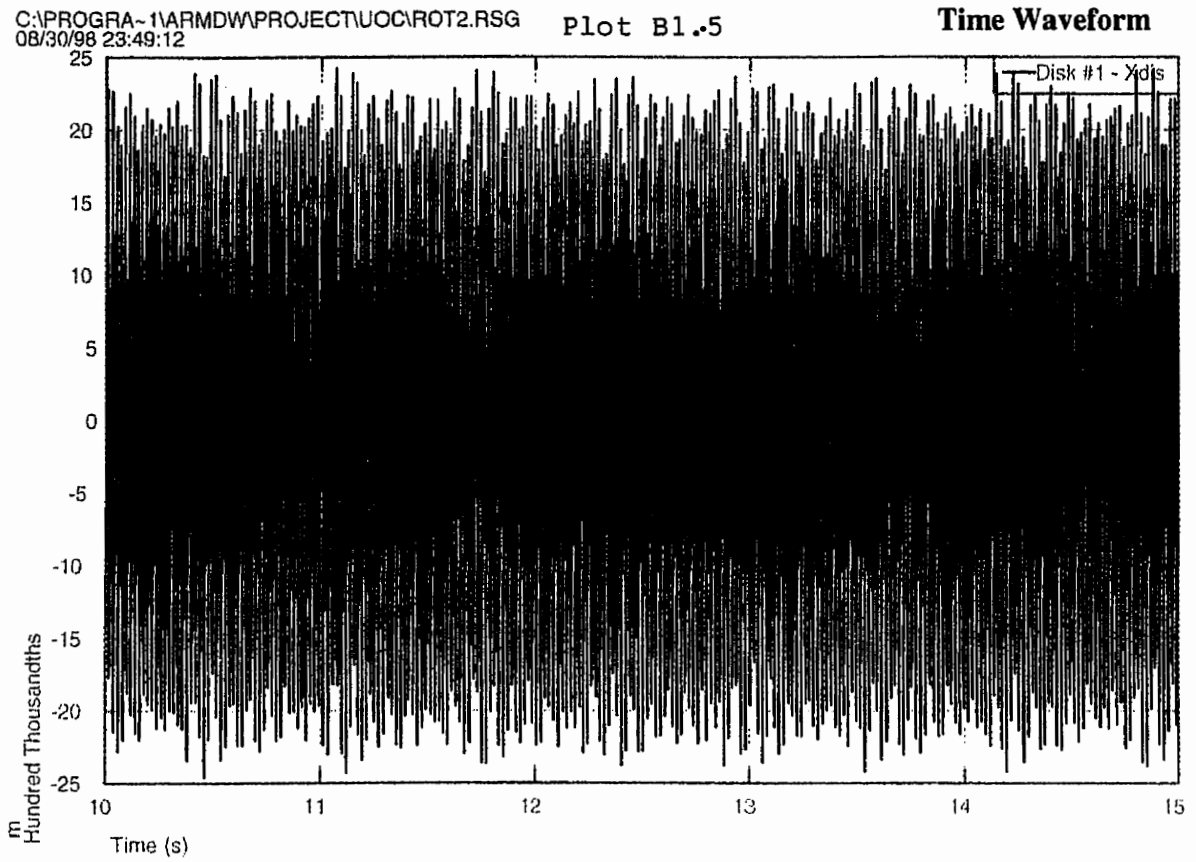

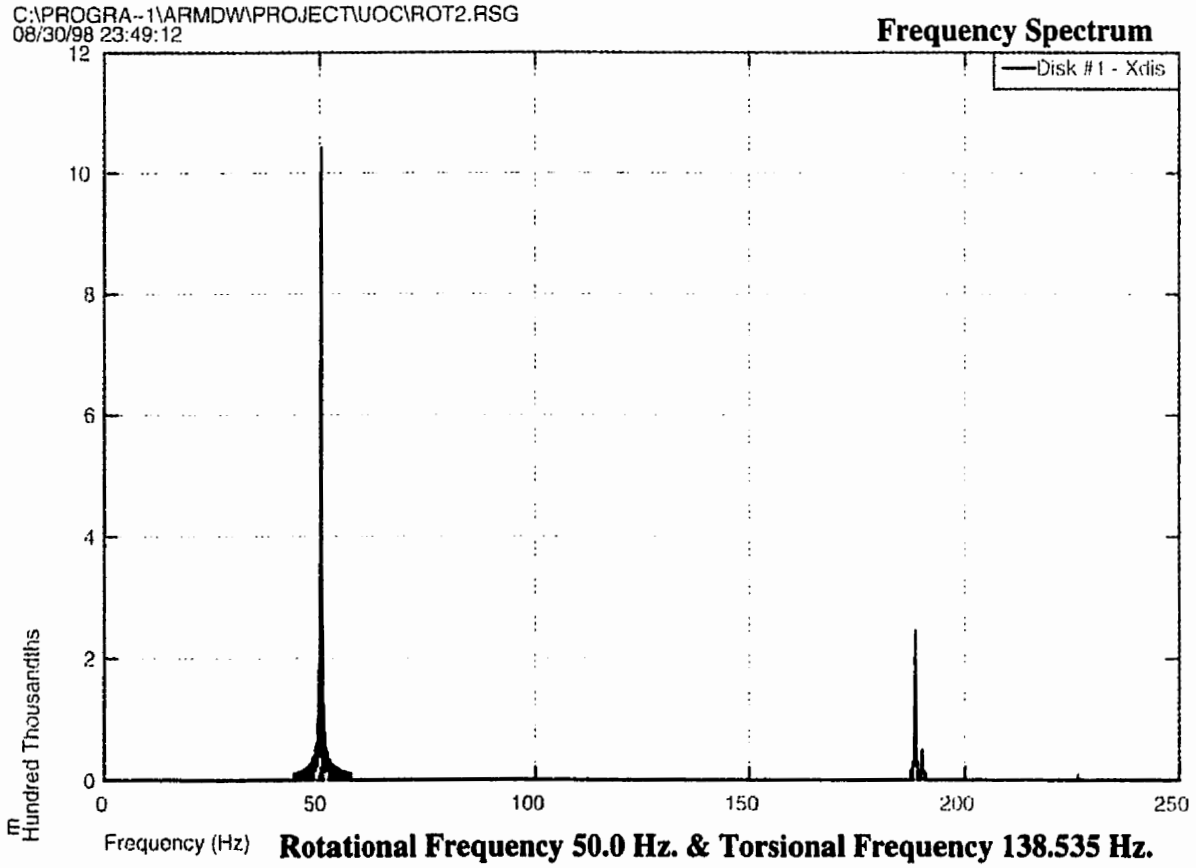

Rotational Frequency 50.0 Hz. & Torsional Frequency 138.535 Hz.

C:\PROGRA~1\ARMDW\PROJECT\UOC\ROT2.RSG
08/30/98 23:44:34

Plot B1.6

Time Waveform

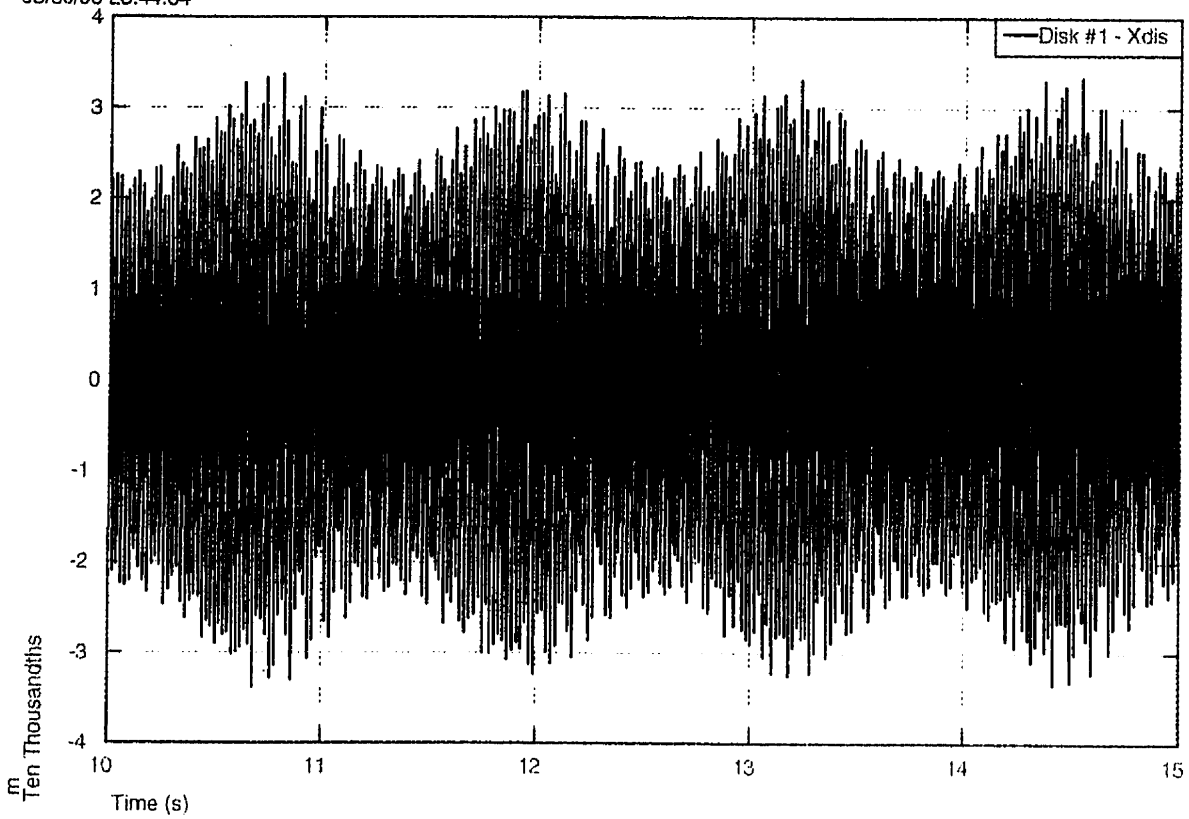

C:\PROGRA~1\ARMDW\PROJECT\UOC\ROT2.RSG
08/30/98 23:44:34

Frequency Spectrum

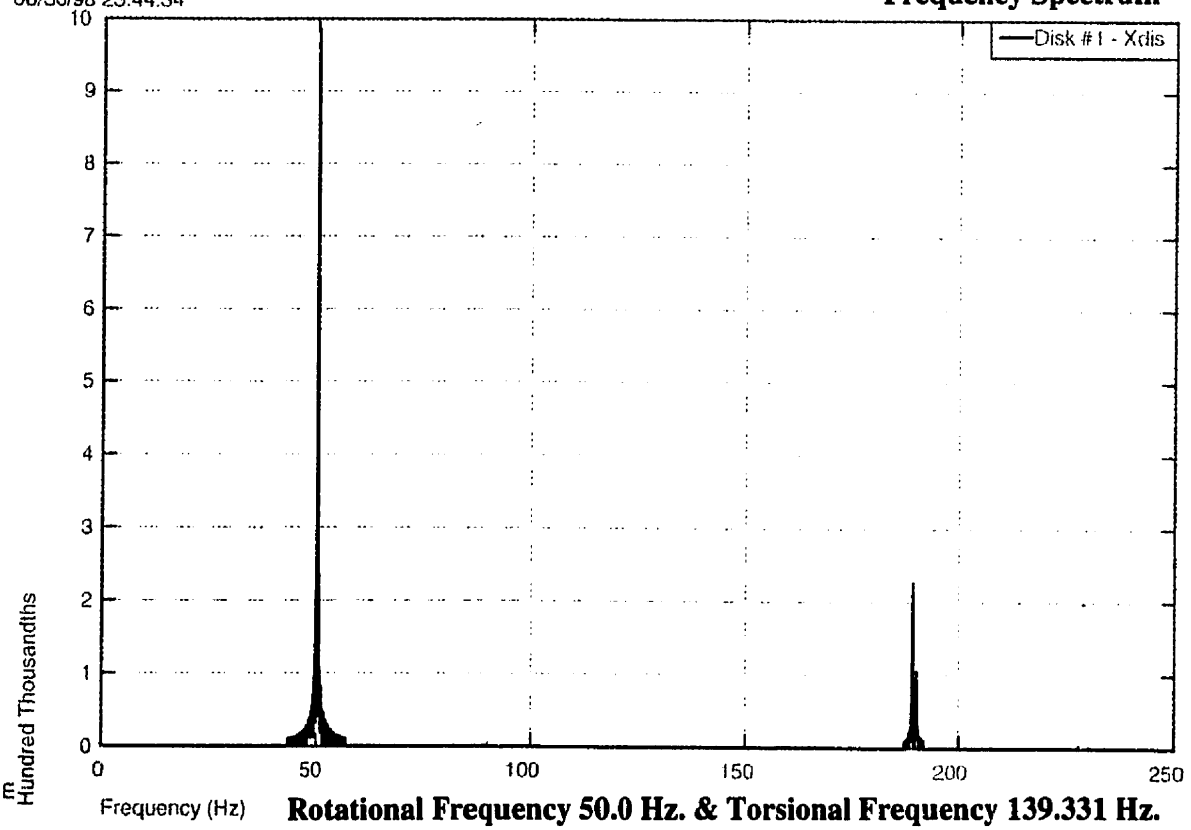

Rotational Frequency 50.0 Hz. & Torsional Frequency 139.331 Hz.

Plot B1.7

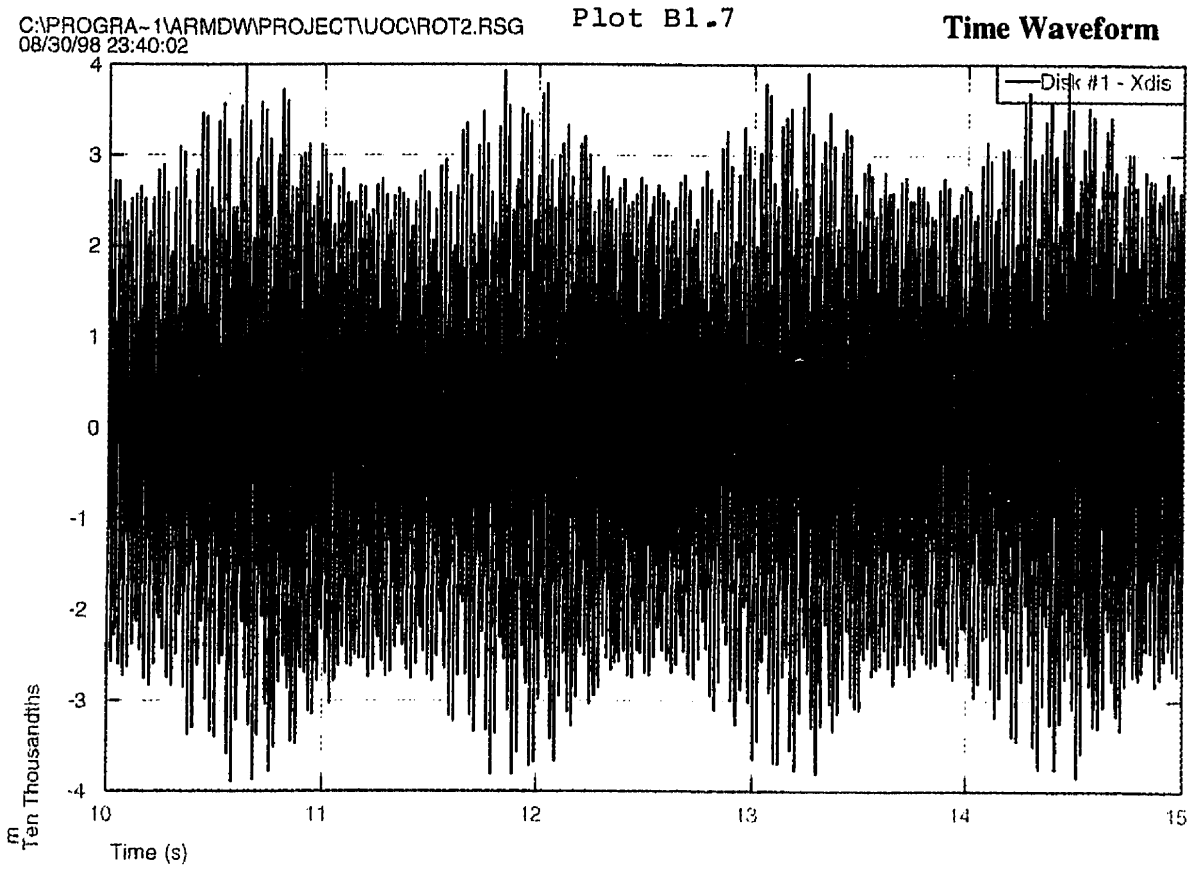

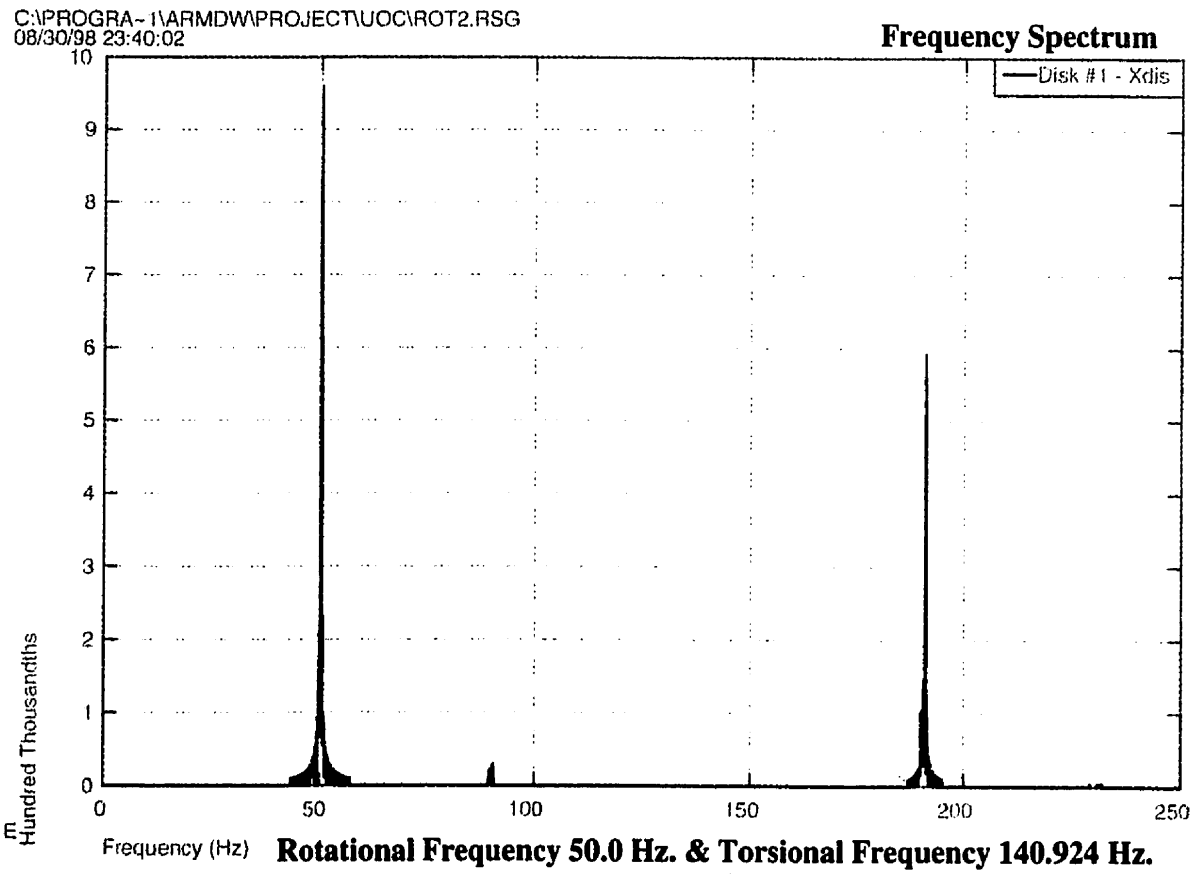

Rotational Frequency 50.0 Hz. & Torsional Frequency 140.924 Hz.

C:\PROGRA~1\ARMDW\PROJECT\UOC\ROT2.RSG
08/30/98 23:24:18

Plot B1.8

Time Waveform

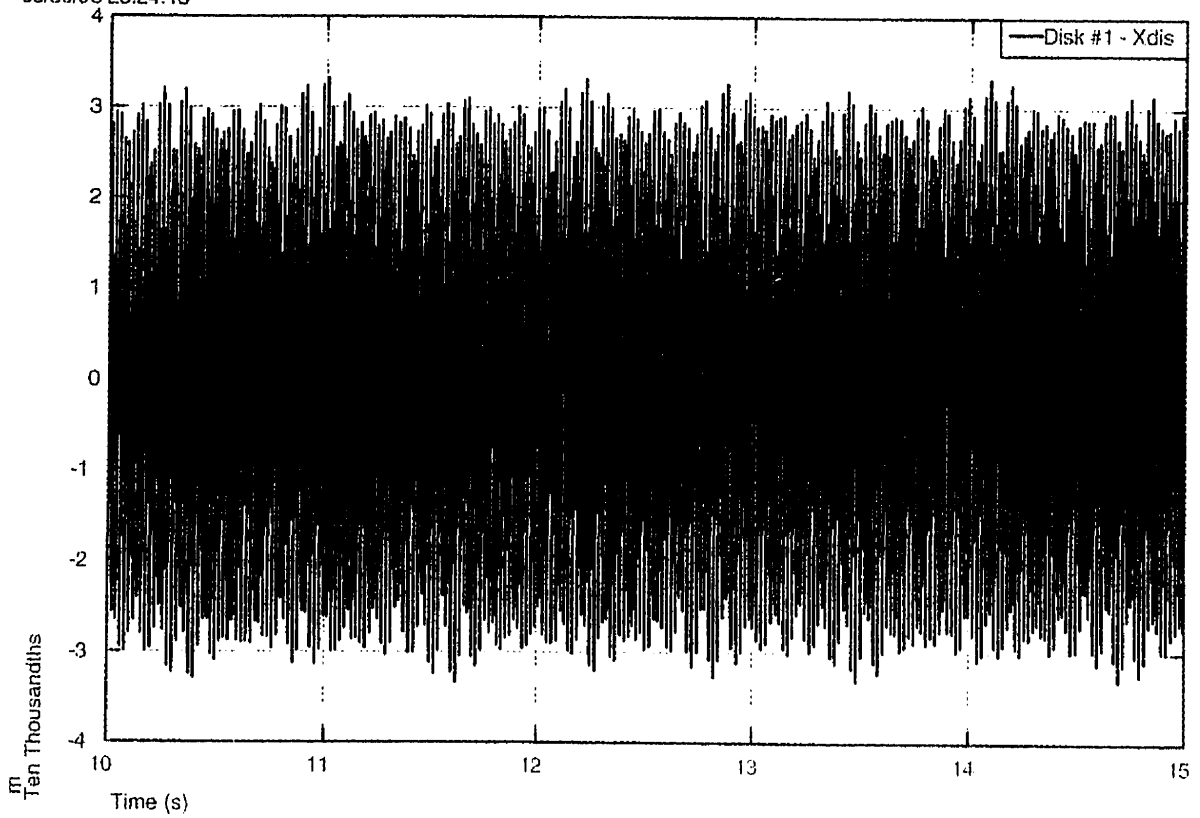

C:\PROGRA~1\ARMDW\PROJECT\UOC\ROT2.RSG
08/30/98 23:24:18

Frequency Spectrum

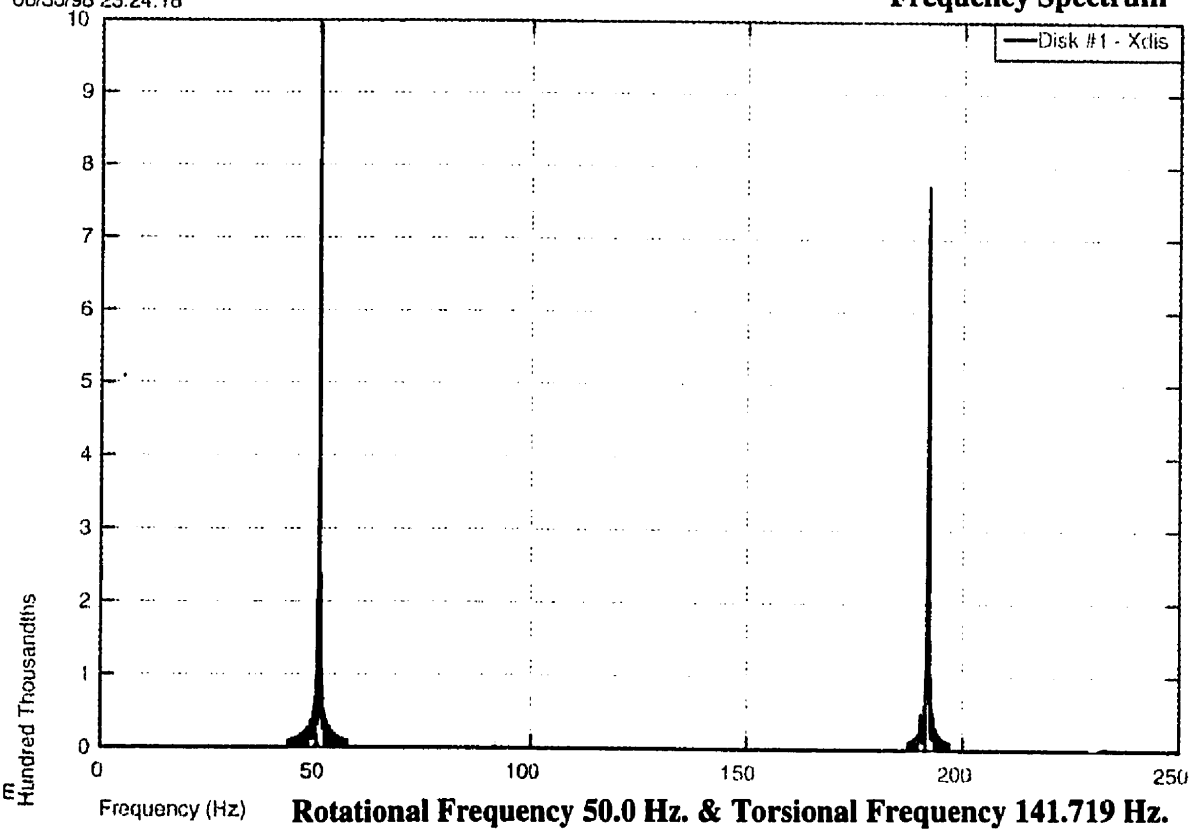

Rotational Frequency 50.0 Hz. & Torsional Frequency 141.719 Hz.

C:\PROGRA~1\ARMDW\PROJECT\UOC\ROT2.RSG
08/30/98 23:18:30

Plot B1.9

Time Waveform

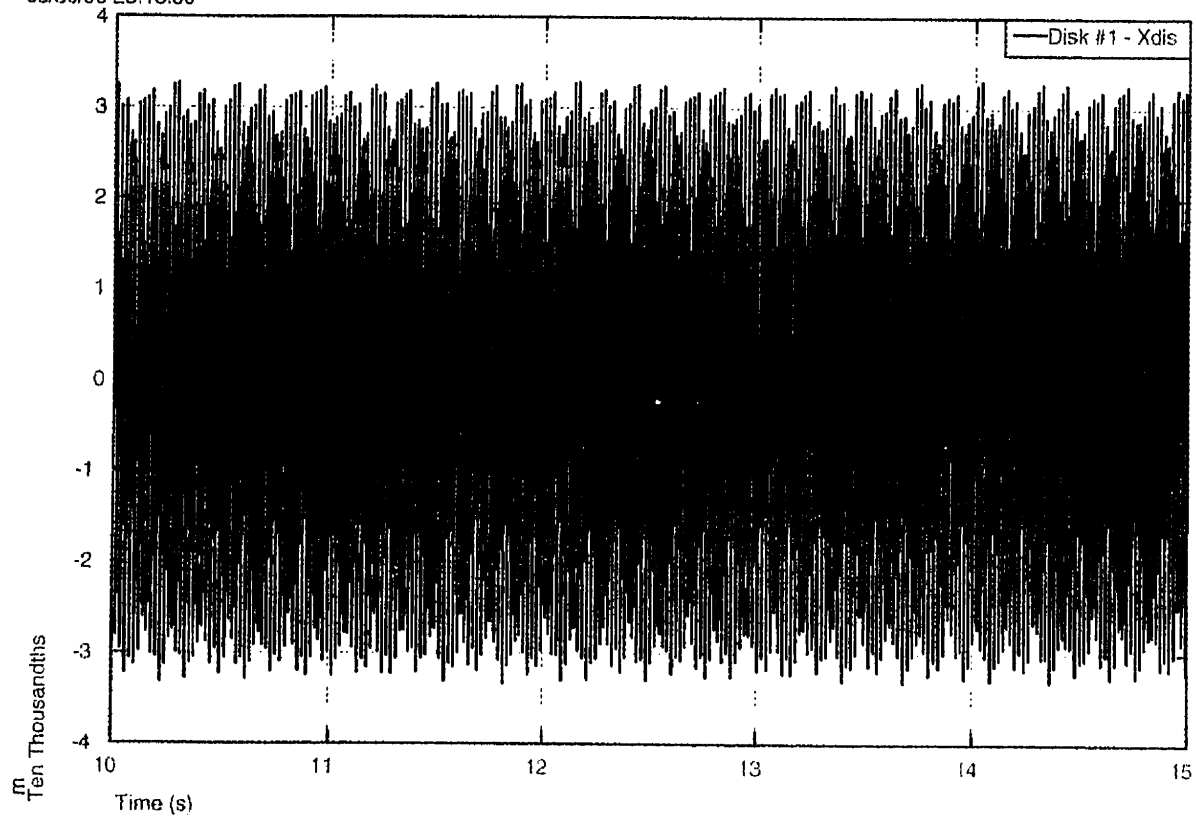

C:\PROGRA~1\ARMDW\PROJECT\UOC\ROT2.RSG
08/30/98 23:18:30

Frequency Spectrum

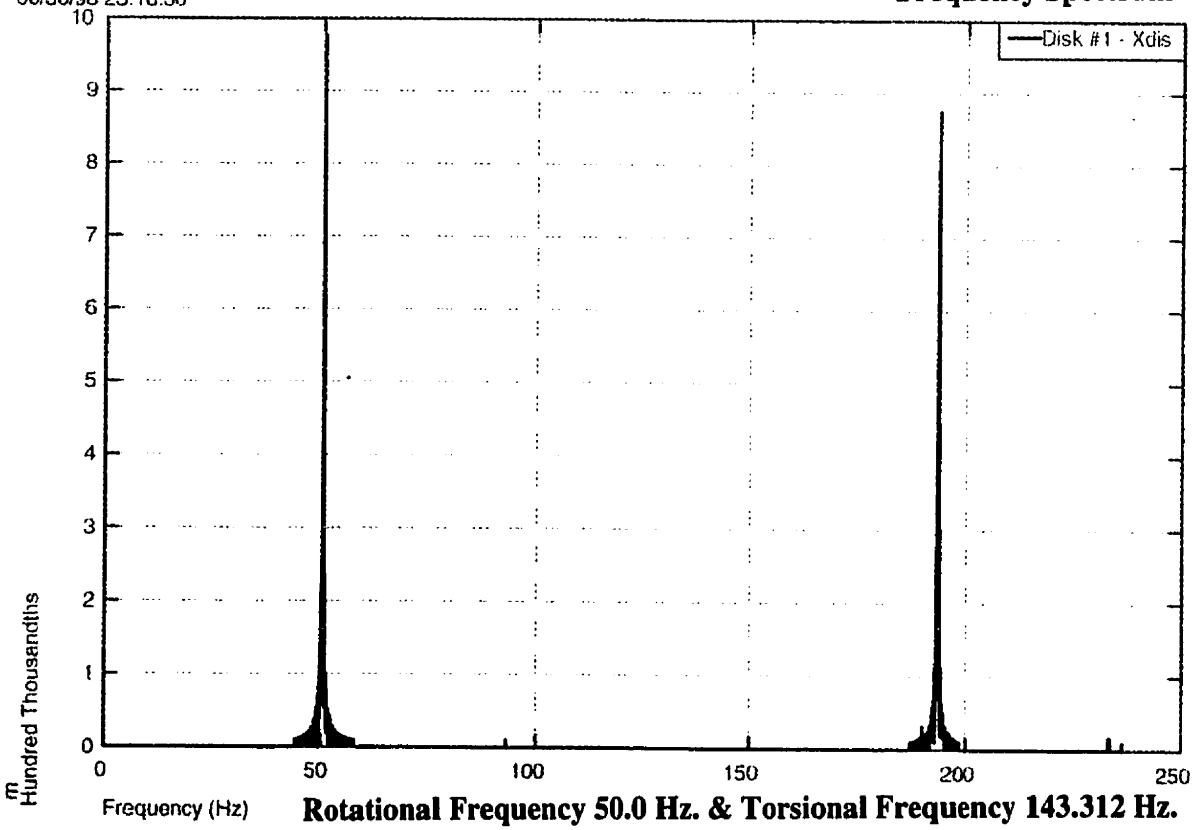

Rotational Frequency 50.0 Hz. & Torsional Frequency 143.312 Hz.

C:\PROGRA~1\ARMDW\PROJECT\UOC\ROT2.RSG
08/30/98 23:03:46

Plot B1.10

Time Waveform

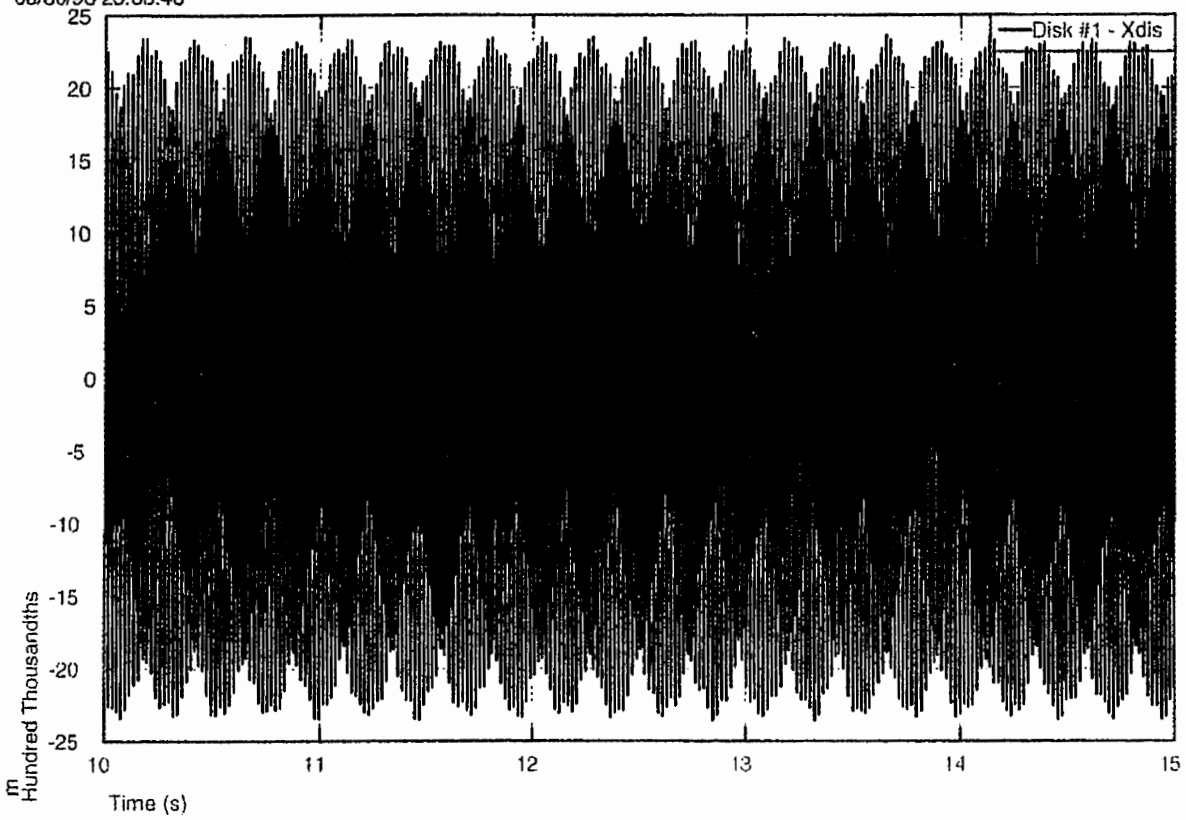

C:\PROGRA~1\ARMDW\PROJECT\UOC\ROT2.RSG
08/30/98 23:03:46

Frequency Spectrum

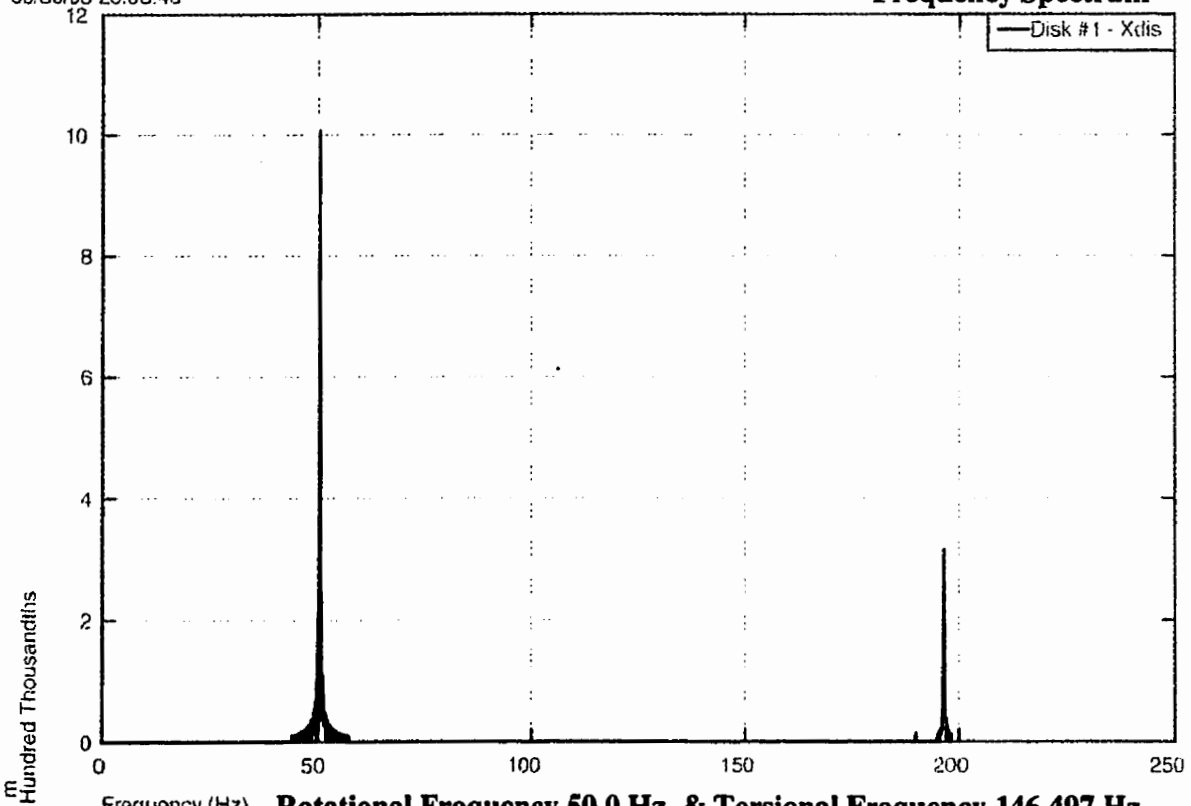

Rotational Frequency 50.0 Hz. & Torsional Frequency 146.497 Hz.

C:\PROGRA~1\ARMDW\PROJECT\UOC\ROT2.RSG
08/30/98 22:51:50

Plot B1.11

Time Waveform

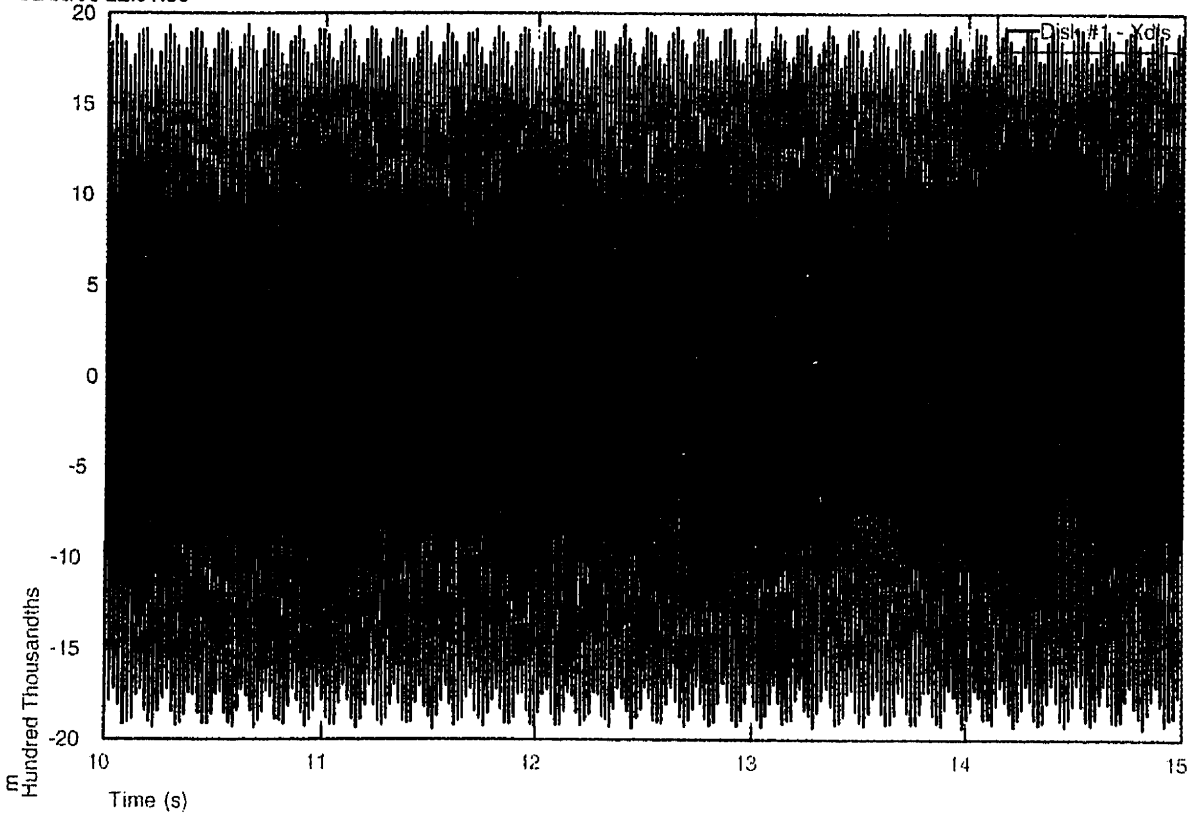

C:\PROGRA~1\ARMDW\PROJECT\UOC\ROT2.RSG
08/30/98 22:51:50

Frequency Spectrum

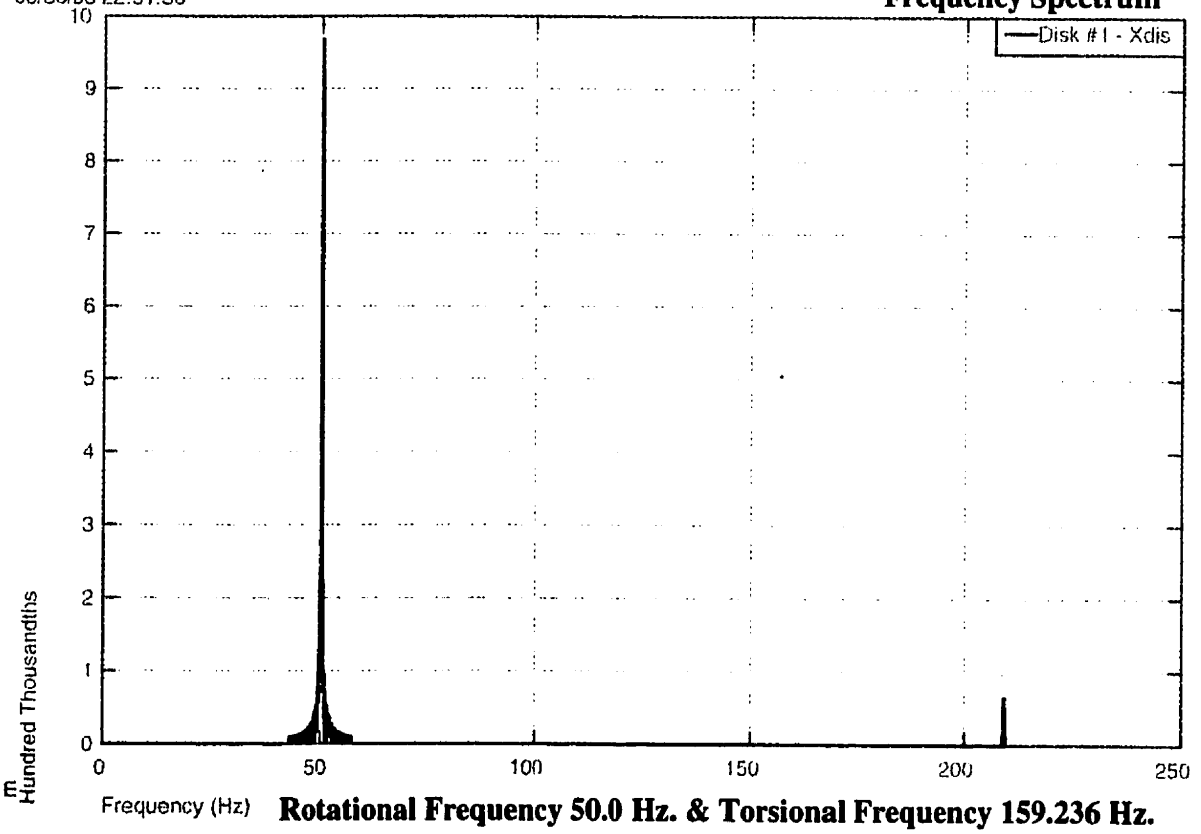

Rotational Frequency 50.0 Hz. & Torsional Frequency 159.236 Hz.

C:\PROGRA~1\ARMDW\PROJECT\UOC\ROT2.RSG
08/30/98 22:46:38

Plot B1.12

Time Waveform

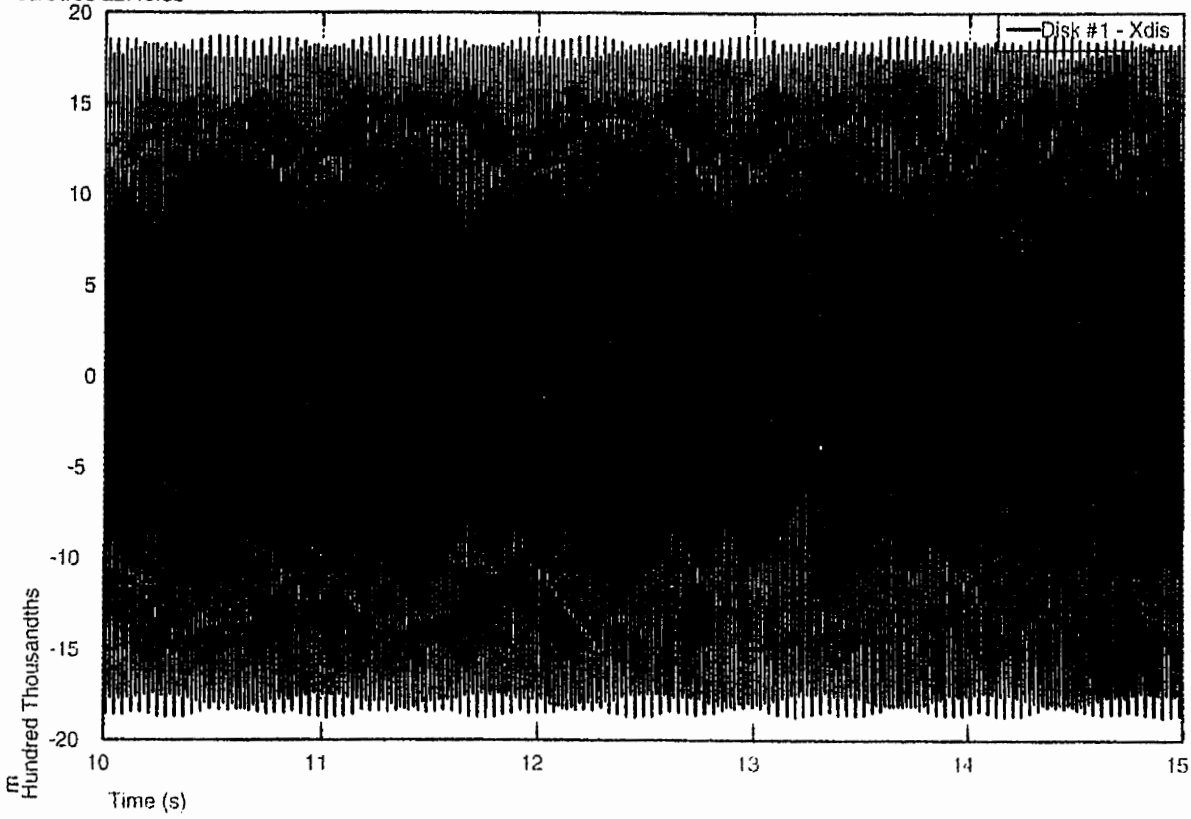

C:\PROGRA~1\ARMDW\PROJECT\UOC\ROT2.RSG
08/30/98 22:46:38

Frequency Spectrum

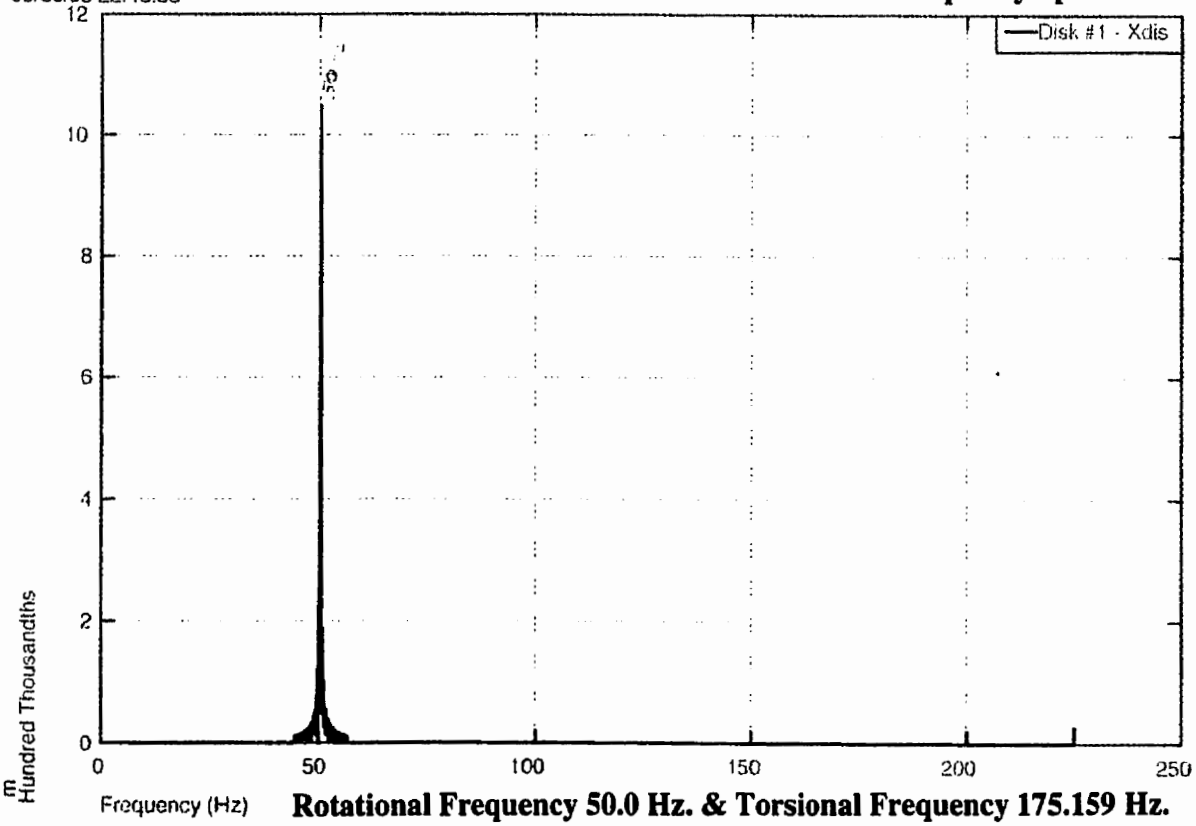

Rotational Frequency 50.0 Hz. & Torsional Frequency 175.159 Hz.

Plot B1.13

Time Waveform

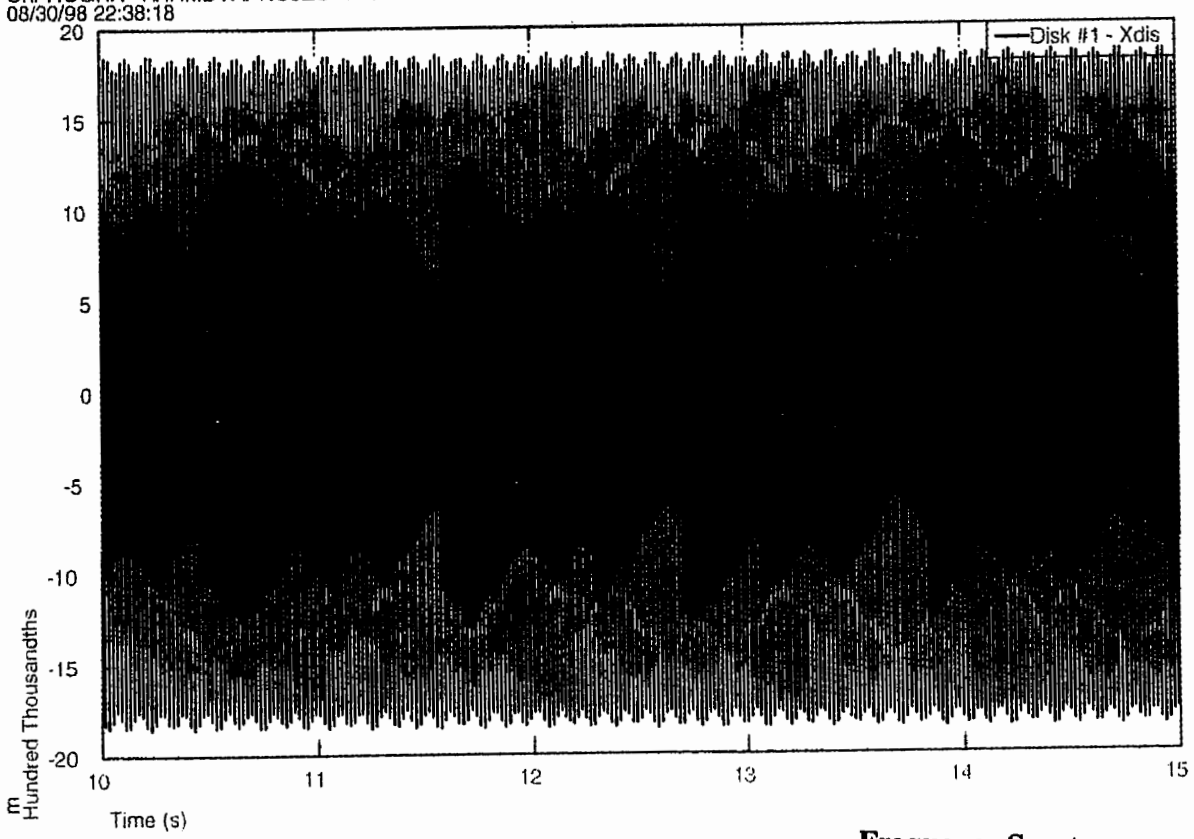

Frequency Spectrum

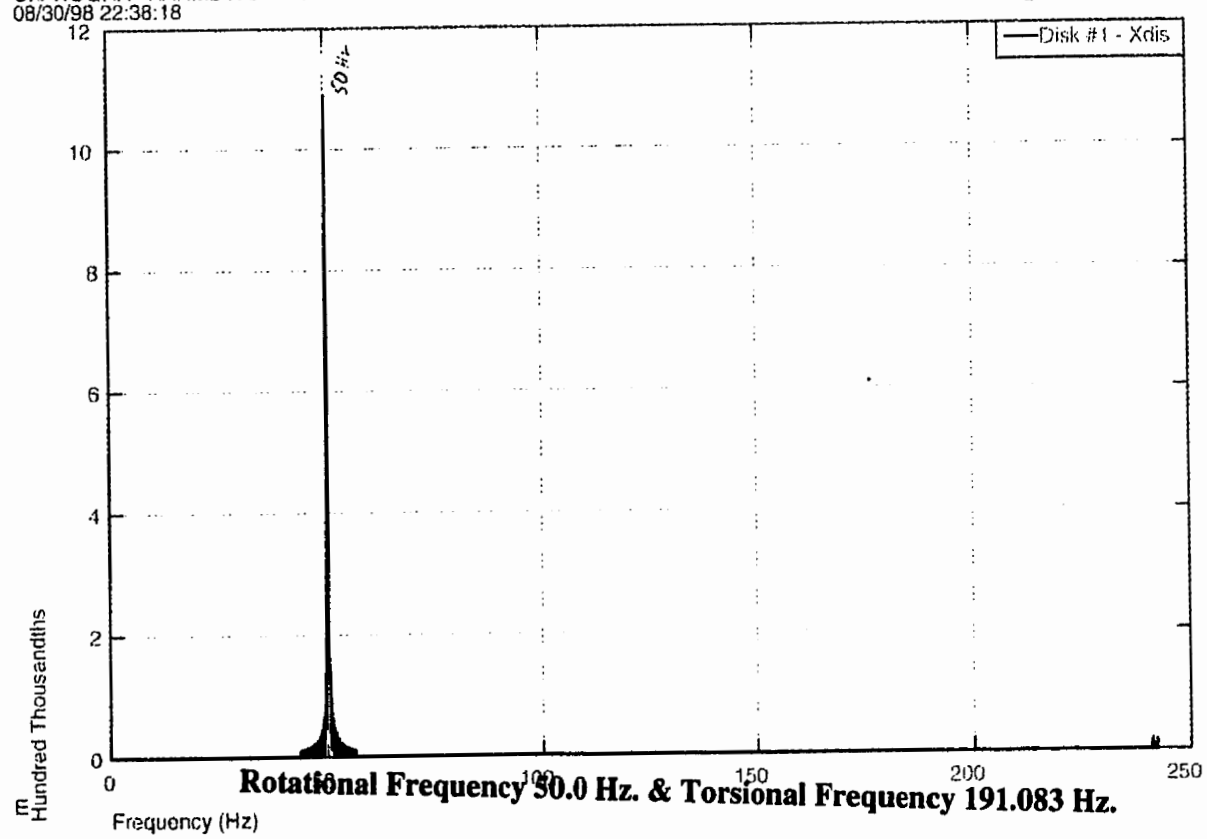

Rotational Frequency 50.0 Hz. & Torsional Frequency 191.083 Hz.

Appendix B2

Computed lateral vibration response plots as per Case 12 of Chapter 4, Section 4.6 are attached in this appendix.

```
Two Disk Test File
7 150000  0.00010 100000  10 3600.0  9.8
138.723  10.2544  138.723 10.2544
0.038   0.000
5000.
1.25264e9  -1.0481e9  -1.0481e9  1.25264e9  3.97572e6
30000.0   1000.0    0.0
    0.0     0.0    0.0
```

Input Guide

```
LINE 1:TITLE (72 CHARACTERS)
LINE 2:NUMB. OF DEGREES OF FREEDOM (ALWAYS 7 = 6 + 1 RIGID BODY ROTATION)
       NUMB. OF TIME STEPS
       TIME STEP INCREMENT (DELTA T - SECONDS)
       NUMB. OF TIME STEPS TO SKIP BEFORE BEGINNING TO PRINT OUTPUT
       NUMB. OF TIME STEPS TO SKIP BETWEEN OUTPUT PRINTING (EVERY 10TH STEP)
       SHAFT SPEED (RPM)
       GRAVITY (M/S^2)
LINE 3:DISK #1 MASS (KG)
       DISK #1 POLAR INERTIA (KG-M^2)
       DISK #2 MASS (KG)
       DISK #2 POLAR INERTIA (KG-M^2)
LINE 4:DISK #1 ECC. FROM SHAFT CENTER TO CENTER OF MASS (M)
       DISK #2 ECC. FROM SHAFT CENTER TO CENTER OF MASS (M)
LINE 5:DAMPING FOR LATERAL BEAM BENDING

LINE 6:K11 LATERAL SHAFT STIFFNESS
       K12 LATERAL SHAFT STIFFNESS
       K21 LATERAL SHAFT STIFFNESS
       K22 LATERAL SHAFT STIFFNESS
       TAU TORSIONAL STIFFNESS
LINE 7:DISK #1 TORQUE AMPLITUDE (N-M)
       DISK #1 TORQUE FREQUENCY (RAD/SEC)
       DISK #1 TORQUE PHASE ANGLE (RAD)
       DISK #2 TORQUE AMPLITUDE (N-M)
       DISK #2 TORQUE FREQUENCY (RAD/SEC)
       DISK #2 TORQUE PHASE ANGLE (RAD)
```

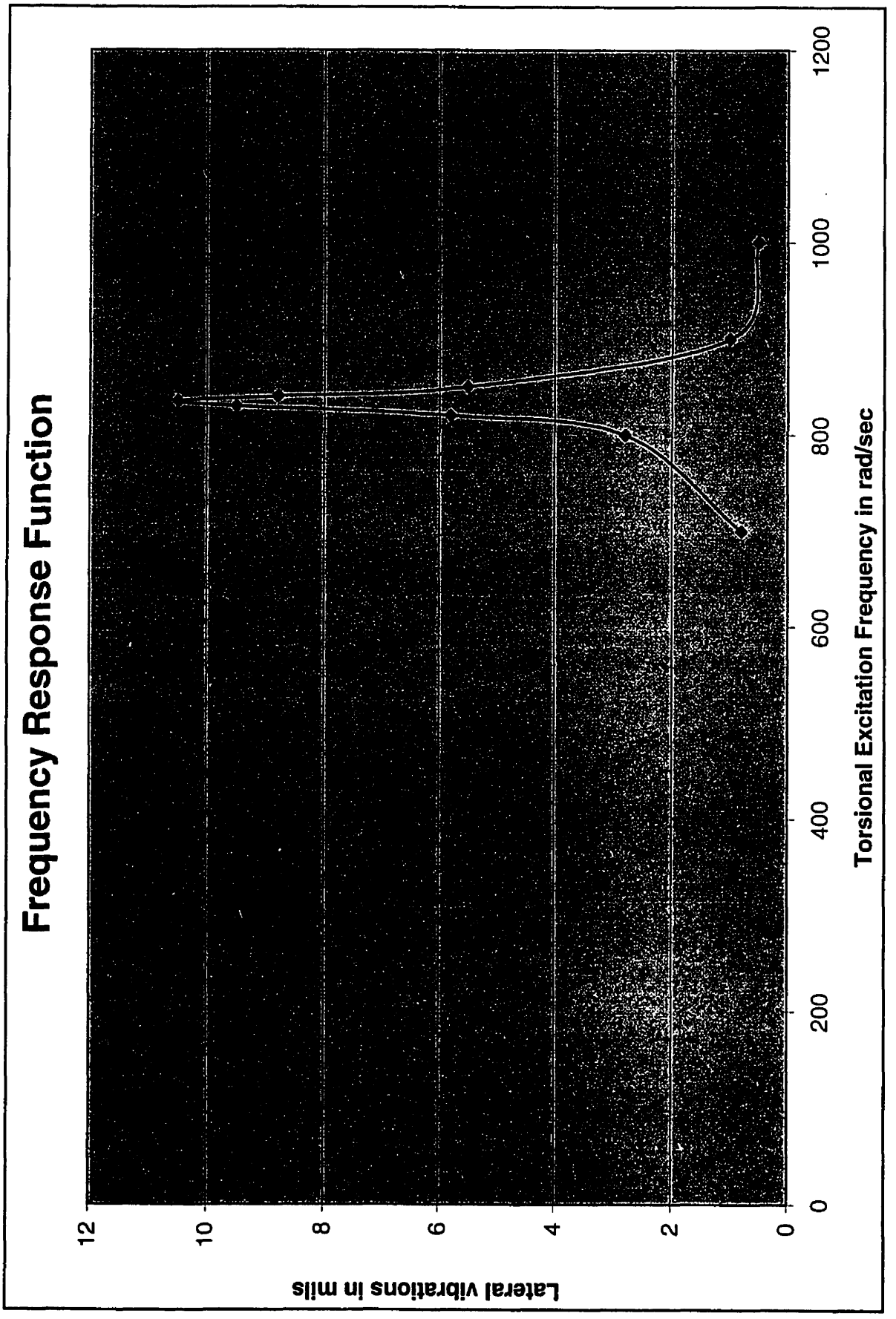
Frequency Response Function
Lateral Vibrations in mils
Torsional Excitation Frequency in rad/sec
0
2
4
6
8
10
12
0
200
400
600
800
1000
1200

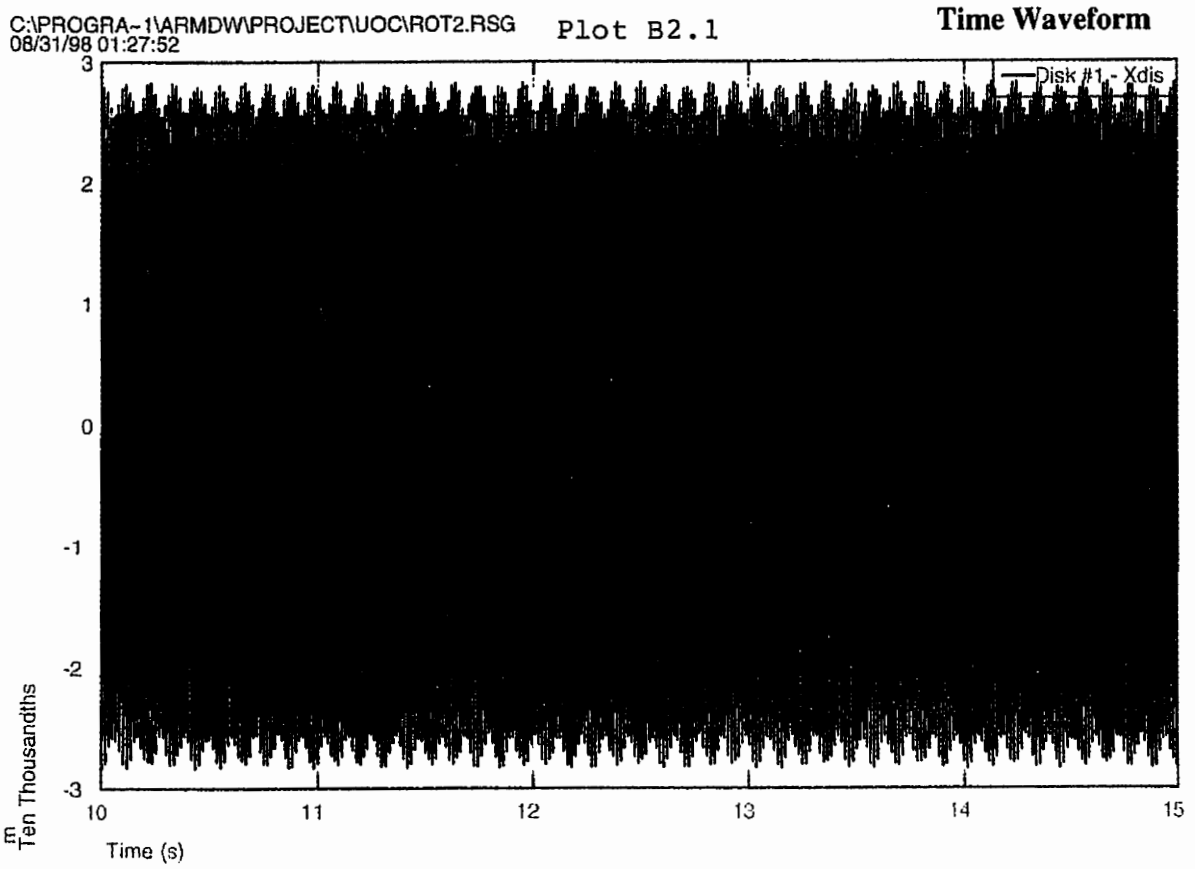

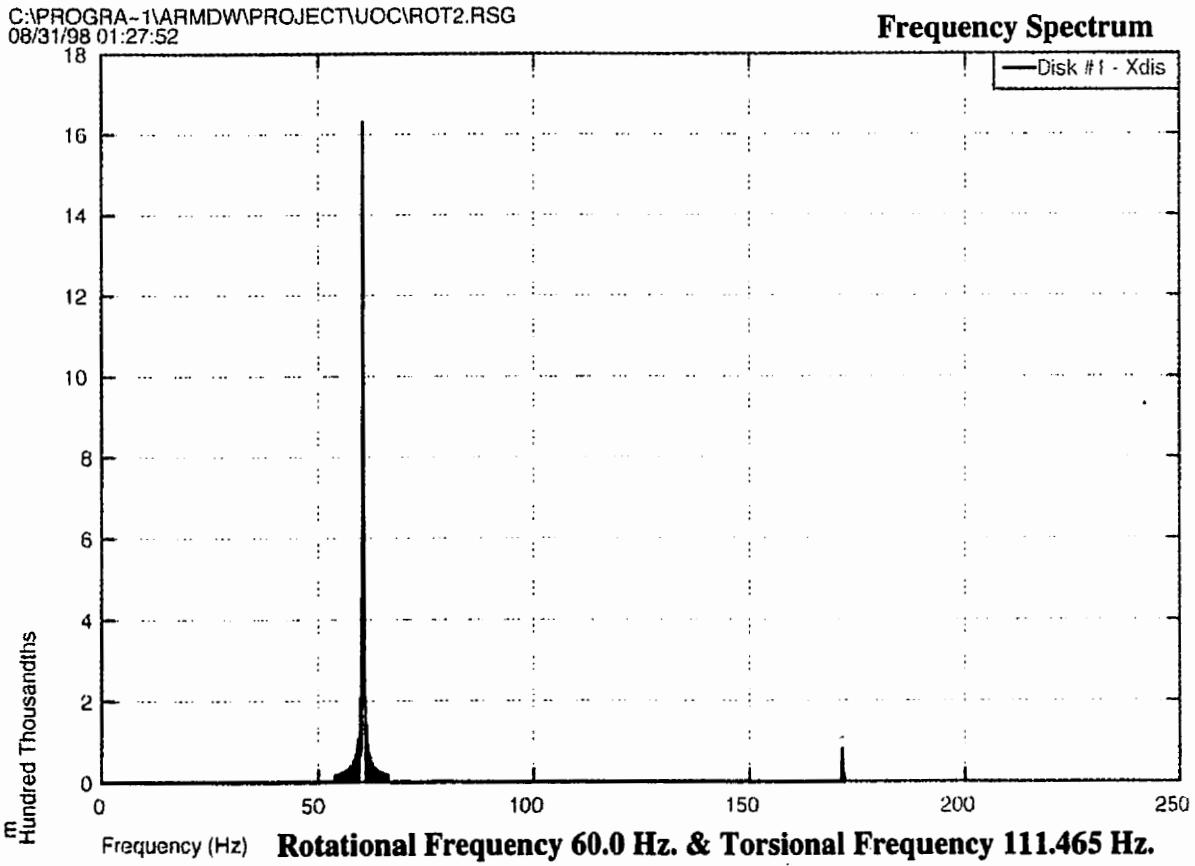

Rotational Frequency 60.0 Hz. & Torsional Frequency 111.465 Hz.

C:\PROGRA~1\ARMDW\PROJECT\UOC\ROT2.RSG
08/31/98 01:36:22

Plot B2.2

Time Waveform

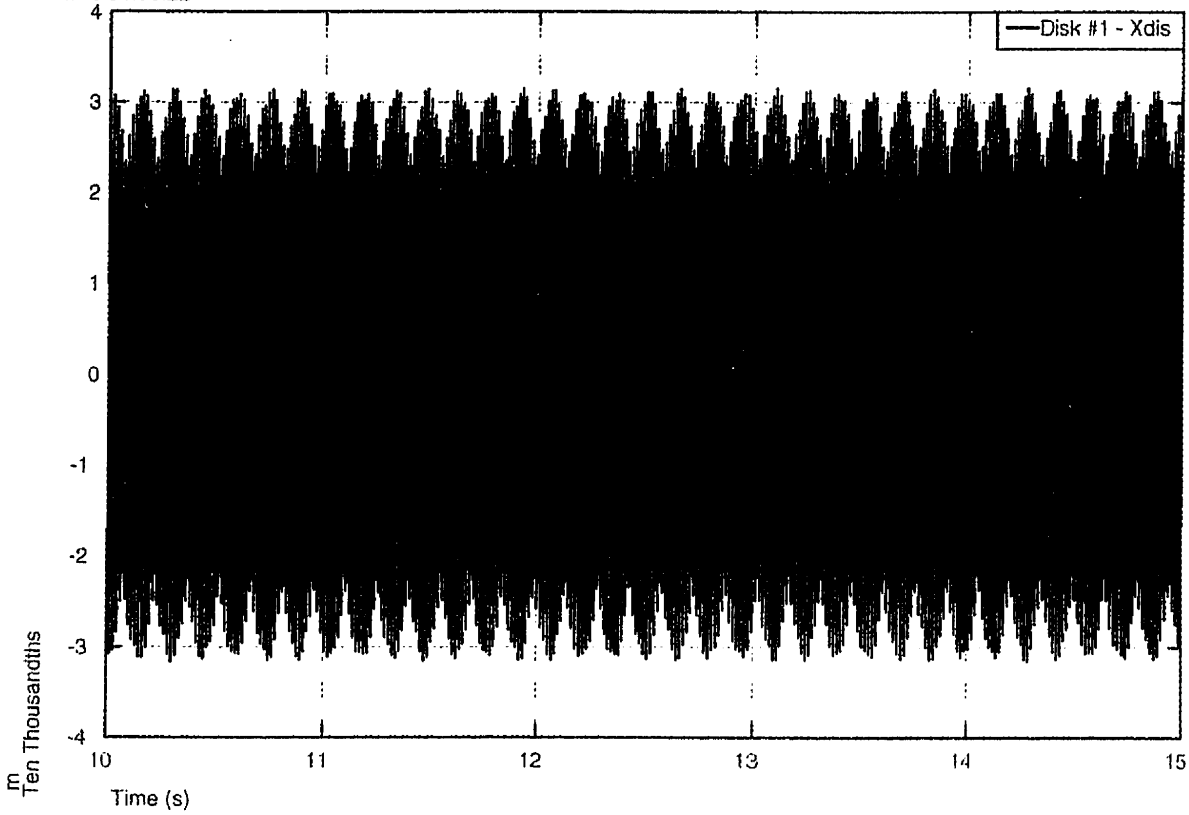

C:\PROGRA~1\ARMDW\PROJECT\UOC\ROT2.RSG
08/31/98 01:36:22

Frequency Spectrum

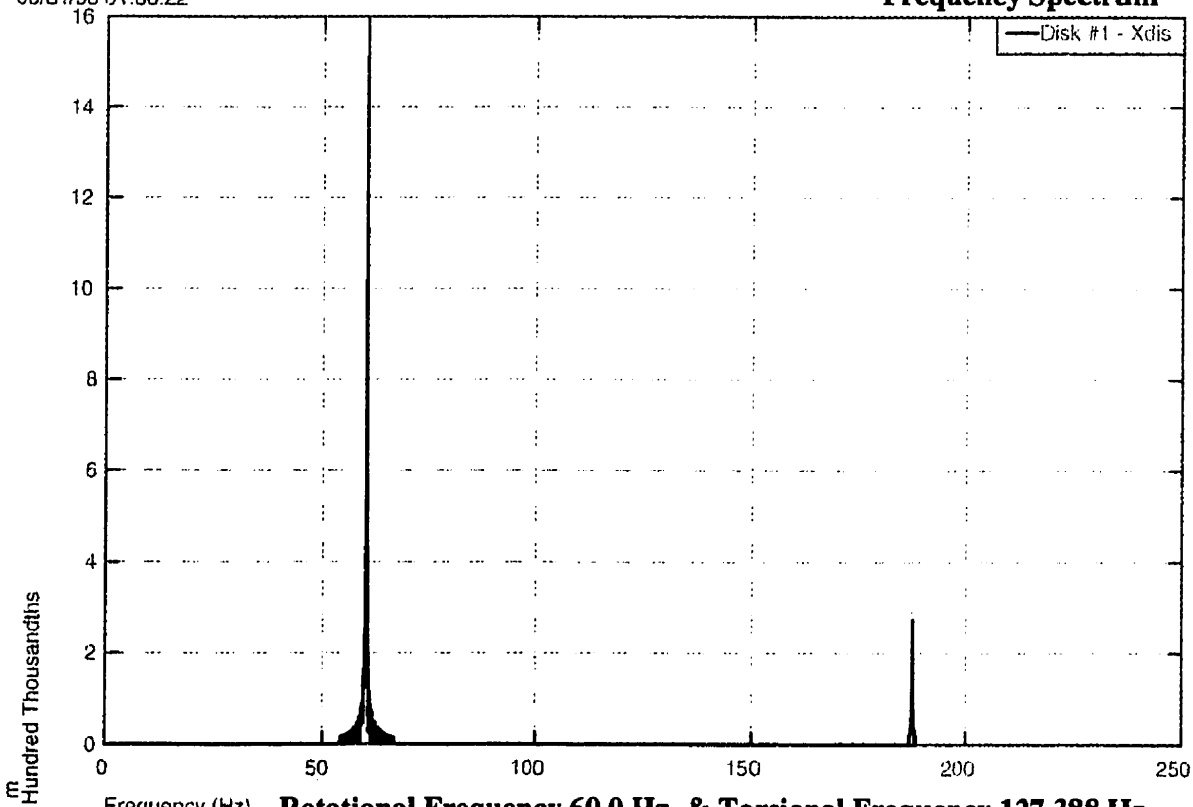

Rotational Frequency 60.0 Hz. & Torsional Frequency 127.388 Hz.

C:\PROGRA~1\ARMDW\PROJECT\UOC\ROT2.RSG
08/31/98 01:45:00

Plot B2.3

Time Waveform

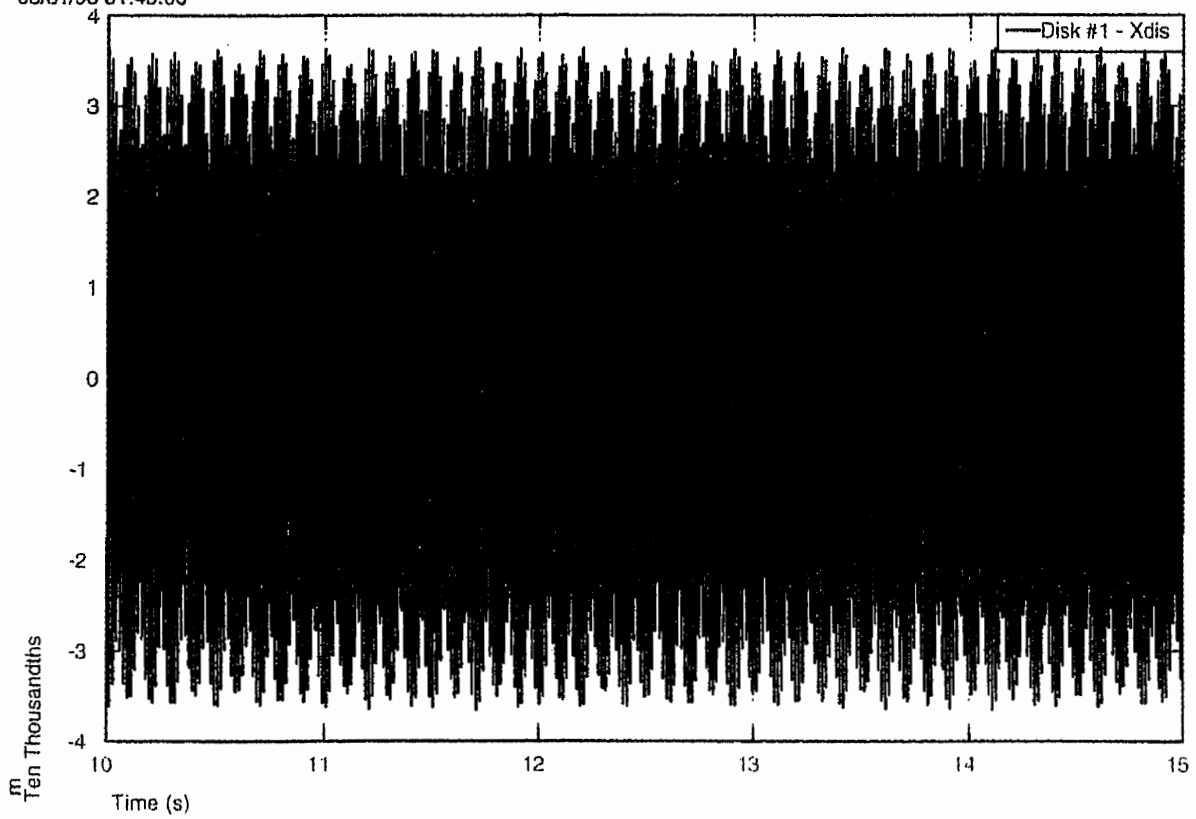

C:\PROGRA~1\ARMDW\PROJECT\UOC\ROT2.RSG
08/31/98 01:45:00

Frequency Spectrum

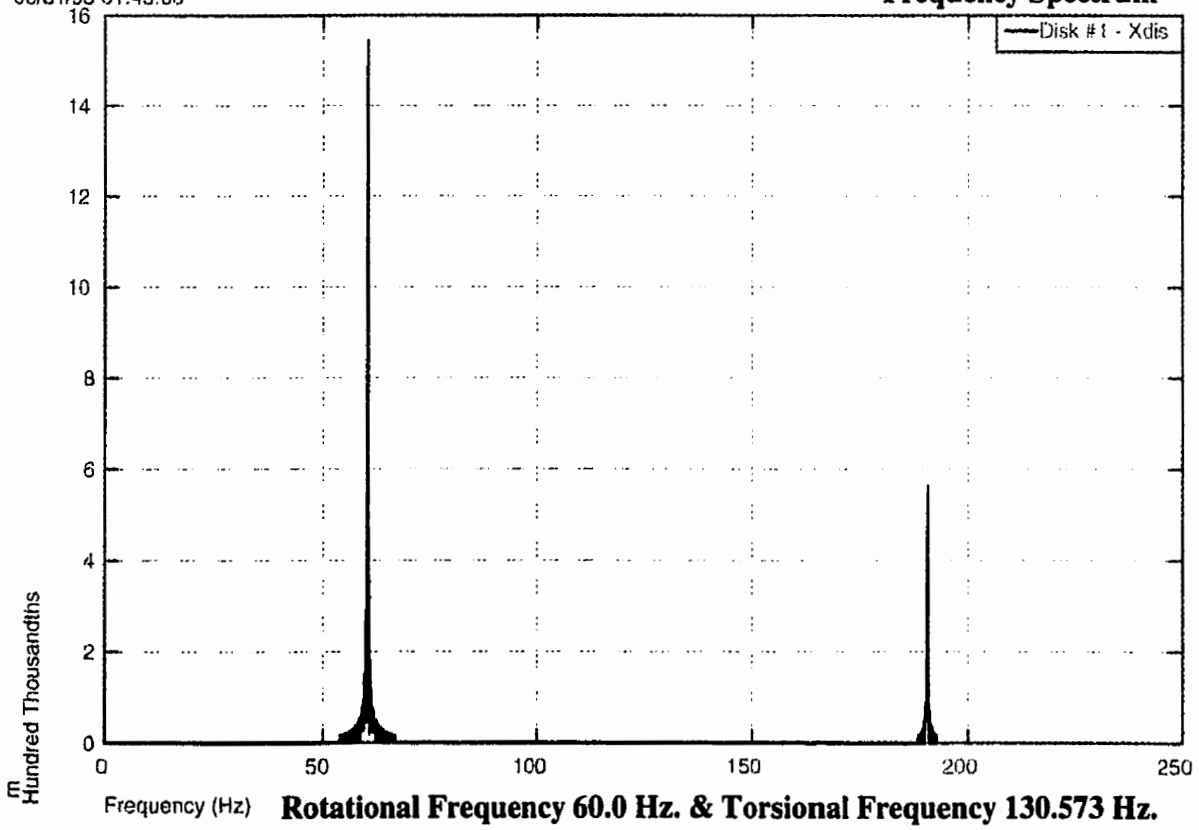

Rotational Frequency 60.0 Hz. & Torsional Frequency 130.573 Hz.

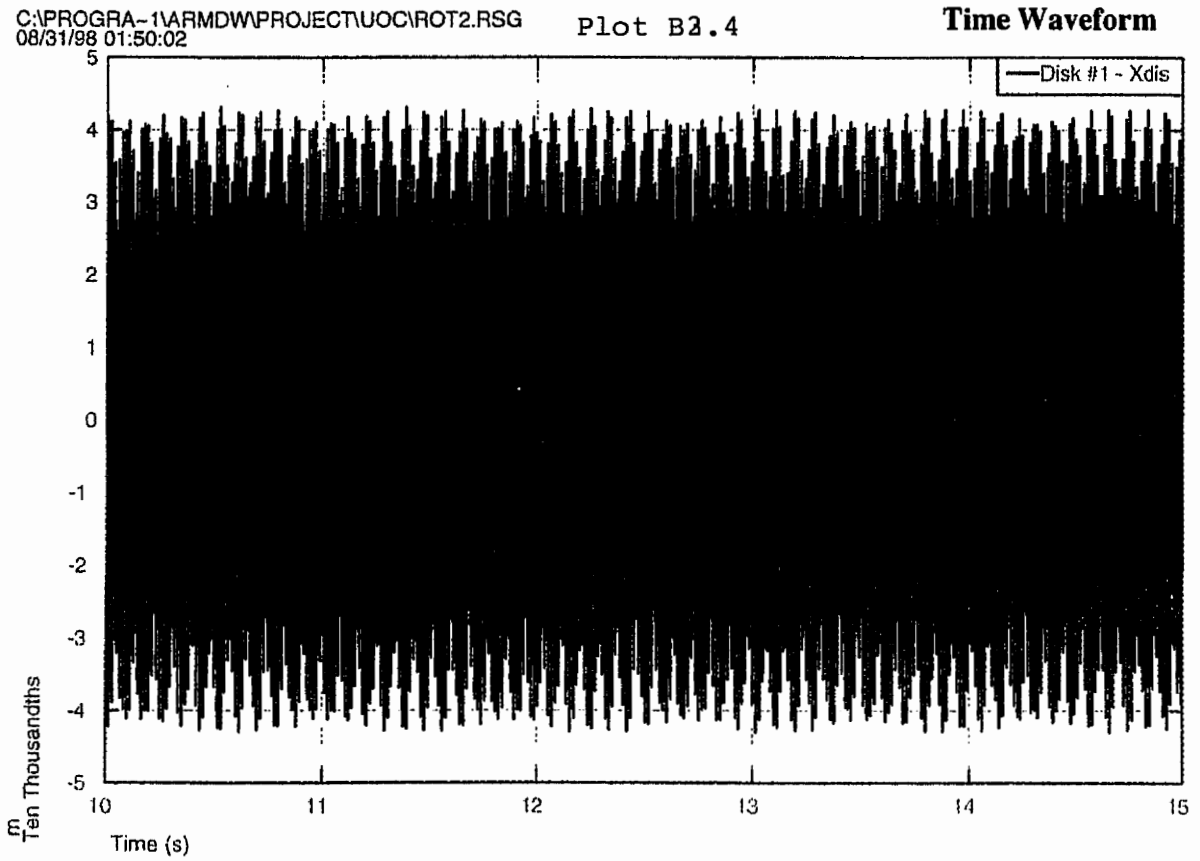

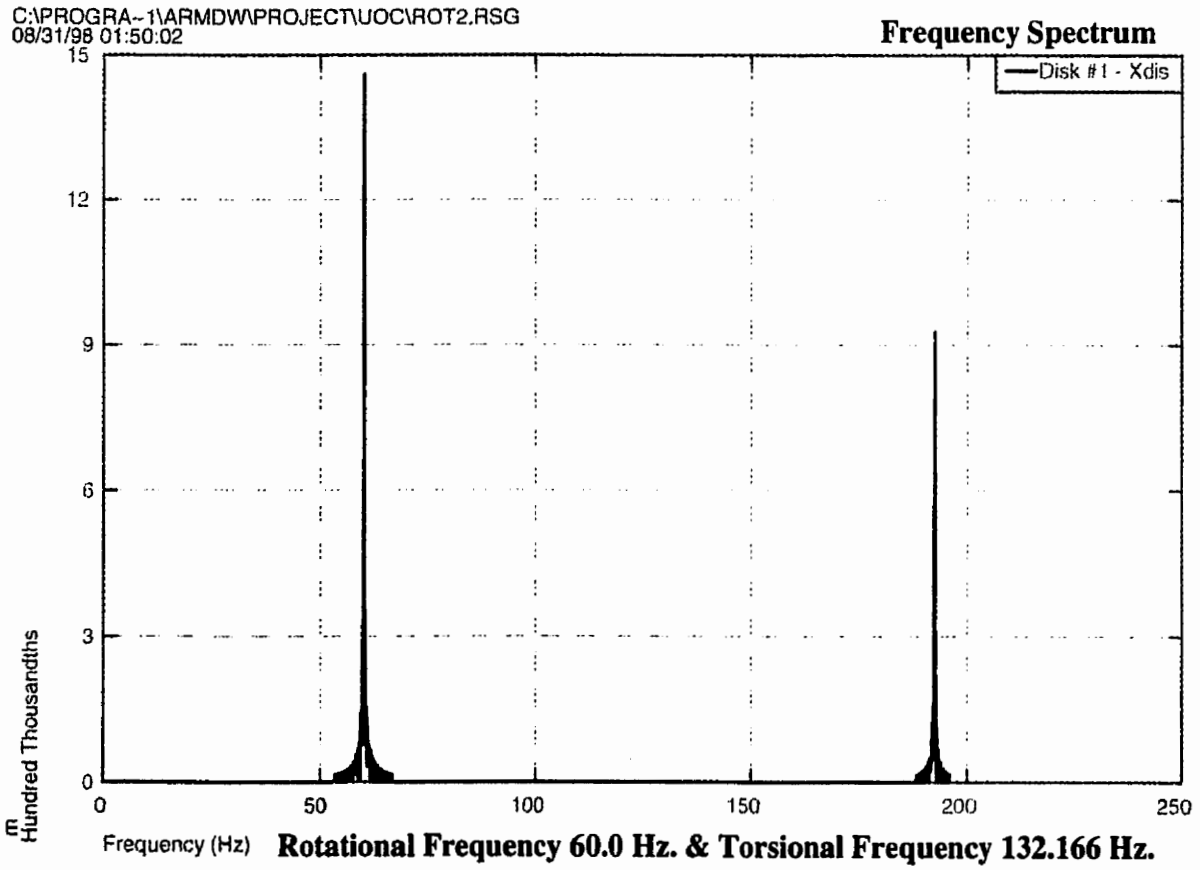

Rotational Frequency 60.0 Hz. & Torsional Frequency 132.166 Hz.

C:\PROGRA~1\ARMDW\PROJECT\UOC\ROT2.RSG
08/31/98 01:55:30

Plot B2.5

Time Waveform

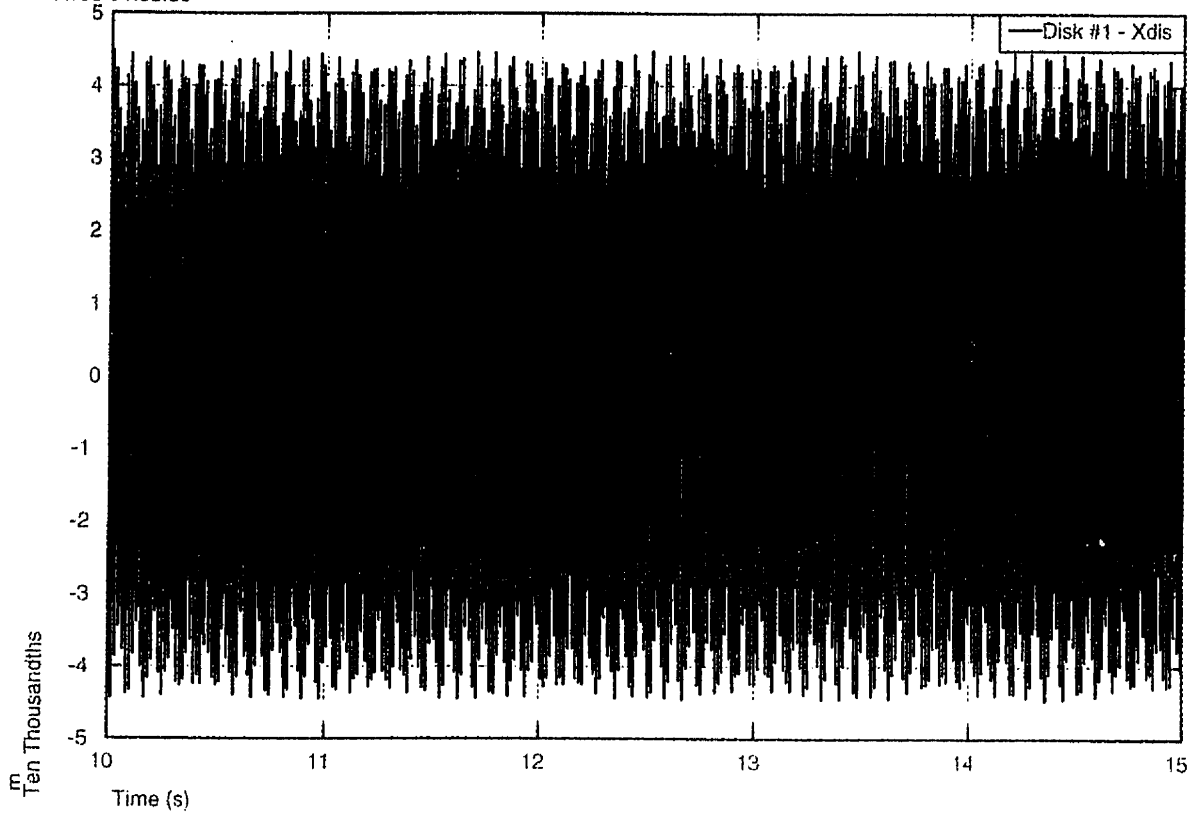

C:\PROGRA~1\ARMDW\PROJECT\UOC\ROT2.RSG
08/31/98 01:55:30

Frequency Spectrum

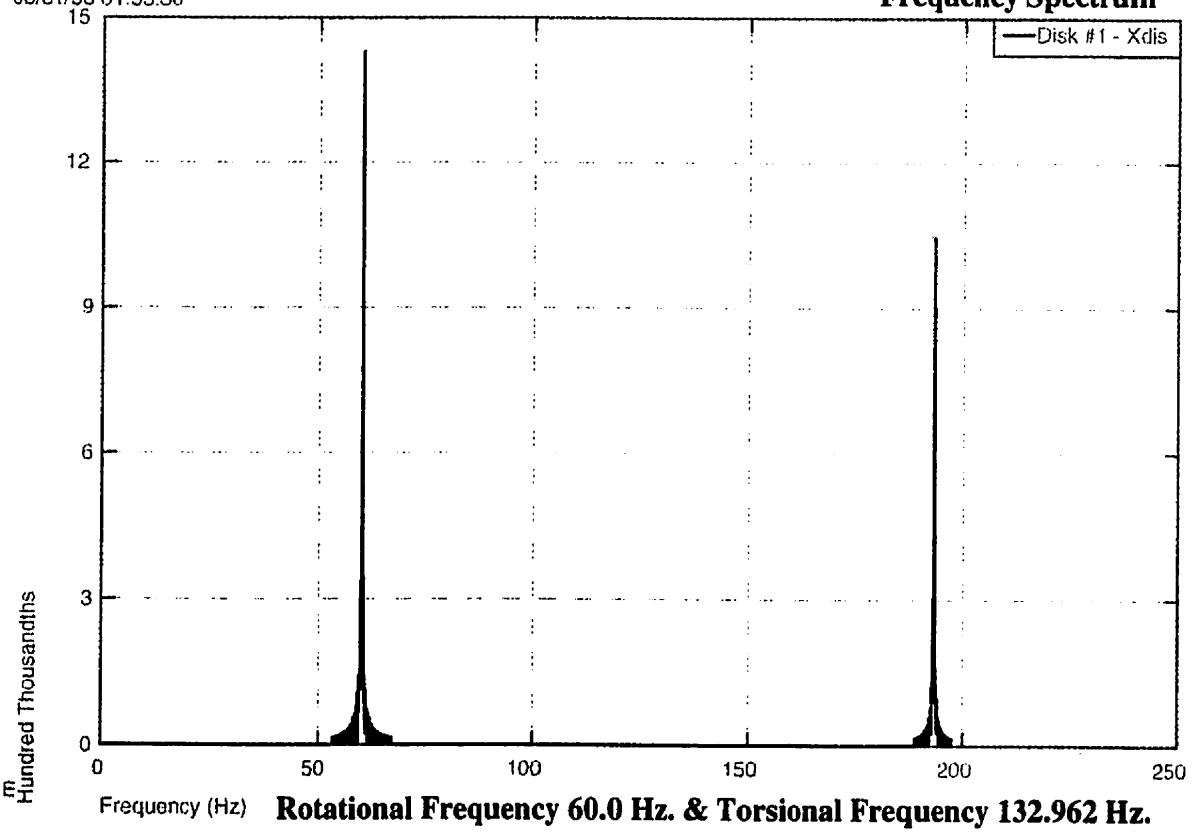

Rotational Frequency 60.0 Hz. & Torsional Frequency 132.962 Hz.

C:\PROGRA~1\ARMDW\PROJECT\UOC\ROT2.RSG
08/31/98 01:58:46

Plot B2.6

Time Waveform

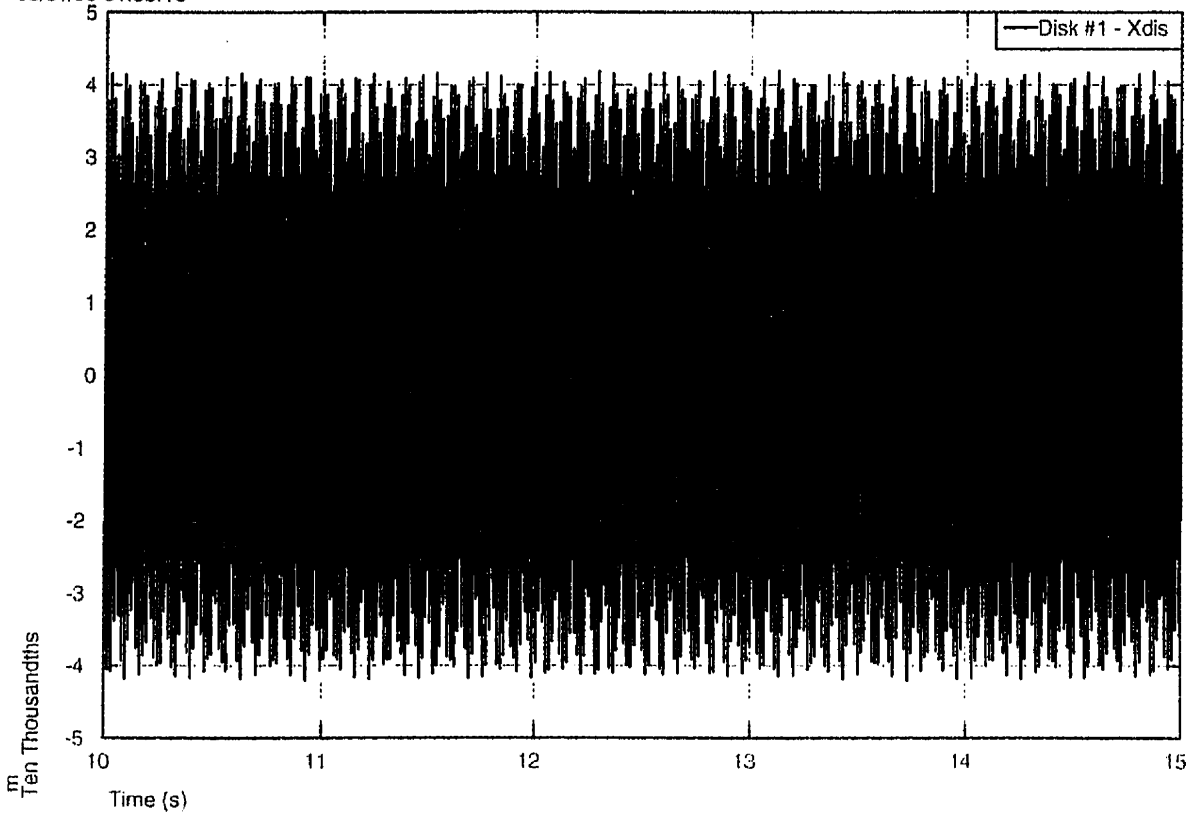

C:\PROGRA~1\ARMDW\PROJECT\UOC\ROT2.RSG
08/31/98 01:58:46

Frequency Spectrum

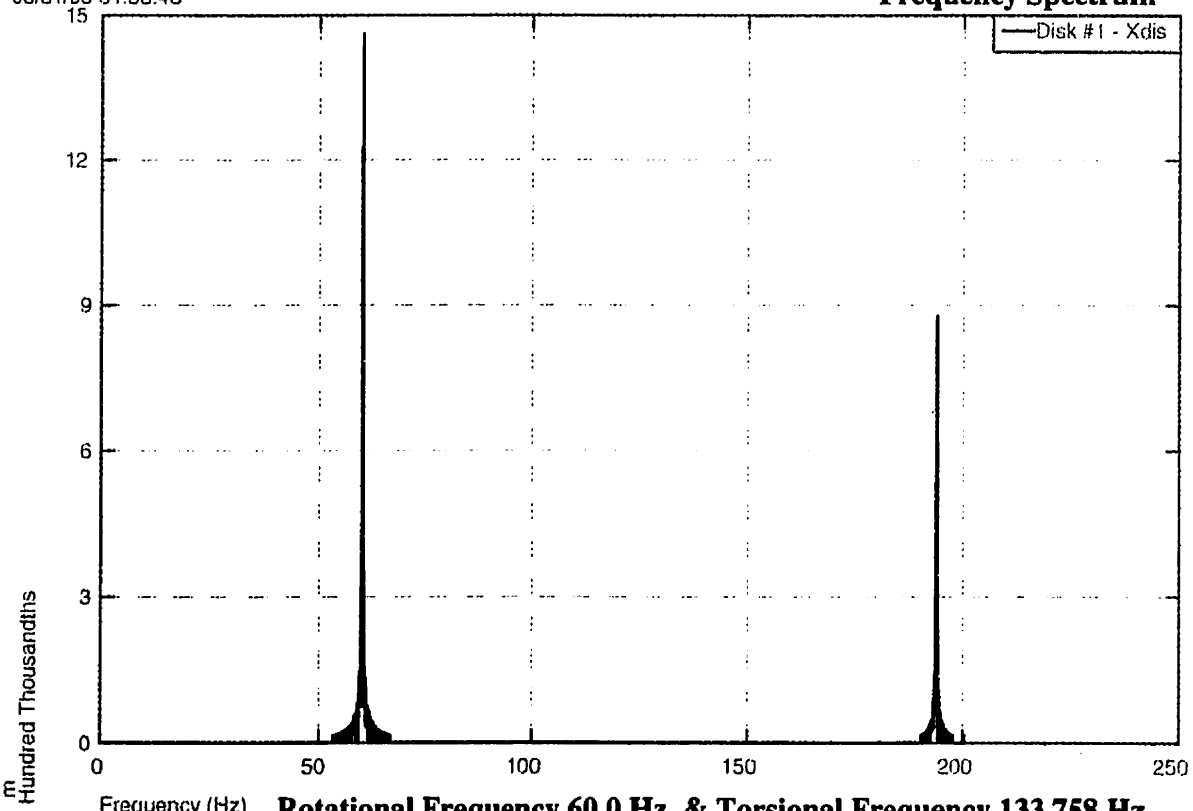

Rotational Frequency 60.0 Hz. & Torsional Frequency 133.758 Hz.

C:\PROGRA~1\ARMDW\PROJECT\UOC\ROT2.RSG
08/31/98 02:02:34

Plot B2.7

Time Waveform

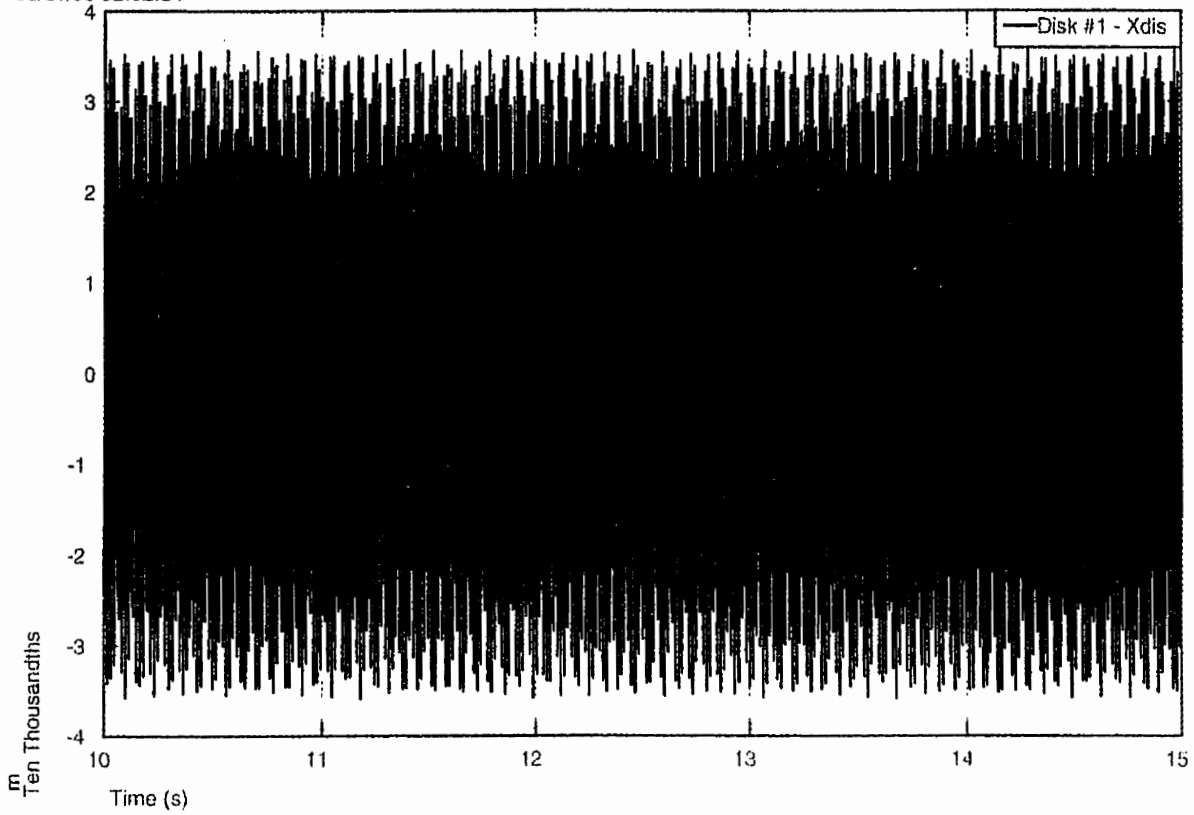

C:\PROGRA~1\ARMDW\PROJECT\UOC\ROT2.RSG
08/31/98 02:02:34

Frequency Spectrum

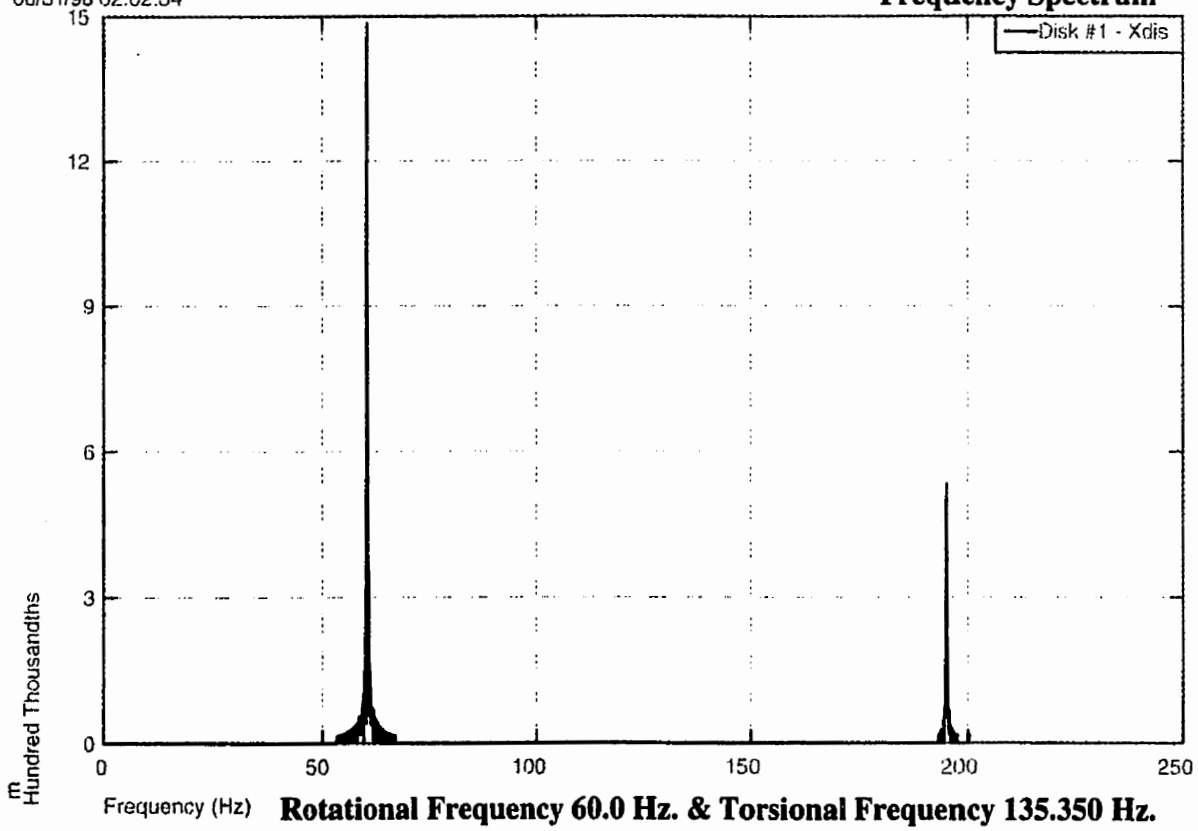

Rotational Frequency 60.0 Hz. & Torsional Frequency 135.350 Hz.

Plot B2.8

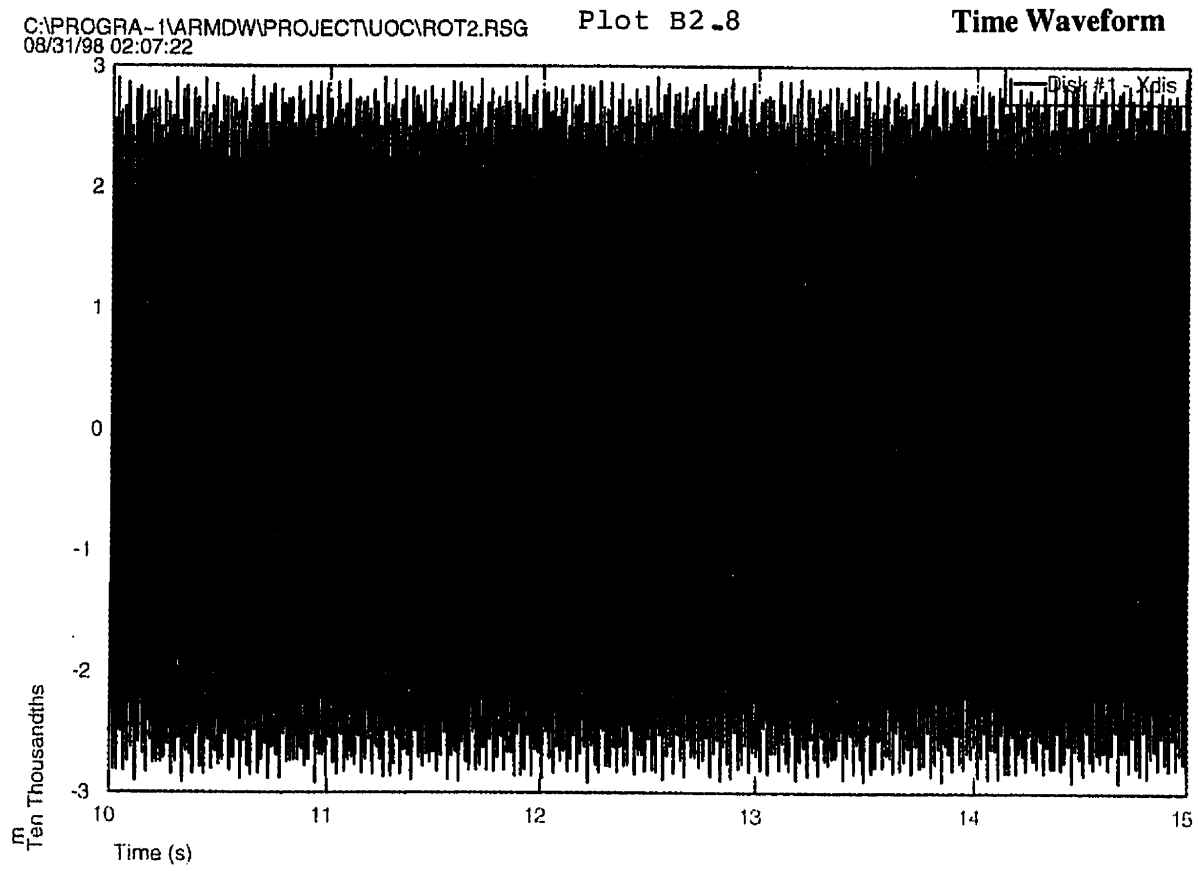

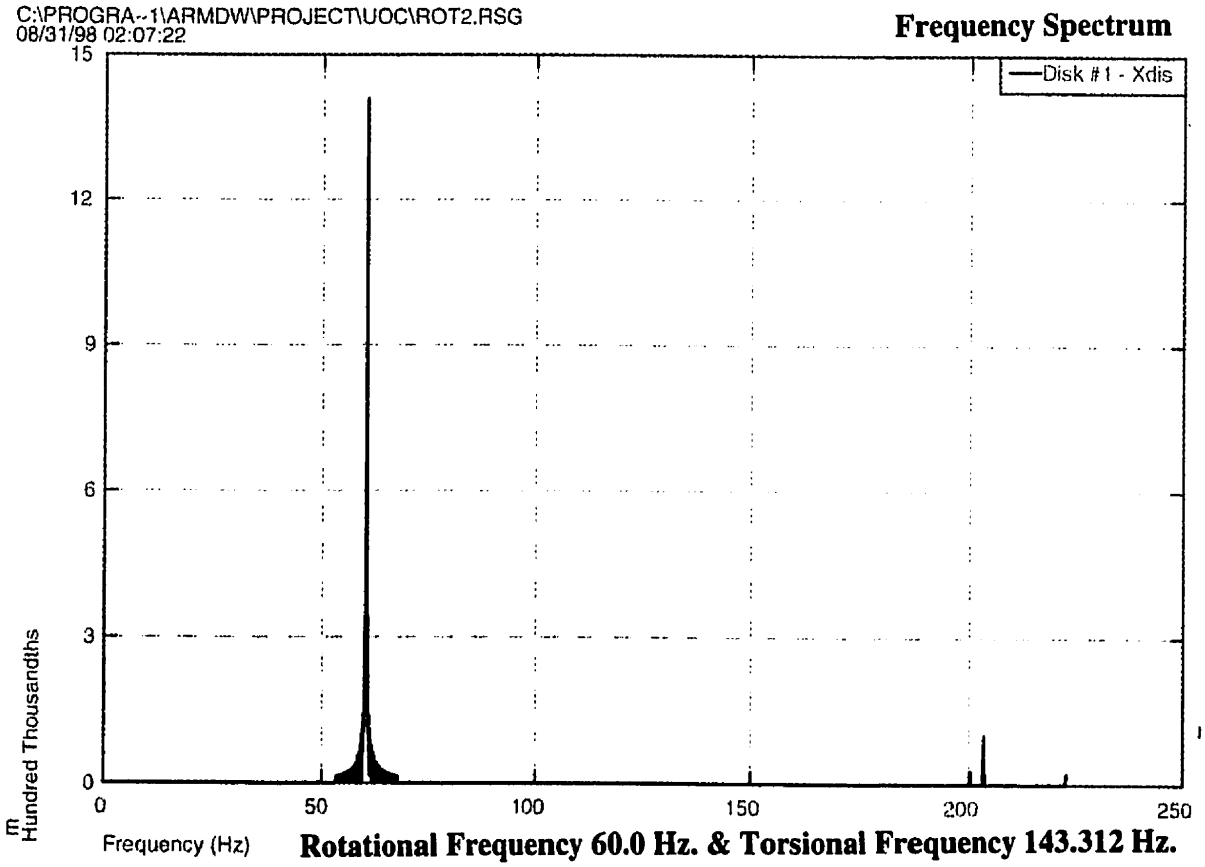

Rotational Frequency 60.0 Hz. & Torsional Frequency 143.312 Hz.

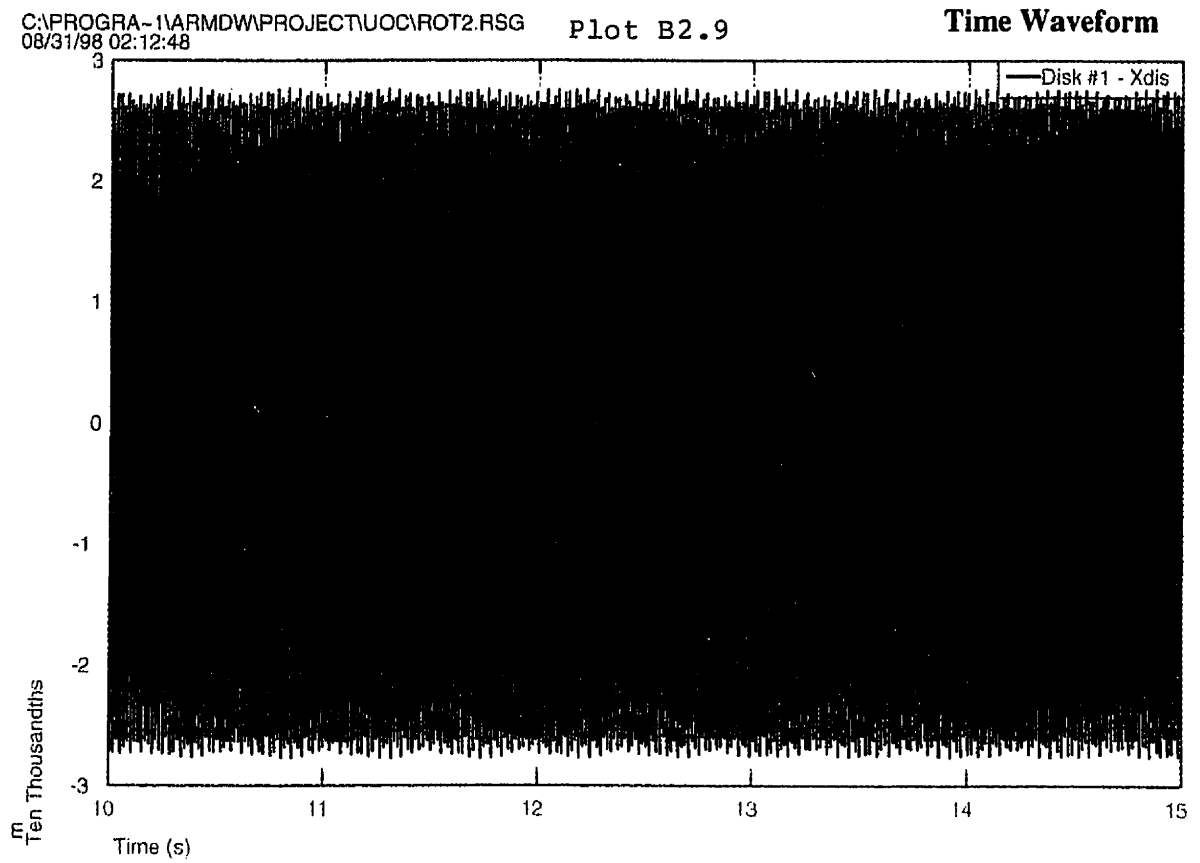

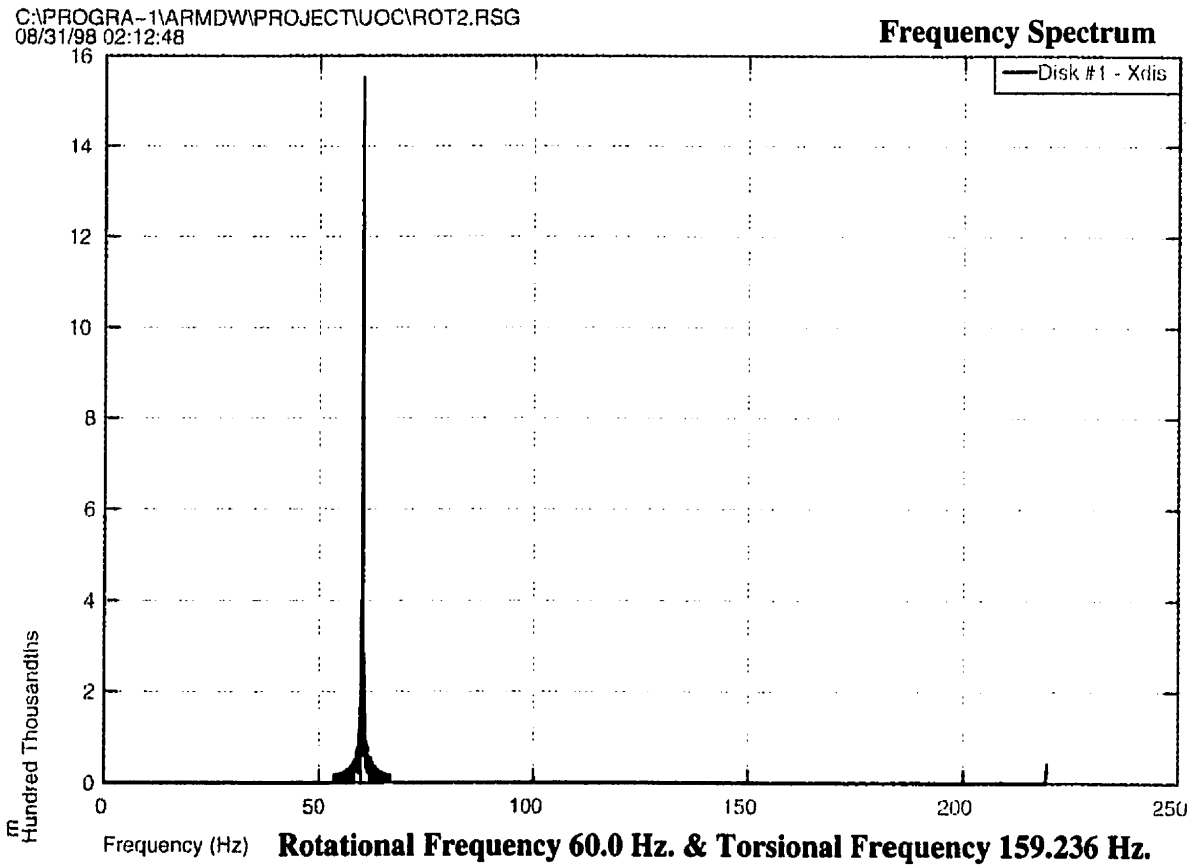

Rotational Frequency 60.0 Hz. & Torsional Frequency 159.236 Hz.

Appendix C1

Program for calculating disk mass, inertia and rotor stiffness.

```
(*Two rotor disk torsional and lateral coupling.*)

(*Data: distance in meters, modulus of elasticity in Pa,
density in kg/m^3*)

density=7.86 10^3; disk1Diam=.769; disk1Thick=0.038;
disk2Diam=.769; disk2Thick=0.038; shaftDiam=.154;

mass1=1/4 density Pi disk1Diam^2 disk1Thick//N
138.723
mass2=1/4 density Pi disk2Diam^2 disk2Thick//N
138.723
mass1Inertia=1/8 mass1 disk1Diam^2//N
10.2544
mass2Inertia=1/8 mass2 disk2Diam^2
10.2544
disk1Inertia=1/64 Pi disk1Diam^4//N
0.0171662
disk2Inertia=1/64 Pi disk2Diam^4//N
0.0171662

shaftDiam
0.154
shaftInertia= (Pi shaftDiam^4) 1/64 //N
0.0000276091
l1=.3; l2=.4; l3=.3; shaftl=1; modulElast=2 10^11;

alpha11=l1^2 (shaftl-l1)^2/
        (3 modulElast shaftInertia shaftl)
          -9
2.66216 10
alpha12=l1 l3 (shaftl^2-l1^2-l3^2)/
              (6 modulElast shaftInertia shaftl)
          -9
2.22752 10
alpha22=(l1+l2)^2 l3^2/(3 modulElast shaftInertia shaftl)
          -9
2.66216 10
```

```
flexMatrix={{alpha11, alpha12}, {alpha12, alpha22}}
                -9                -9
{{2.66216 10   , 2.22752 10   },
                -9                -9
  {2.22752 10   , 2.66216 10   }}
stifMatrix=Inverse[flexMatrix]
                9                 9
{{1.25264 10 , -1.04812 10 },
                 9                 9
  {-1.04812 10 , 1.25264 10 }}
k11=stifMatrix[[1,1]]
            9
1.25264 10
k12=stifMatrix[[1,2]]
             9
-1.04812 10
k21=stifMatrix[[2,1]]
             9
-1.04812 10
k22=stifMatrix[[2,2]]
            9
1.25264 10
modulrigid=72 10^9;
torsionstif=(Pi modulrigid shaftDiam^4)/(32 shaftl)//N
            6
3.97572 10
```

Appendix C2

Program for calculating the natural frequencies of the two-disk rotor system.

```
massMatrix={{138.723,0},{0,138.723}}
{{138.723, 0}, {0, 138.723}}
stifMatrix={{1.25264 10^9,-1.0481 10^9},
            {-1.0481 10^9,1.25264 10^9}}
             9            9
{{1.25264 10 , -1.0481 10 },
              9            9
  {-1.0481 10 , 1.25264 10 }}
charEq=Det[-omega^2 massMatrix+stifMatrix]==0/.
        {omega^2->crS,omega^4->crS^2}
          17             11                    2
4.70593 10   - 3.4754 10   crS + 19244.1 crS  == 0
criticalSpeeds=Solve[charEq,crS]
                     6                      7
{{crS -> 1.47445 10 }, {crS -> 1.65851 10 }}
crSpeedOne=Sqrt[crS]/.criticalSpeeds[[1]] (*in rad/sec*)
1214.27
crSpeedOneHz=1/2 crSpeedOne/Pi//N
193.257

crSpeedTwo=Sqrt[crS]/.criticalSpeeds[[2]] (*in rad/sec*)
4072.49
crSpeedTwoHz=1/2 crSpeedTwo/Pi//N
648.156
```

Appendix D

Rotor dynamic analysis of the experimental rotor model. Dimensional data of the shaft as given in figure 5.5 on page 70 was used for this model. Advanced Rotating Machinery Dynamic program of Rotor Bearing Technology and Software Inc. was used to compute the damped natural frequencies of the model.

*** ROTOR BEARING TECHNOLOGY & SOFTWARE, INC. ***
STABILITY AND NATURAL FREQUENCY ANALYSIS PROGRAM FOR
AXISYMETRIC ROTATING SHAFTS *** ROSTAB *** [V4.0G1]

UOC project two rotor bingham pump

THE ANALYSIS PERFORMED FOR THE FOLLOWING
ROTOR SYSTEM CONFIGURATION >>>>>>>>>>>>>

NUMBER OF * STATIONS *	THE SHAFT IS MODELED BY ------->	21
NUMBER OF * SHAFT *	ELEMENTS IN THE ROTOR SYSTEM -->	20
NUMBER OF * DISCS *	IN THE ROTOR SYSTEM ---------->	2
NUMBER OF * BEARINGS *	IN THE ROTOR SYSTEM ---------->	2
NUMBER OF * MATERIALS*	THE SHAFTING IS COMPOSED OF --->	1
NUMBER OF * MODES *	(Mode Shapes) TO BE PLOTTED --->	6
* GRAVITY *	---- (Inch/SEC^2) ---------->	.38640E+03

Units of measures used for this problem are ----------> [US (English)]

>>> MATERIAL DATA <<<

MATERIAL NUMBER #	MODULUS OF ELASTICITY (LB/IN^2)	SHEAR MODULUS (LB/IN^2)	DENSITY (LB/IN^3)	MATERIAL DAMPING
1	.2900E+08	.1150E+08	.2830E+00	.0000E+00

UOC project two rotor bingham pump

>>> SHAFT ELEMENT DATA <<<

Shaft No.	* E L E M E N T * STATIONS		TYPE	MAT.	LENGTH (Inch)	O.D. (Left End Of Element) (Inch)	I.D. (Left End Of Element) (Inch)	O.D. (Right End Of Element) (Inch)	I.D. (Right End Of Element) (Inch)
1	1	2	1	1	.6900E+00	.2250E+01	.0000E+00	.2250E+01	.0000E+00
2	2	3	1	1	.2810E+01	.3540E+01	.0000E+00	.3540E+01	.0000E+00
3	3	4	1	1	.2250E+01	.3680E+01	.0000E+00	.3680E+01	.0000E+00
4	4	5	1	1	.4380E+01	.3750E+01	.0000E+00	.3750E+01	.0000E+00
5	5	6	1	1	.3940E+01	.3750E+01	.0000E+00	.3750E+01	.0000E+00
6	6	7	1	1	.1144E+02	.3750E+01	.0000E+00	.3750E+01	.0000E+00
7	7	8	1	1	.7500E+01	.3810E+01	.0000E+00	.3810E+01	.0000E+00
8	8	9	1	1	.1880E+01	.3880E+01	.0000E+00	.3880E+01	.0000E+00
9	9	10	1	1	.1880E+01	.3880E+01	.0000E+00	.3880E+01	.0000E+00
10	10	11	1	1	.7680E+01	.4120E+01	.0000E+00	.4120E+01	.0000E+00
11	11	12	1	1	.4070E+01	.4130E+01	.0000E+00	.4130E+01	.0000E+00
12	12	13	1	1	.6300E+00	.4130E+01	.0000E+00	.4130E+01	.0000E+00
13	13	14	1	1	.9800E+00	.3970E+01	.0000E+00	.3970E+01	.0000E+00
14	14	15	1	1	.4390E+01	.3810E+01	.0000E+00	.3810E+01	.0000E+00
15	15	16	1	1	.4500E+01	.3880E+01	.0000E+00	.3880E+01	.0000E+00
16	16	17	1	1	.2750E+01	.3810E+01	.0000E+00	.3810E+01	.0000E+00
17	17	18	1	1	.1144E+02	.3760E+01	.0000E+00	.3760E+01	.0000E+00
18	18	19	1	1	.3940E+01	.3750E+01	.0000E+00	.3750E+01	.0000E+00
19	19	20	1	1	.3250E+01	.3750E+01	.0000E+00	.3750E+01	.0000E+00
20	20	21	-1	1	.5250E+01	.3130E+01	.0000E+00	.1960E+01	.0000E+00

>>> DISC PROPERTY DATA <<<

DISC NUMBER	NODE NUMBER	WEIGHT (LBS)	POLAR MOMENT OF INERTIA (LB-IN^2)	TRANSVERSE MOMENT OF INERTIA (LB-IN^2)
1	9	.13100E+03	.35700E+04	.17850E+04
2	12	.11700E+03	.30700E+04	.15350E+04

```
      ***     ROTOR BEARING TECHNOLOGY & SOFTWARE, INC.    ***
      STABILITY AND NATURAL FREQUENCY ANALYSIS PROGRAM FOR
     AXISYMETRIC ROTATING SHAFTS    *** ROSTAB ***   [V4.0G1]
     ======================================================

  UOC project two rotor bingham pump


  THE STABILITY ANALYSIS PERFORMED WAS FOR
  SHAFT OPERATING SPEED OF ---------------->   3600.0000   (RPM)


  WITH BEARING & HOUSING STIFFNESS AND DAMPING MATRICES
.........................................................


   BEARING NUMBER (  1 ); AT Node/Station NUMBER (  5 )

   BEARING STIFFNESS MATRIX Size Specified =  2
   [ Units are in LB/IN ]

 .8750E+06   .9500E+05
-.3700E+05   .2000E+06


   BEARING DAMPING MATRIX :-
   [ Units are in LB-SEC/IN ]

 .4250E+03 -.1900E+03
-.1600E+03   .1400E+04


   BEARING NUMBER (  2 ); AT Node/Station NUMBER ( 19 )

   BEARING STIFFNESS MATRIX Size Specified =  2
   [ Units are in LB/IN ]

 .8750E+06   .9500E+05
-.3700E+05   .2000E+06


   BEARING DAMPING MATRIX :-
   [ Units are in LB-SEC/IN ]

 .4250E+03 -.1900E+03
-.1600E+03   .1400E+04
```

*** ROTOR BEARING TECHNOLOGY & SOFTWARE, INC. *** Page #
STABILITY AND NATURAL FREQUENCY ANALYSIS PROGRAM FOR
AXISYMETRIC ROTATING SHAFTS *** ROSTAB *** [V4.0G1]
==========

UOC project two rotor bingham pump

>>> Analysis Performed With The Following Externally Applied Loads <<<

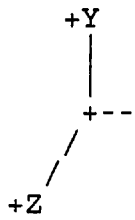

Number of Concentrated Nodal Force & Moment Components ---------->	0
Gravity Loading Factor in X Direction --->	.000
Gravity Loading Factor in Y Direction --->	-1.000
Gravity Constant (In/Sec^2) ---------->	.38640E+03

>>> COMPUTED DEFLECTIONS (Displ. & Rot.) at EACH SHAFT STATION <<<
[* Calculations Consider Housing Stiffness Not Bearings *]

Station Number	Axial Location (Inch)	Horizontal X-Deflection (Inch)	Vertical Y-Deflection (Inch)	Rotations About - X (In/In)	Rotations About - Y (In/In)
1	.00000E+00	.00000E+00	.32704E-02	.32253E-03	.00000E+00
2	.69000E+00	.00000E+00	.30479E-02	.32253E-03	.00000E+00
3	.35000E+01	.00000E+00	.21416E-02	.32262E-03	.00000E+00
4	.57500E+01	.00000E+00	.14157E-02	.32285E-03	.00000E+00
5	.10130E+02	.00000E+00	-.27352E-29	.32424E-03	.00000E+00
6	.14070E+02	.00000E+00	-.12809E-02	.31960E-03	.00000E+00
7	.25510E+02	.00000E+00	-.45825E-02	.23726E-03	.00000E+00
8	.33010E+02	.00000E+00	-.60256E-02	.13868E-03	.00000E+00
9	.34890E+02	.00000E+00	-.62630E-02	.11075E-03	.00000E+00
10	.36770E+02	.00000E+00	-.64444E-02	.81726E-04	.00000E+00
11	.44450E+02	.00000E+00	-.67100E-02	-.13112E-04	.00000E+00
12	.48520E+02	.00000E+00	-.65542E-02	-.63255E-04	.00000E+00
13	.49150E+02	.00000E+00	-.65113E-02	-.70927E-04	.00000E+00
14	.50130E+02	.00000E+00	-.64340E-02	-.84602E-04	.00000E+00
15	.54520E+02	.00000E+00	-.59077E-02	-.15115E-03	.00000E+00
16	.59020E+02	.00000E+00	-.50965E-02	-.20508E-03	.00000E+00
17	.61770E+02	.00000E+00	-.44864E-02	-.23504E-03	.00000E+00
18	.73210E+02	.00000E+00	-.12516E-02	-.31215E-03	.00000E+00
19	.77150E+02	.00000E+00	-.24288E-29	-.31736E-03	.00000E+00
20	.80400E+02	.00000E+00	.10302E-02	-.31692E-03	.00000E+00
21	.85650E+02	.00000E+00	.26919E-02	-.31629E-03	.00000E+00

*** ROTOR BEARING TECHNOLOGY & SOFTWARE, INC. *** Page #
STABILITY AND NATURAL FREQUENCY ANALYSIS PROGRAM FOR
AXISYMETRIC ROTATING SHAFTS *** ROSTAB *** [V4.0G1]

UOC project two rotor bingham pump

>>> COMPUTED ROTOR PARAMETERS <<<

Shaft Station #	Axial Location (Inch)	Shaft Weight (lbs)	Shaft Moment of Inertia (lb-in^2)	Disc Weight (lbs)	Bearing Station
1	.00000E+00	.38820E+00	.24566E+00	.00000E+00	
2	.69000E+00	.43016E+01	.63759E+01	.00000E+00	
3	.35000E+01	.72997E+01	.11863E+02	.00000E+00	
4	.57500E+01	.10231E+02	.17765E+02	.00000E+00	
5	.10130E+02	.13003E+02	.22856E+02	.00000E+00	Yes
6	.14070E+02	.24036E+02	.42251E+02	.00000E+00	
7	.25510E+02	.29978E+02	.53382E+02	.00000E+00	
8	.33010E+02	.15245E+02	.27873E+02	.00000E+00	
9	.34890E+02	.62907E+01	.11838E+02	.13100E+03	
10	.36770E+02	.17633E+02	.36659E+02	.00000E+00	
11	.44450E+02	.22203E+02	.47190E+02	.00000E+00	
12	.48520E+02	.89093E+01	.18996E+02	.11700E+03	
13	.49150E+02	.29108E+01	.59280E+01	.00000E+00	
14	.50130E+02	.87986E+01	.16232E+02	.00000E+00	
15	.54520E+02	.14611E+02	.27018E+02	.00000E+00	
16	.59020E+02	.11965E+02	.22217E+02	.00000E+00	
17	.61770E+02	.22411E+02	.39814E+02	.00000E+00	
18	.73210E+02	.24132E+02	.42588E+02	.00000E+00	
19	.77150E+02	.11237E+02	.19752E+02	.00000E+00	Yes
20	.80400E+02	.95039E+01	.12823E+02	.00000E+00	
21	.85650E+02	.32665E+01	.28750E+01	.00000E+00	
Total =	.85650E+02	.26835E+03	.48654E+03	.24800E+03	

Total Shaft Weight (LBS) ----------> 268.35280
Total Disc Weight (LBS) ----------> 248.00000
OVER ALL Rotor Weight (LBS) ----------> 516.35280
Total Shaft Length (Inch) ----------> 85.65000
C. G. Location from Station 1 (Inch) ---> 41.65440

>>> Computed Bearing REACTIONS <<<

Bearing Number.	Station Number.	Force (lbs) X-Direction	Force (lbs) Y-Direction	Resultant (lbs)	Angle (Deg.) From +X Axis
1	5	.00000E+00	.27352E+03	.27352E+03	.90000E+02
2	19	.00000E+00	.24289E+03	.24289E+03	.90000E+02

*** ROTOR BEARING TECHNOLOGY & SOFTWARE, INC. ***
STABILITY AND NATURAL FREQUENCY ANALYSIS PROGRAM FOR
AXISYMETRIC ROTATING SHAFTS *** ROSTAB *** [V4.0G1]

UOC project two rotor bingham pump

Shaft Element FORCES, MOMENTS and STRESSES

ELEMENT #	Node	FORCE-X (Shear)	FORCE-Y (Shear)	MOMENT-X (IN-LB)	MOMENT-Y (IN-LB)	FIBER-STR. Max. (KSI)	SHEAR-STR. Max. (KSI)
1	1	0.000E+00	1.789E-02	2.908E-04	0.000E+00	2.601E-07	6.001E-06
	2	0.000E+00	7.835E-01	2.775E-01	0.000E+00	2.482E-04	2.627E-04
2	2	0.000E+00	7.783E-01	2.697E-01	0.000E+00	6.192E-05	1.054E-04
	3	0.000E+00	8.606E+00	1.348E+01	0.000E+00	3.095E-03	1.166E-03
3	3	0.000E+00	8.621E+00	1.348E+01	0.000E+00	2.756E-03	1.081E-03
	4	0.000E+00	1.539E+01	4.051E+01	0.000E+00	8.280E-03	1.930E-03
4	4	0.000E+00	1.540E+01	4.052E+01	0.000E+00	7.826E-03	1.859E-03
	5	0.000E+00	2.909E+01	1.380E+02	0.000E+00	2.665E-02	3.512E-03
5	5	0.000E+00	-2.444E+02	1.379E+02	0.000E+00	2.664E-02	2.951E-02
	6	0.000E+00	-2.321E+02	-8.008E+02	0.000E+00	1.547E-01	2.802E-02
6	6	0.000E+00	-2.321E+02	-8.008E+02	0.000E+00	1.547E-01	2.802E-02
	7	0.000E+00	-1.964E+02	-3.252E+03	0.000E+00	6.281E-01	2.370E-02
7	7	0.000E+00	-1.964E+02	-3.252E+03	0.000E+00	5.989E-01	2.296E-02
	8	0.000E+00	-1.722E+02	-4.634E+03	0.000E+00	8.534E-01	2.013E-02
8	8	0.000E+00	-1.722E+02	-4.634E+03	0.000E+00	8.080E-01	1.942E-02
	9	0.000E+00	-1.659E+02	-4.951E+03	0.000E+00	8.634E-01	1.871E-02
9	9	0.000E+00	-3.486E+01	-4.951E+03	0.000E+00	8.634E-01	3.931E-03
	10	0.000E+00	-2.855E+01	-5.011E+03	0.000E+00	8.738E-01	3.220E-03
10	10	0.000E+00	-2.856E+01	-5.011E+03	0.000E+00	7.298E-01	2.856E-03
	11	0.000E+00	4.212E-01	-5.119E+03	0.000E+00	7.456E-01	4.213E-05
11	11	0.000E+00	4.442E-01	-5.119E+03	0.000E+00	7.402E-01	4.421E-05
	12	0.000E+00	1.587E+01	-5.086E+03	0.000E+00	7.354E-01	1.579E-03
12	12	0.000E+00	1.329E+02	-5.086E+03	0.000E+00	7.354E-01	1.323E-02
	13	0.000E+00	1.353E+02	-5.001E+03	0.000E+00	7.232E-01	1.347E-02
13	13	0.000E+00	1.353E+02	-5.001E+03	0.000E+00	8.142E-01	1.457E-02
	14	0.000E+00	1.387E+02	-4.867E+03	0.000E+00	7.923E-01	1.494E-02
14	14	0.000E+00	1.387E+02	-4.867E+03	0.000E+00	8.964E-01	1.622E-02
	15	0.000E+00	1.528E+02	-4.227E+03	0.000E+00	7.785E-01	1.788E-02
15	15	0.000E+00	1.529E+02	-4.227E+03	0.000E+00	7.372E-01	1.724E-02
	16	0.000E+00	1.679E+02	-3.505E+03	0.000E+00	6.113E-01	1.893E-02

16	16	0.000E+00	1.679E+02	-3.505E+03	0.000E+00	6.456E-01	1.963E-02
	17	0.000E+00	1.768E+02	-3.032E+03	0.000E+00	5.583E-01	2.067E-02
17	17	0.000E+00	1.768E+02	-3.032E+03	0.000E+00	5.809E-01	2.123E-02
	18	0.000E+00	2.127E+02	-8.037E+02	0.000E+00	1.540E-01	2.554E-02
18	18	0.000E+00	2.127E+02	-8.037E+02	0.000E+00	1.552E-01	2.568E-02
	19	0.000E+00	2.250E+02	5.866E+01	0.000E+00	1.133E-02	2.717E-02
19	19	0.000E+00	-1.785E+01	5.866E+01	0.000E+00	1.133E-02	2.155E-03
	20	0.000E+00	-7.695E+00	1.715E+01	0.000E+00	3.313E-03	9.289E-04
20	20	0.000E+00	-7.692E+00	1.715E+01	0.000E+00	5.696E-03	1.333E-03
	21	0.000E+00	-4.914E-04	-4.249E-04	0.000E+00	5.748E-07	2.171E-07

*** ROTOR BEARING TECHNOLOGY & SOFTWARE, INC. *** Page #
STABILITY AND NATURAL FREQUENCY ANALYSIS PROGRAM FOR
AXISYMETRIC ROTATING SHAFTS *** ROSTAB *** [V4.0G1]

UOC project two rotor bingham pump

>>> STABILITY ANALYSIS <<<

Number	Growth Factor	Logarithmic Decrement	Critical Damping	* F R E Q U E N C Y * Hz Cyc/Sec	REV/MIN
1	-.54851E-02	.15637E-06	.24887E-07	.35078E+05	.21047E+07
3	.23636E-02	-.67382E-07	-.10724E-07	.35078E+05	.21047E+07
5	.65693E-03	-.19010E-07	-.30255E-08	.34557E+05	.20734E+07
7	-.65698E-03	.19011E-07	.30258E-08	.34557E+05	.20734E+07
9	-.11163E+03	.10622E-01	.16905E-02	.10509E+05	.63057E+06
11	-.26385E+03	.25175E-01	.40067E-02	.10480E+05	.62883E+06
13	-.29959E-01	.29641E-05	.47175E-06	.10107E+05	.60645E+06
15	-.29497E-01	.29185E-05	.46449E-06	.10107E+05	.60642E+06
17	-.39444E+04	.62724E+00	.99335E-01	.62885E+04	.37731E+06
19	-.69199E+01	.10552E-02	.16794E-03	.65580E+04	.39348E+06
21	-.46845E+01	.71439E-03	.11370E-03	.65573E+04	.39344E+06
23	-.41379E+02	.63373E-02	.10086E-02	.65294E+04	.39176E+06
25	-.15119E+03	.23140E-01	.36829E-02	.65336E+04	.39201E+06
27	-.44108E+01	.72873E-03	.11598E-03	.60528E+04	.36317E+06
29	-.38138E+01	.63036E-03	.10033E-03	.60502E+04	.36301E+06
31	-.27901E+04	.51726E+00	.82047E-01	.53939E+04	.32363E+06
33	-.88370E+04	.18438E+01	.28157E+00	.47929E+04	.28757E+06
35	-.44795E+04	.10103E+01	.15876E+00	.44338E+04	.26603E+06
37	-.24986E+05	.00000E+00	.00000E+00	.00000E+00	.00000E+00
38	-.26470E+05	.00000E+00	.00000E+00	.00000E+00	.00000E+00
39	-.30247E-01	.85311E-05	.13578E-05	.35455E+04	.21273E+06
41	-.45682E-01	.12911E-04	.20549E-05	.35382E+04	.21229E+06
43	-.11447E+04	.38599E+00	.61317E-01	.29656E+04	.17793E+06
45	-.32912E+02	.10174E-01	.16192E-02	.32350E+04	.19410E+06
47	-.20255E+02	.62477E-02	.99435E-03	.32420E+04	.19452E+06
49	-.30332E+04	.12159E+01	.18999E+00	.24947E+04	.14968E+06
51	-.82065E+03	.31351E+00	.49834E-01	.26177E+04	.15706E+06
53	-.20048E+04	.86006E+00	.13562E+00	.23310E+04	.13986E+06
55	-.33762E+03	.23580E+00	.37502E-01	.14318E+04	.85910E+05
57	-.25078E+03	.19003E+00	.30231E-01	.13197E+04	.79182E+05
59	-.38342E+03	.29072E+00	.46221E-01	.13188E+04	.79130E+05
61	-.29011E+03	.23308E+00	.37070E-01	.12447E+04	.74680E+05
63	-.19348E+03	.18118E+00	.28823E-01	.10679E+04	.64074E+05
65	-.16639E+03	.16492E+00	.26238E-01	.10090E+04	.60537E+05
67	-.25229E+03	.29156E+00	.46354E-01	.86531E+03	.51919E+05
69	-.19464E+03	.24834E+00	.39494E-01	.78377E+03	.47026E+05
71	-.17641E+03	.27866E+00	.44307E-01	.63306E+03	.37983E+05
73	-.13479E+03	.22767E+00	.36211E-01	.59205E+03	.35523E+05
75	-.47464E+02	.10332E+00	.16442E-01	.45939E+03	.27563E+05
77	-.28273E+02	.65185E-01	.10374E-01	.43373E+03	.26024E+05
79	-.15214E+04	.42033E+01	.55603E+00	.36196E+03	.21718E+05
81	-.90326E+03	.27917E+01	.40604E+00	.32355E+03	.19413E+05

83	-.16901E+02	.92084E-01	.14654E-01	.18354E+03	.11012E+05
85	-.15622E+02	.90309E-01	.14372E-01	.17298E+03	.10379E+05
87	-.42789E+00	.11035E-01	.17563E-02	.38775E+02	.23265E+04
89	-.83663E+01	.21641E+00	.34422E-01	.38659E+02	.23196E+04
91	-.15308E+03	.00000E+00	.00000E+00	.00000E+00	.00000E+00
92	-.14713E+03	.00000E+00	.00000E+00	.00000E+00	.00000E+00

CODE: 603061622

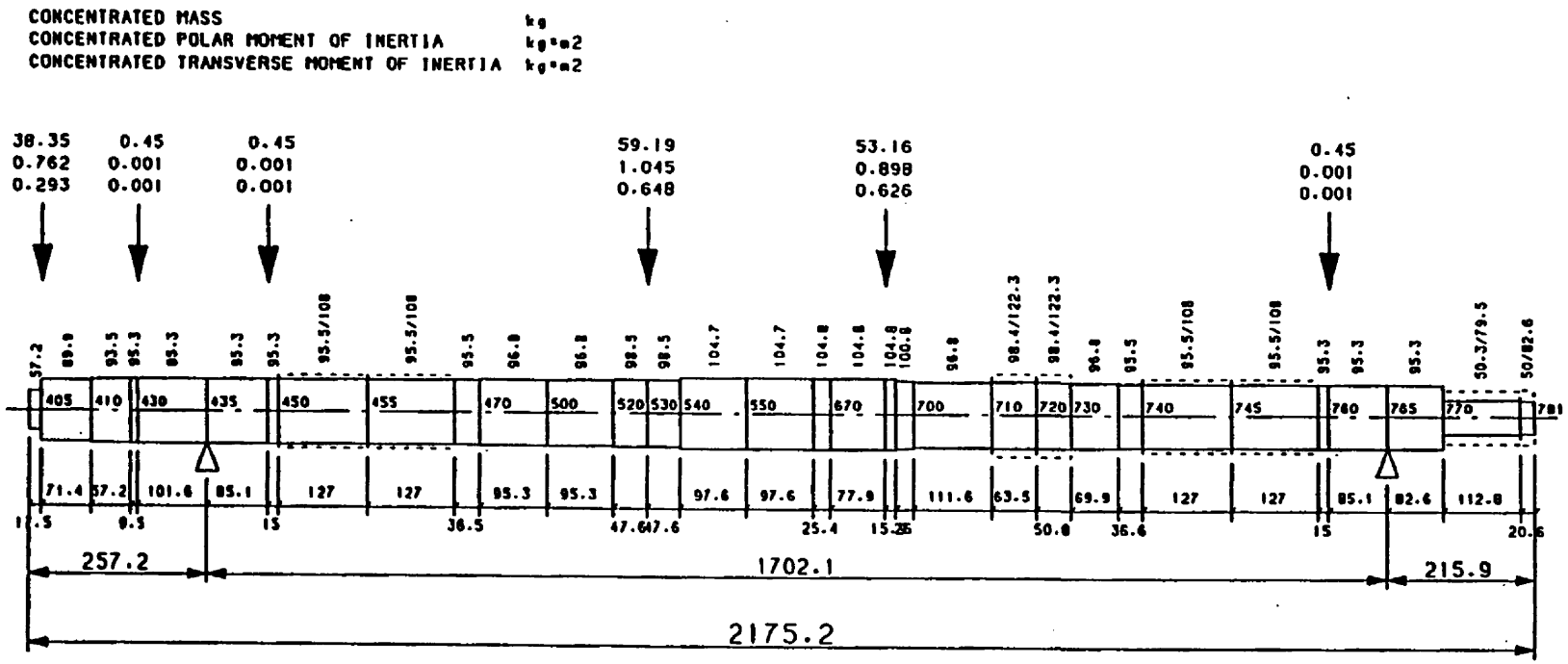

Plot 5.5: Dimensional Details of the Pump Rotor

LATERAL ROTOR MODEL	SCALE 1 : 6.6	DATE: 06.03.96
1E725 Pump Type 12x12x15.5 MSD-D 2 Stg.		
SULZER BINGHAM PUMPS INC - PORTLAND, OREGON, USA		Fig. A1

ROTOR MASS = 2.872E+02kg
ROTOR POLAR
MASS MOMENT = 2.886E+00kg-m2

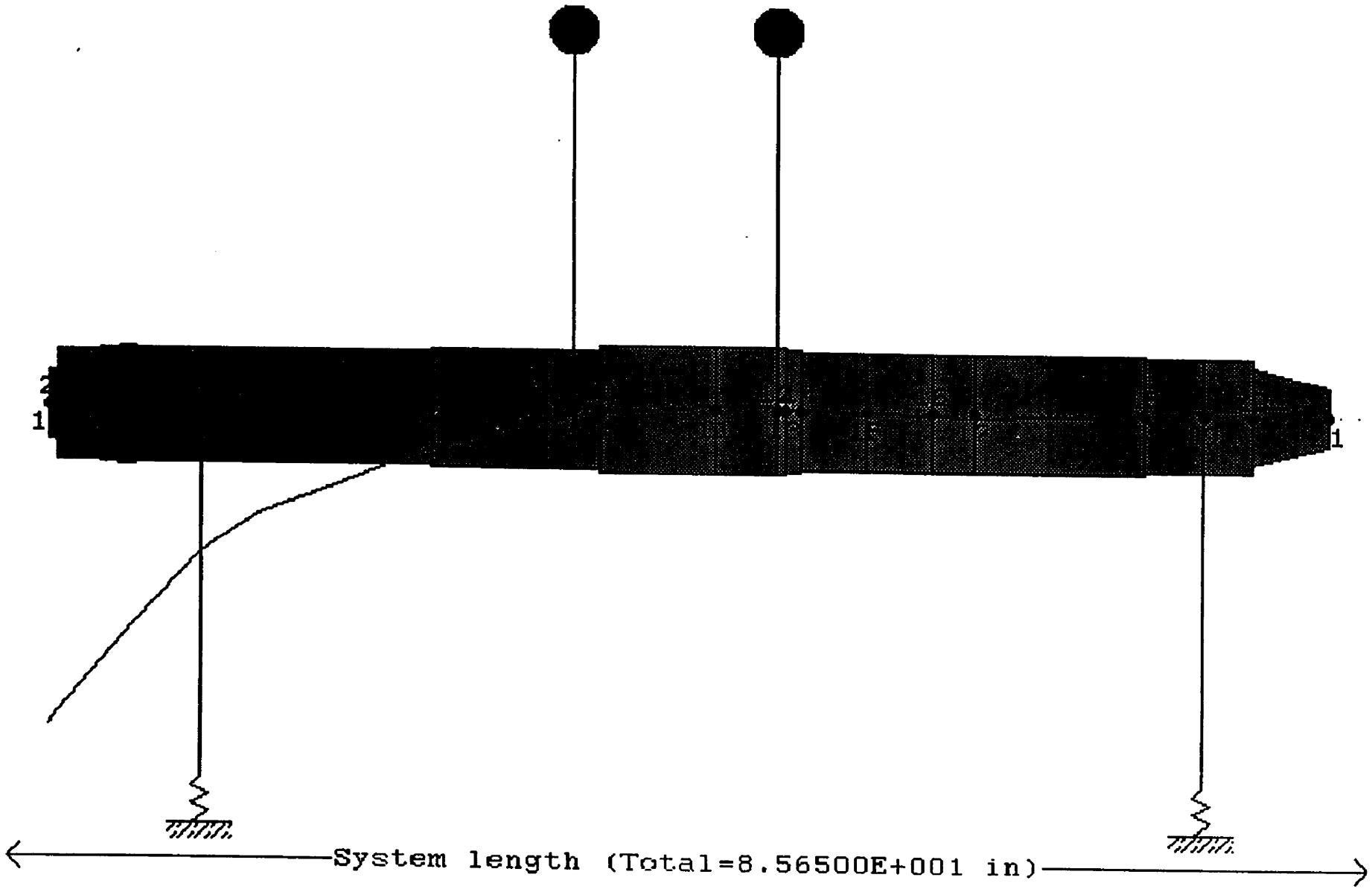

Plot 5.8: **Third Flexing Mode of the Pump Rotor**

At 323.5 Hz.

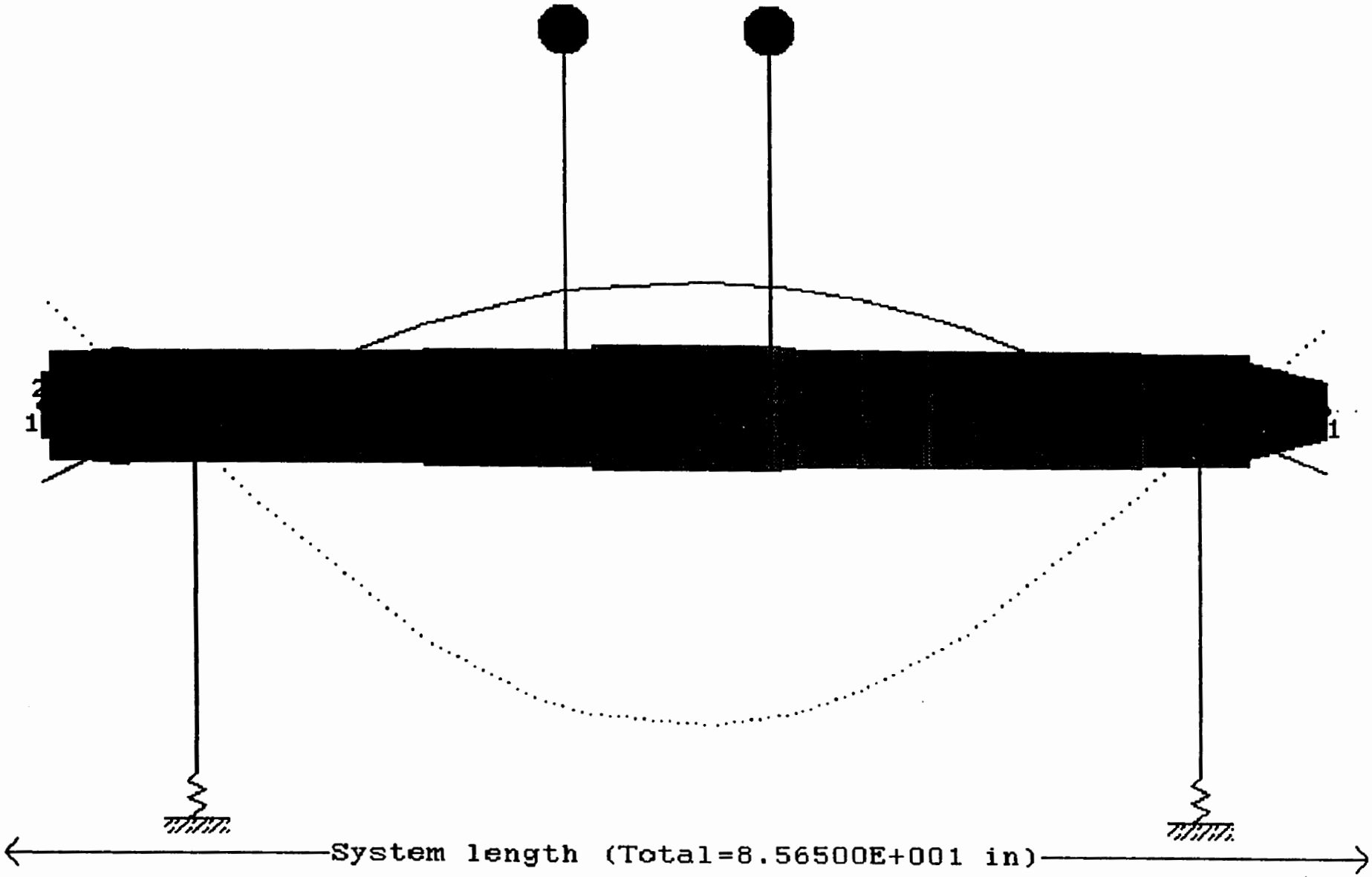

Page 127

Plot 5.6: **First Bending Mode of the Pump Rotor**

At 38.7 Hz.

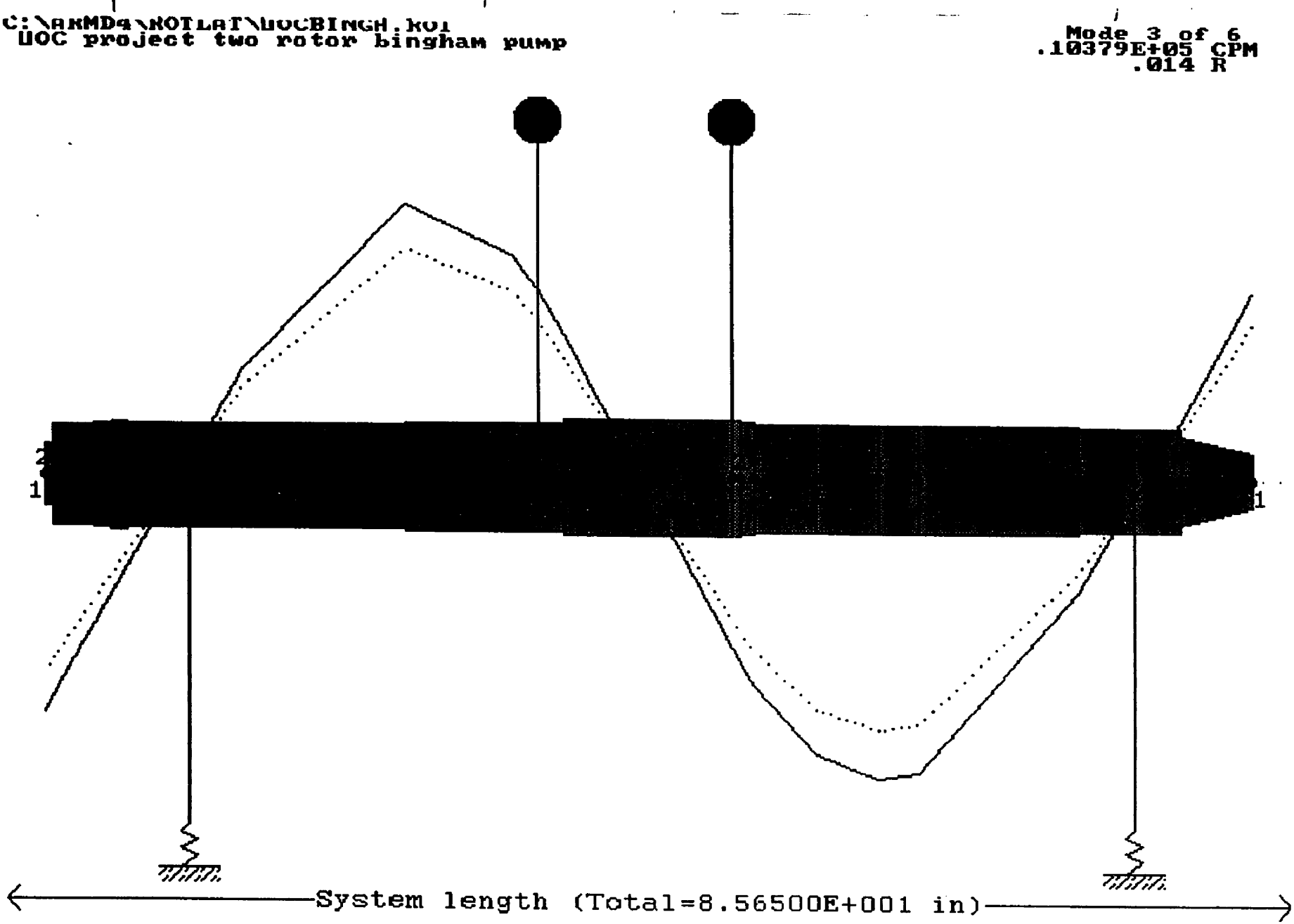

Plot 5.7: **Second Bending Mode of the Pump Rotor**

At 172.92 Hz.